Doctoral thesis

Dehydration of 2,3-butanediol into 3-buten-2-ol and 1,3-butadiene over acid-base catalysts

January 2017

CHIBA UNIVERSITY

Hailing Duan

14TD3104

Laboratory of Reaction Engineering

Graduate School of Engineering

Chiba University

(千葉大学学位申請論文)

Dehydration of 2,3-butanediol into 3-buten-2-ol and 1,3-butadiene over acid-base catalysts

2017 年 1 月

CHIBA UNIVERSITY

千葉大学大学院工学研究科

共生応用化学専攻共生応用化学コース

資源反応工学研究室

段　海玲

14TD3104

Abstract

1,3-Butadiene (BD) is among the most important bulk chemicals for manufacturing polymers and rubbers. Especially, the major products such as styrene-butadiene rubbers and butadiene rubbers are in great demand to produce tires of automobiles. However, the supply of BD mainly depends on the production of ethylene and it is not stable under the situation changing supply of petroleum recently.

On the other hand, in order to realize the low-carbon society and to diminish the use of fossil sources, recent days the demand for sustainable chemical compounds is growing rapidly. Since 2,3-butanediol (2,3-BDO) is one of the respective biomass-derived chemical compounds and its production by fermentation of glycerol, glucose, sucrose, xylose, ect. with various bacteria has been greatly developed, 2,3-BDO shows the widely future prospect for widely bio-based chemicals application via catalytic technologies.

Studies on 2,3-BDO dehydration were reported even before 1938, but the products distributed variously over different catalysts relying on their properties. 2-Butanone (MEK) can be produced from 2,3-BDO easily via the methyl groups rearrangement in the acidic aqueous solution, resins or over several acid solid catalysts such as bentonite, alumina, silica-alumina, heteropoly acids, and zeolites. In addition, the presence of Brønsted acid sites from zeolites also leaded to the formation competition of MPA and MEK, together with some heavy condensation products. Sometimes, BD can be also produced over the only acidic solid catalysts, but it is very difficult to control the proper acidity for the efficiently selective BD production. On the other hand, the basic sites also lead to dehydrogenate for acetoin and diacetyl or dehydrate to 2,3-epoxybutane.

I also studied the 2,3-BDO dehydration over the bare base-acidic rare earth metal oxides, and found out that the 1,2-elimination for the first one molecular water leading to 3-buten-2-ol (3B2OL) formation, and then further to BD formation only over Sc_2O_3. Formations of BD and 3B2OL are different in activation energy level, thus their distribution could be controlled by reaction temperature simply in the case of Sc_2O_3 and ThO_2.

On the other hand, 1,2-elimination also occurred over the base-acid bifunctional catalysts such as ZrO_2, and the alkaline metal oxide modified ZrO_2 such as CaO/ZrO_2, BaO/ZrO_2, SrO/ZrO_2, and MgO/ZrO_2. They resembled each other greatly with both their reaction activities and their crystal structures. Especially, the modified ZrO_2 samples showed the similar new-formed perovskite compounds, which can generate the new medium basic sites when they are highly dispersed. This new medium basic sites also showed some relativity with the 1,2-elimination activities.

Based on the fact that the direct conversion of 2,3-BDO into BD needs high reaction temperatures while the dehydration into their corresponding unsaturated alcohol 3B2OL proceeds at rather low temperatures, efficient formation of 3B2OL from BDO and then further dehydrated into BD by two steps or in one process with a two-layer catalyst bed were also investigated in this study.

Acknowledgement

I would like to give my sincere gratitude to Prof. Satoshi Sato and Assistant Prof. Yasuhiro Yamada for the valuable advice and discussions, and Prof. Shogo Shimazu, Prof. Masami Sakamoto, Prof. Motoi Machida and Prof. Nobuyuki Ichikuni giving me for his insightful comments and suggestions. Acknowledgments are also made to Mr. Shingo Kubo in Kagoshima University for his support in measuring samples by XPS. I also want to thank Dr. Daolai Sun for his assistant of XRD measurement.

I would like to express my acknowledgement to JST, Strategic International Collaborative Research Program, SICORP for their support. I also would like to give my sincere thanks to Rotary Yoneyama Memoria Foundation for their scholarship and friendship support during the last two years of my doctoral program.

I would like to thank the members of Sato Laboratory (Laboratory of Reaction Engineering) for their friendly memberships.

Finally, I would also like to express my gratitude to my family for their warm encouragement and moral support.

Hailing Duan

January 2017

Table of Contents

Chapter I: Introduction

1.1 Energy & resources supply and demand

Energy has been enforced human's civilization and development for millions of years. Currently, the shares of energy sources are mainly considered as coal, oil, gas, nuclear, biofuels and also some other renewable fuel resources, as shown in **Figure 1-1**. Among them, the fossil fuel resources such as oil, coal and natural gas show the highest shares of total world primary energy, which have significantly accelerated global economic development. **Figure 1-1** also shows that global energy demand will still increase rapidly with the global economic development in the next two decades. Even with some environmental problems such as the CO_2 emission issue, the demand of fossil energy shows no decline since oil has been supplied as not only the global energy but also the bulk chemicals for our daily life. And also the demand of natural gas increases greatly mainly as a fuel due to its low CO_2 emission.[1]

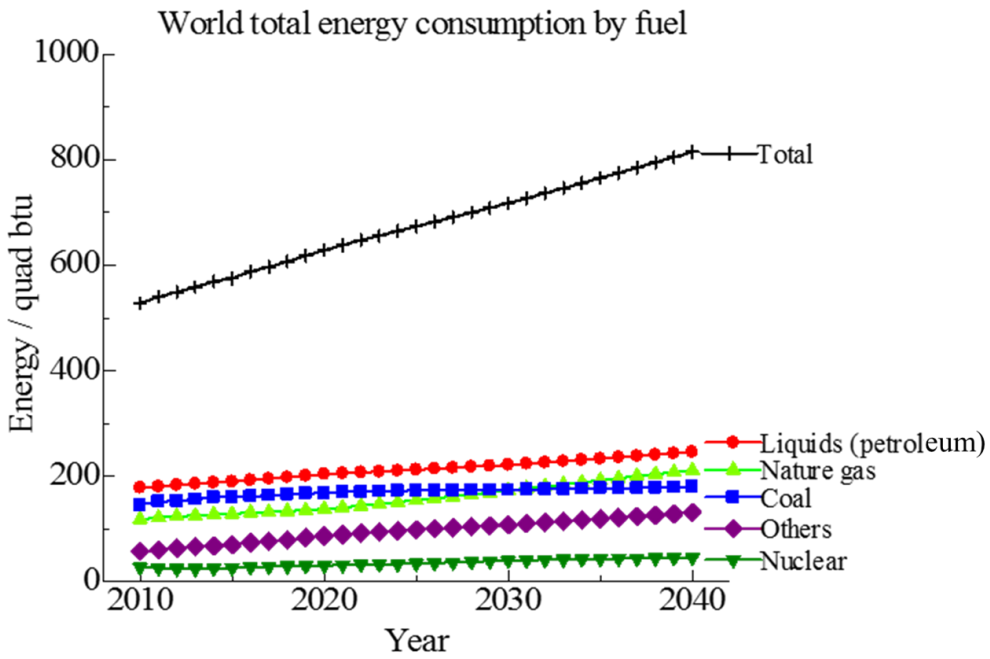

Figure 1-1 A consumption for the global total primary energy from 2010 to 2040.[1]

1.2 The existing circumstances of fossil resources

It is well known that fossil resources are formed when a large amount of dead organisms had been buried under earth deeply for a long periods of time. The application of fossil resources can be dated back to 1853 and the first oil well for industry usage opened at 1858 in Ontrario, Canada.[2] Then, oil became the significant resources for industry and the important pillar for global economy. United States, Saudi Arabia and then Soviet Union, presently Russia, have been led the oil trade for more than

150 years. Because the oil facilities were the important strategic asset, fossil resources monopoly has also caused some military conflicts including the World War II.[3]

Currently, oil is not only used as the main fuels for vehicles but also widely used as the resources of some bulk chemical compounds for pharmaceuticals, solvents, fertilizers, pesticides, plastics, etc. **Figure 1-2** shows the daily production of petroleum and other liquids in 1979 and 2015 by the main countries. The total daily production has increased greatly from 67135 to 95741 thousand barrels. About 80% of the global oil resource is located in the Middle East. The top three, U.S., Saudi Arabia and Russia, changed little on their global shares in the past 20 years, but their unstable daily production and supplies also resulted in serious problems.[4] Since no data and proof are available to show the total amount of oil all over the world, thus, reports on the current oil storage are only based on the estimated amount of oil deposits at that time. Therefore, the unstable daily production of oil can even effect the price of fuel and then the global economy.

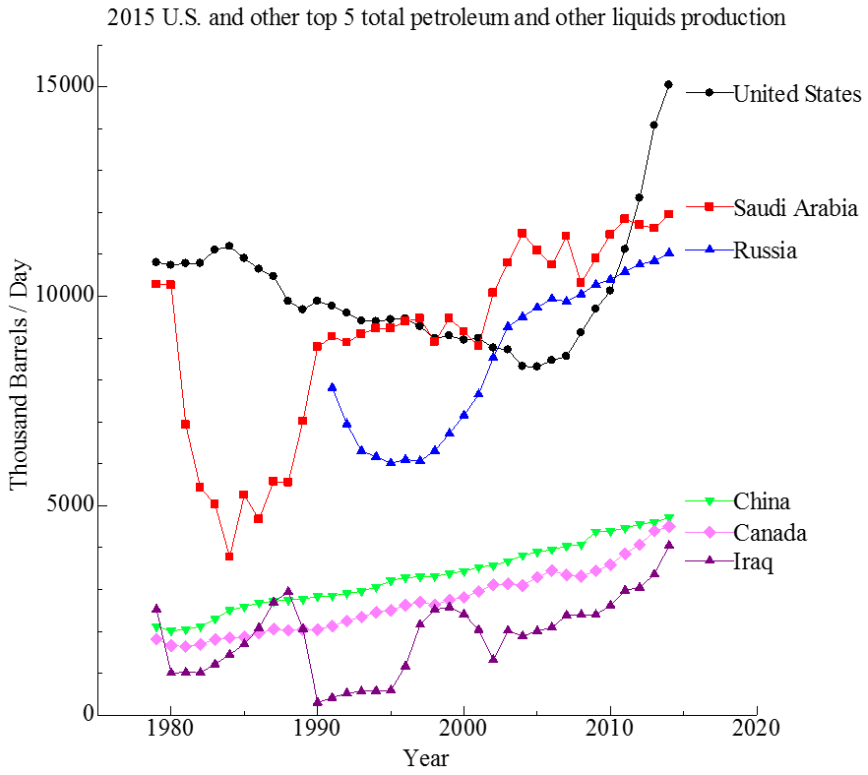

Figure 1-2 The total petroleum and other liquids daily production of the top 6 countries. [4]

1.3 The application of petroleum

Petroleum in common means crude oil, including gaseous, liquid, and solid hydrocarbons formed under different temperature and pressure conditions. Lower hydrocarbons such as C_1-C_4

alkanes are formed as gases, while C_5 or the heavier ones are in liquid or solid states. In most case, crude oil exists as their mixtures. Crude oil mainly includes alkanes, cycloalkanes, and some other compounds containing nitrogen, oxygen and sulfur, as well as a small amount of metals such as iron, copper, nickel, vanadium, etc. Of course, there are not only the organic and inorganic substances but also some live bacteria, which can decompose the crude oil into various compounds.[5,6]

As summarized in **Figure 1-3**, our daily life has been supported by a large amount of products derived from petroleum for more than 100 years.[7] Petroleum can be refined by distillation into benzene, xylene, toluene, butanes, etc. Based on these compounds, the further products such as plastics, nylons, resins, solvent, films, rubber, etc. can be produced for the next generation goods such as cushion, spandex, vitamins, bumpers, paints, clothes, pen, aspirin, etc. which are necessary as the textiles, safe food supply, transportation, housing, recreation, communications, health and even hygiene.[8] In other words, we cannot live without petroleum. Unfortunately, the unpredictable oil supply cannot give us a stable future for long time and we must find some renewable and alternative resources to replace those fossil resources intermediately.

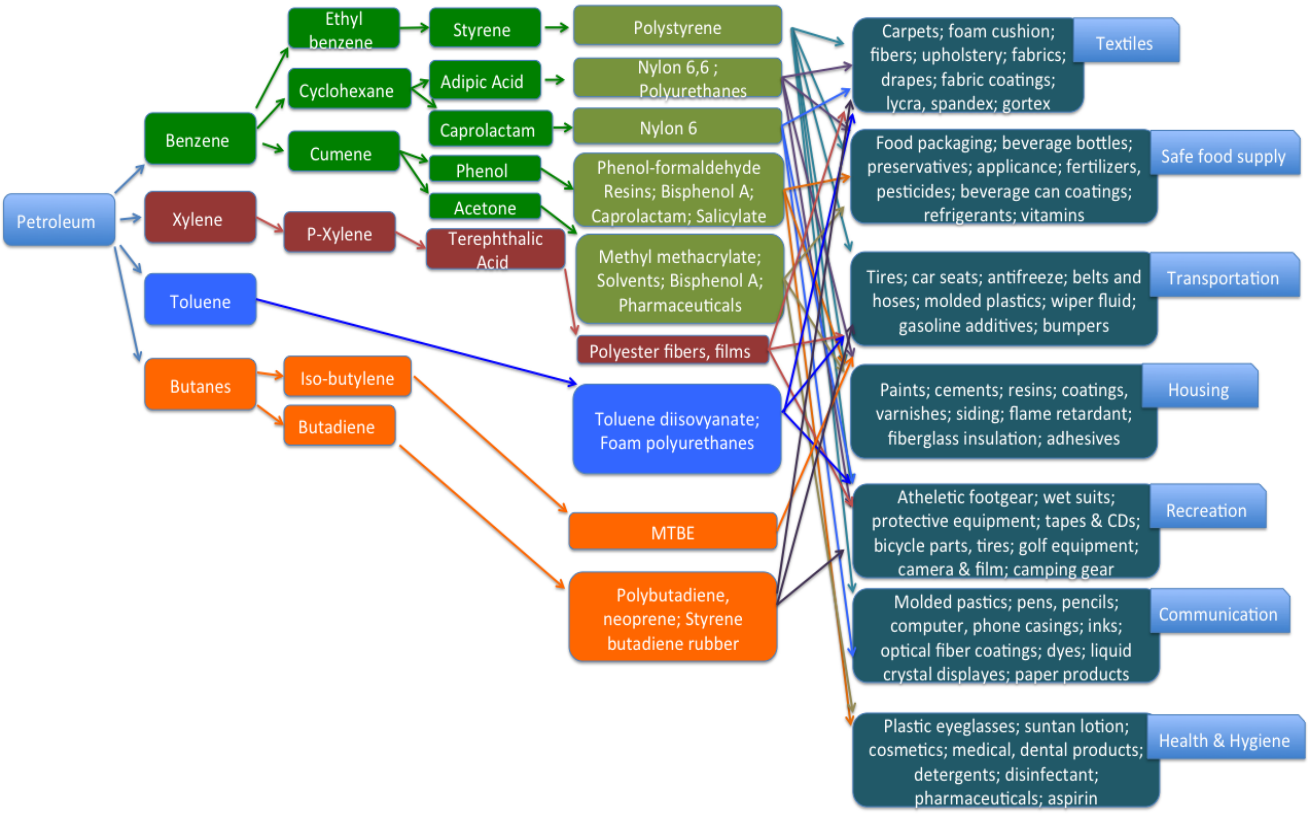

Figure 1-3 Products from Petroleum-based Feedstocks.[8]

However, the fossil resources bring to us not only the abundant life, but also a lot of serious problems every day. Some of the problems are also destroying human's future as follows:

1. Incompleted combustion of these fossil fuels, petroleum or gasoline resulted in some toxic by-products, such as MP2.5, CO, NO_x, SO_x, etc. into air, especially the NO_x compounds, which is responsible for the famous photochemical-smog.[9]

2. The global warming problems and also the ocean acidification problems are going worse to worse with the problems of increasing CO_2 emission. When burned, fossil fuels and the petroluem-direvied products release CO_2, the main greenhouse gas.The concentration of the atmospheric CO_2 has risen over the last 150 years, which can result in the global temperature increasing and then the iceberg in polarzone dissolving. In fact, world surface temperature has been increasing about 0.2°C per decade in the past 30 years.[10] It is worried that the living systems will be changed and result in a large amount of organisms dying with increasing global temperature.

3. Oil extraction is costly and sometimes brings environmental destruction. Exploration and extraction of oil and coal disturb the surroundings. Crude oil shipping and purification also caused accidents which have damaged many natural ecosystems deeply.

1.4 The future energy and chemical resources we can depend on

Currently, the choices of future energy and alternative resources is determined by a large number of important factors. The future price of fossil fuels and the magnitude of efforts affect the alternatives. As shown in **Figure 1-4**, in the past 20 years, oil price changed greatly, and has also affected the global economy and development markedly.

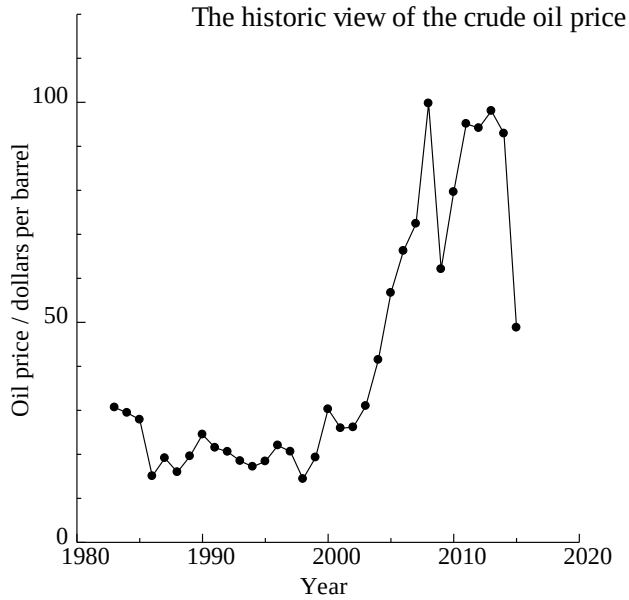

Figure 1-4 Overview of the crude oil price. [11]

On the other hand, differences in CO_2 emissions are also one of the very important factors for our

decisions. As an effective example, in the past decade, the U.S. has taken some efficient actions in reforming their fuel resources composition for the electric generation. Nuclear generation kept stable over the past decade as one of the largest share for generation with no-CO_2 emissions. Besides, renewable energy sources are increasing in the shares, together with the share of natural gas increasing for its low CO_2 emission, as shown in **Figure 1-5**.[12]

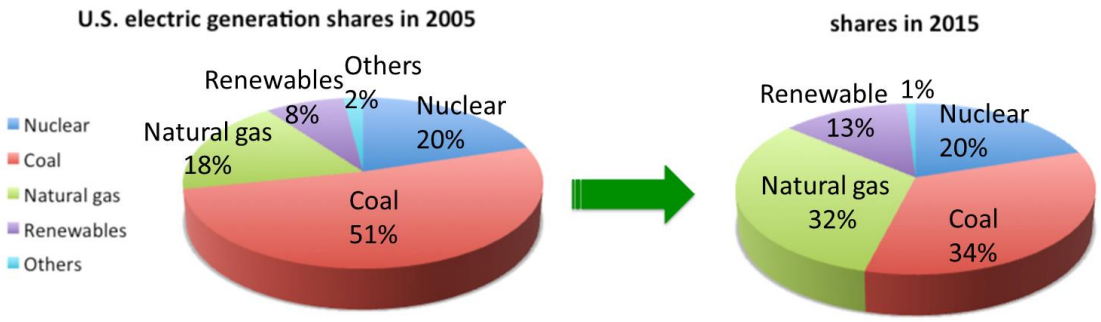

Figure 1-5 The changes of U.S. electric generation shares for environment consideration.[12]

As another important fossil resource, the global natural gas production is aimed to grow from 342 billion cubic feet per day (Bcf/d) in 2015 to 554 Bcf/d by 2040. It is mainly judged from the the increasing production of shale gas resources, which is expected to *ca.* 30% of the total natural gas.[13] However, even with its high combusion heat density and low CO_2 emission, as one of the fossil resources natural gas still accelerates the greenhouse warming worse when compared with renewable resources. Thus, more efforts should be concentrated on enhancing the applied research of renewable resources.

Renewable energy technologies such as solar, wind power, hydropower, and biomass are available and under consideration, but currently, the primary alternatives still depend on hydroelectricity and nuclear generation (**Figure 1-6**). On the other hand, in Japan, people cannot forget the destructive damage from the burst of nuclear generation. Thus, we should not image our living with nuclear power in the future, and we can only live on the renewable resources such as solar power and biomass since Japan has only the limited hydropower, wind power and geothermal energy. Biomass is the most abundant all over the world. If the application technologies of biomass are enhanced, not only the environment problems but also the renewable resources for fuel and industrial chemical compounds could be solved.

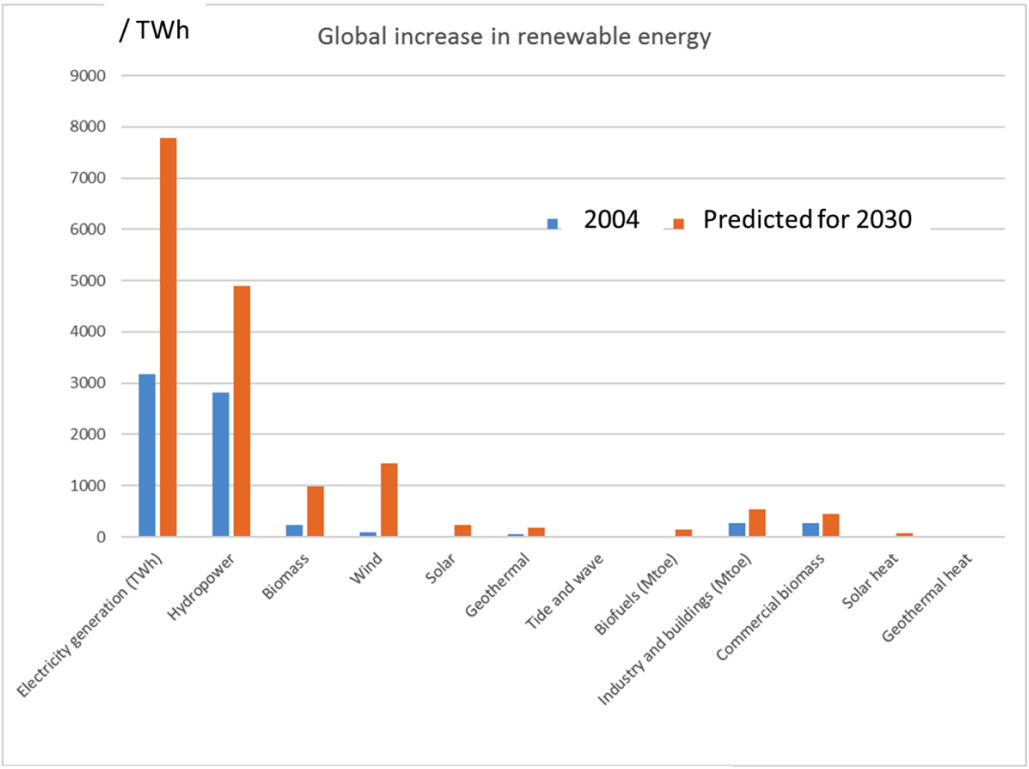

Figure 1-6 The predication of global increase in renewable energy.[14]

1.5 Biomass storage and application

Biomass is organic material derived from the waste plants, or agriculture-derived materials which should not be edible materials for food or feed usage. The estimated biomass production in the world is about 105 billion metric tons by carbon per year, and about half of them is in the ocean and the other half is on land.[15] Industrial biomass consists of a large number of plants and a variety of species. Plants can convert CO_2 into organic compounds for their growth or fruits. When it turned into biomass and was burned or decomposed by microorganism, the CO_2 will return into the environment recycle system. If biomass is applicated to take the place of fossil resources for fuel and industrial compounds, CO_2 emission from fossil resources will be cut efficiently and the global warming can be prevented successfully. Different from fossil resources, biomass contains less nitrogen and sulfur, and is biologically-produced materials made from hydrogen, carbon and oxygen. Especially, for the most recent decades (2003-2012) almost 90% of the total CO_2 emission (9.5 billion tons per year) has been resulted from fossil fuel combustion but only ca. 60% of the total can be recycled back to the earth. It was also reported that the application of biomass to replace fossil resources can save up to 38 billion tons of carbon.[16] Therefore, biomass fuel is more environmental friendly than fossil fuel and could be the most alternative fuel resource to replace fossil fuel. But the incompleted combustion of biomass

also resulted in some environmental problems such as PM2.5, PM10, NOx, etc., similarly to the fossil fuels. Biomass combusion for energy is of low efficiency in utilization and also causes serious air pollution. In many developing countries, people are still burning biomass to make fire. Thus, high technologies for the conversion of biomass is needed to produce the environmental fuels.

Biomass can also be converted into some industrial chemicals for our daily life, if the carbon of biomass is converted into industrial chemical compounds, the CO_2 cycle will take longer, which can also solve the global warming efficiently. Even in the early 19th century, the implementation of bio-based economy was proposed. However, at that time oil was always cheaper than other alternative resources-derived products. After the oil production peak, the increasing oil price drastically impacts the petroleum based materials in cost and also leaving some serious environment problems. European Union (EU) has approved laws to reduce the environmental-unfriendly materials and began to take great efforts on the application of eco-friendly resources. Therefore, alternative solutions would be found to decrease the current application of fossil resources and then to reduce the amount of CO_2 to normal.[17-19]

1.6 Biomass application technologies and the biomass-derived chemical compounds

Biomass is an eco-friendly renewable resource for energy and industrial compounds. Waste-based biomass, including animal waste, the waste from agriculture, forestry construction, sewage sludge etc. should be greatly potential as a resource.

As to the biomass conversion technologies, various products must be available, and they vary with the characteristics and types of biomass material. Conversion of biomass to biofuel can be achieved with some methods mainly classified into: thermal, chemical, and biochemical methods or the combination of them. As the targets, currently biomass is mainly used for energy. For example, the waste wood, sludge, industrial waste, etc. can be dried and then burned directly to make the steam for electric power generation. The direct combusion method provides over 90% of the energy worldwide generated from biomass. Biomass of different forms can also be used to produce power in small-scale distributed generation facilities for rural and industrial scale electrification. It is also a significant part of traditional uses for cooking and heating especially in developing countries.[20] As to the indirect combustion method, generally the biomass can also be thermally decomposed to crack into gas and then purificated as fuel gas such as methane and fuel oil for transports or electricity generation. Biochemical and chemical conversion technologies are significant methods in converting biomass into a variety of chemical products, such as alcohols and lactate purification. Then, they can be used as automotive fuel, and also industrial material as well. In addition, the combination of several feedstocks and conversion technologies is also available to produce energy and valuable chemical compounds from biomass, as shown in **Figure 1-7**.[21]

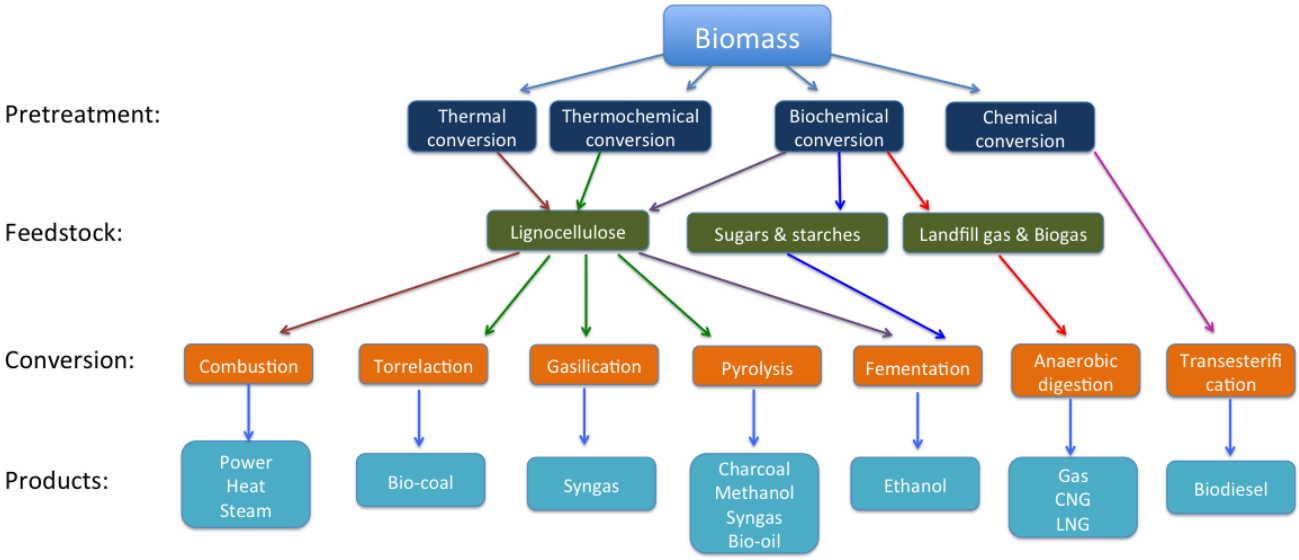

Figure 1-7 Conversion technologies of biomass into energy and chemical compounds.[21]

Currently, it is still a difficult issue on the conversion of biomass into valuable chemical compounds directly. Recent years, with developing biochemical and chemical technologies, fermentation has become one of the most popular methods in biomass conversion. Fermentation metabolically converts sugars such as glucose, fructose, and galactose to acids, gases, alcolhols ect. It occurs with yeasts or in oxygen-starved muscle cells. Fermentation is also used more broadly by modifying the DNA of the cells and then increasing the bulk growth of cells on a medium, to produce a target chemical product. At the present time, industrial chemistry has produced a large range of chemical compounds and almost totally relied on fossil resources. Since biomass is produced from water, the atmospheric CO_2, and sunlight via the biological photosynthesis system, biomass and biomass-derived materials should be one of the most promising alternatives to take the place of fossil resources, and it has been considered as the only sustainable source for fine chemicals without excrescent carbon emission. Especially, lignocellulosic biomass is appointed as an abundant and renewable carbon-compounds source, and it is a promising alternative to diminish the usage of crude oil. Lignocellulosic biomass can be obtained lower-costly than other agricultural feedstocks such as sugar cane, corn starch and soybeans. Lignocellulosic biomass almost includes cellulose, hemicellulose, lignin and also a few other components including minerals, phenolic compounds and acetyl groups (**Figure 1-8**). The structure of cellulose chain consists of the extensive intra- and intermolecular hydrogen bonding for the networks of its units. Since carbon forms more than half of the structure of cellulose, it is very promising to convert cellulose into valuable chemicals. Hemicellulose has a disordered structure consists of several heteropolymers including xyloglucan, glucuronoxylan, xylan, arabinoxylan, galactomannan, and glucomannan. They are 5- or 6-carbon units to form a complex network linking cellulose fibers with lignin. Lignin is the steric polymer of

phenylpropanoid units, functioning as the structure glue to strengthen and protect the plant cell. In general, lignocellulosic biomass is composed of lignin (10-25%), cellulose (35-50%), and hemicellulose (20-35%).[22]

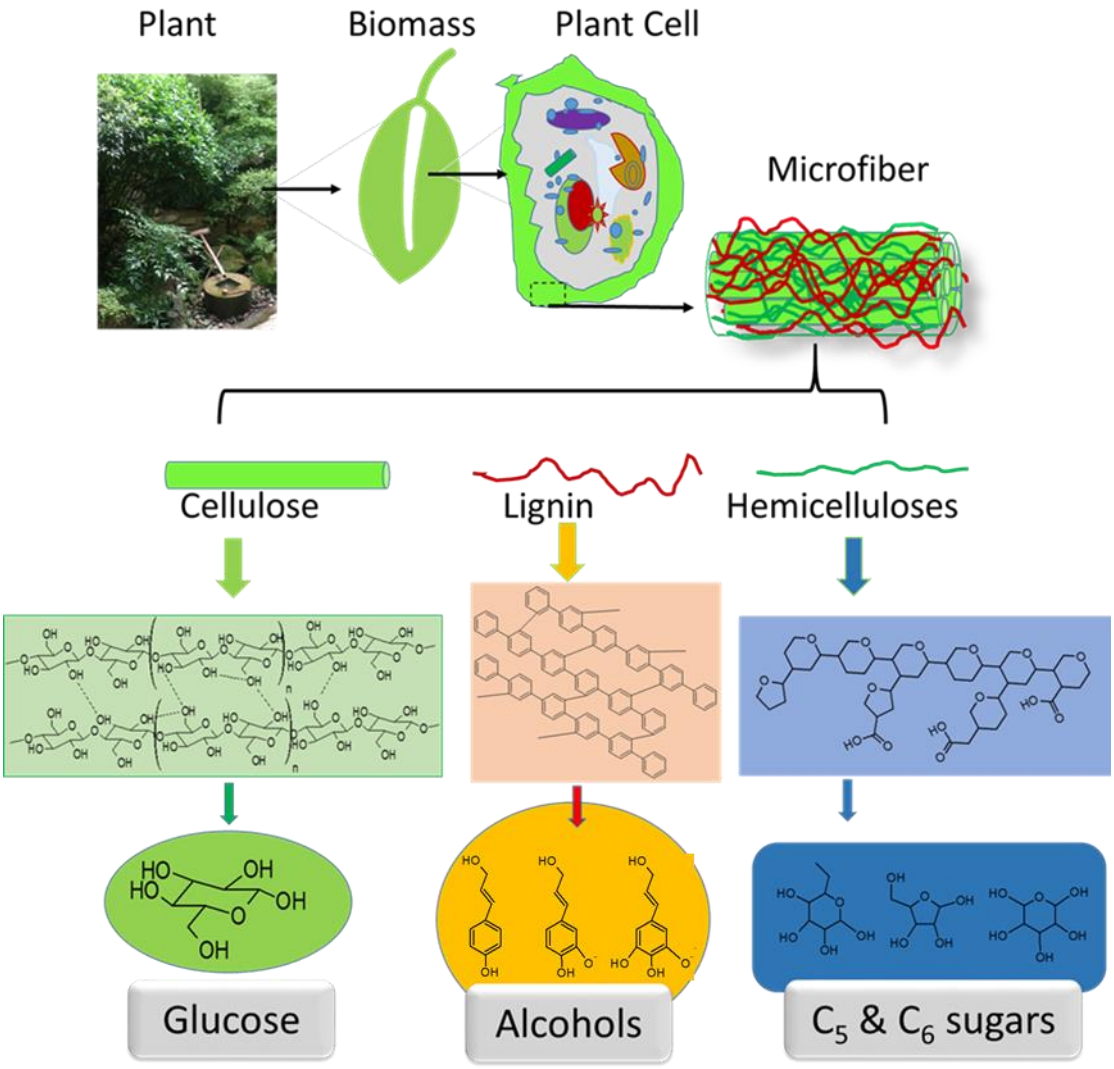

Figure 1-8 The basic structure of lignocellulosic biomass.[22]

Prior to other treatment, pretreatment effects the binding characteristics of lignocellulosic biomass, thus it is an essential step to chip the raw material into little size and then break down its physical structure for the next enzymatic or chemical treatment steps.[22-24] Pretreatment methods can be identified as mechanical, physicochemical, chemical, biological, biochemical technologies etc. or the combination of them.[23] In details, the pretreatment options are reported including fractionation, solubilizing, hydrolysis, irradiation, microwave, explosion, hot-water pretreatment, organosolve

processes, oxidation, ozonolysis etc.[25]

Since lignocellulosic biomass contains higher oxygen, lower carbon and hydrogen contents, and also prior to petroleum in compositional variety, much more chemicals can be obtained from lignocellulosic materials.[26] However, because of the low price of petroleum-derived products, currently only the production of bio-ethanol, bio-deasel i.e. fatty acid esters and bio-lactic acid is well established and commercially available [27], while most technologies of the biorefinery chemicals production are still at the research levels.

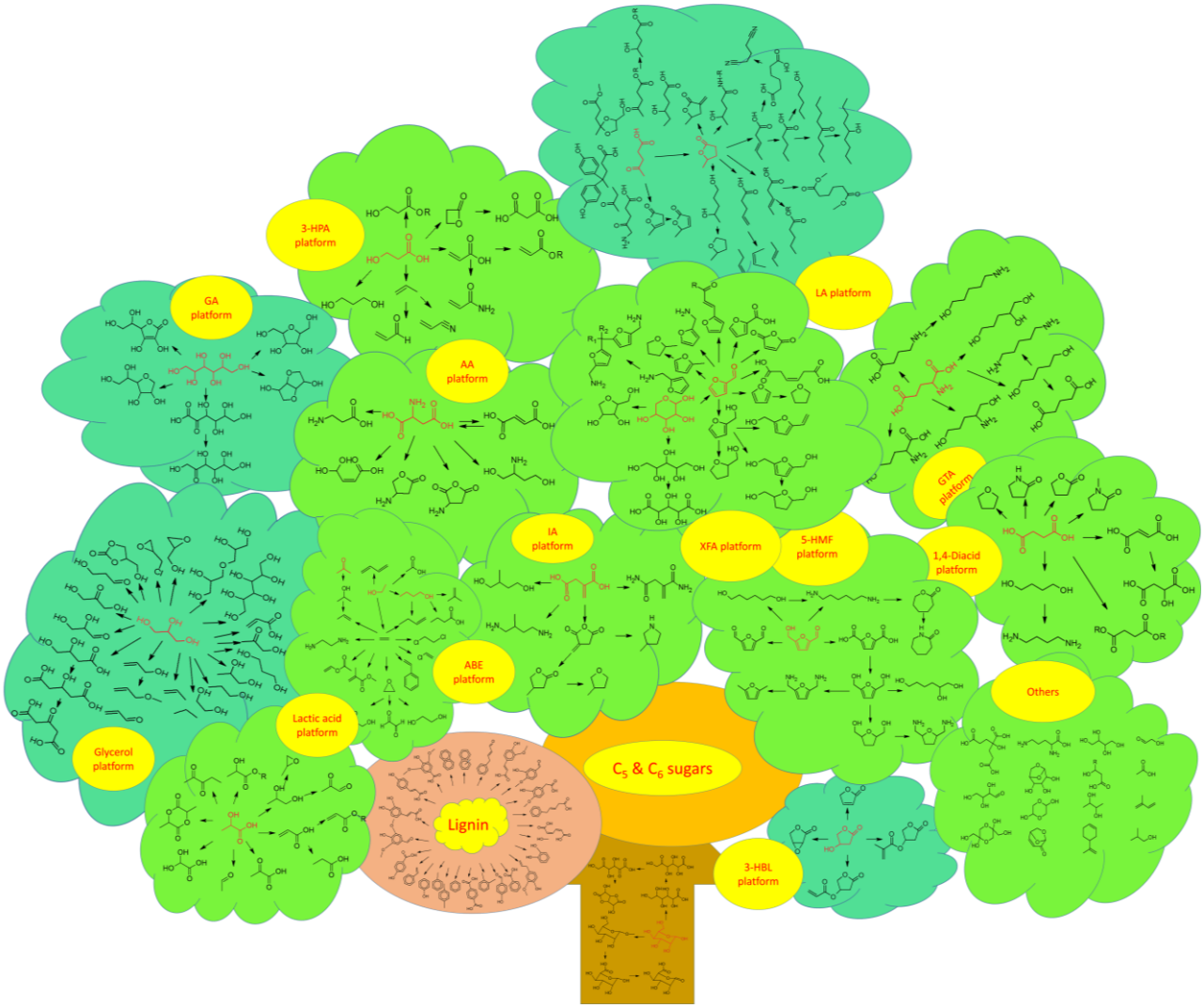

Figure 1-9 A part of the possible chemical compounds from biomass.[22, 28]

Depolymerization of hemicellulose via the concentrated HCl-driven hydrolysis produces glucose, the five membered sugars including arabinose and xylose, and the six membered sugars such as mannose, galactose and rhamnose, just as shown in **Figure 1-8**. **Figure 1-9** shows a part of the

disclosed routes for some fine chemicals derived from biomass.[22, 28] These C_5 and C_6 sugars can be converted into platform chemicals including 1,4-diacids, 3-hydroxy propionic acid (3-HPA), 5-hydroxymethyl furfural (5-HMF), 2,5-furan dicarboxylic acid (2,5-FDCA), glutamic acid (GTA), glucaric acid (GCA), aspartic acid (AA), levulinic acid (LA), itaconic acid (IA), 3-hydroxybutyrolactone (3-HBL), sorbitol, glycerol, etc. Further more, many fine chemicals can be obtained from these platform chemicals with chemical and biochemical technologies. For example, ethanol currently produced with super production volume is considered as one of the important platform chemicals, since it can be converted into a large number of industrial chemicals. In addition, acetone-butanol-ethanol (ABE) fermentation process is now widely researched,[29] because it can be further converted into the chemicals such as ethylene, propene, butadiene, ethylene glycol, etc., the bulk chemicals for industry. Lactic acid is also believed as the building block chemical owing to its further products such as acrylic acid, propionic acid, acetaldehyde, dilactide and 2,3-pentanedione.[30]

1.7 The proposal of this study

In order to realize the low-carbon society and to diminish the use of fossil sources, in my present study, I focused on the catalytical conversion of biomass-derived intermediates into industrial bulk chemical compounds. Since 2,3-butanediol (2,3-BDO) synthesis from cellulose, glucose, glycerol, sucrose, xylose, etc. by fermentation technologies with various bacteria has been greatly developed,[31-33] 2,3-BDO shows the wide future prospect for widely bio-based chemicals. In my work, I investigate the conversion of biomass-derived 2,3-BDO with catalytic technologies and aim to produce some valuable chemical compounds.

The fermentation process from cellulose to 2,3-BDO was imaged as **Scheme 1-1**. At high dissolved-oxygen and glucose-rich conditions, the bacteria such as Klebsiella can convert pyruvate into acetaldehyde or α-acetolactate firstly by acetolactate synthase. In anoxic state, α-acetolactate decarboxylase catalyzes the transformation of α-acetolactate and acetaldehyde into acetoin, while decarboxylation of α-acetolactate produces diacetyl spontaneously in the presence of oxygen. Finally, 2,3-BDO is formed from the reduction of acetoin and diacetyl by butanediol dehydrogenase.[34-36]

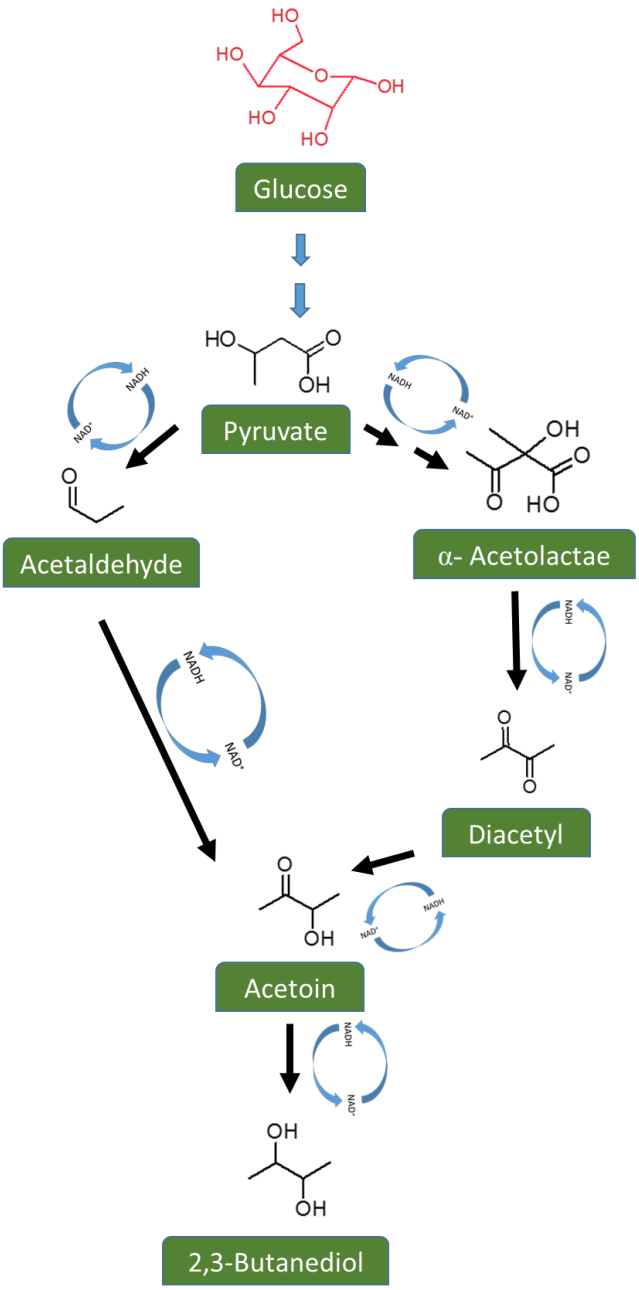

Scheme 1-1 The fermentation process for 2,3-BDO formation from glucose.

In this study, as shown in **Scheme 1-2**, I investigated the transformation of biomass-derived 2,3-BDO into 1,3-butadiene (BD), which is currently derived from petroleum and used as the raw material for rubber. In addition, due to 3-buten-2-ol (3B2OL), the intermediate of the dehydration from 2,3-BDO to BD, is also used as the intermediate for cancer drugs, here I also investigated catalyze the dehydration of 2,3-BDO into 3B2OL firstly and then further dehydate it into 1,3-BDO. In addition, in order to find out and prepare the most selective catalyst, my work also concentrated on investigating the best reaction conditions for industrial production. Besides, in order to decrease the reaction

temperature, I designed a two-layer catalyst-bed process, in which the upper layer catalyst was used for the reaction from 2,3-BDO to 3B2OL and the lower catalyst was for the further dehydration of 3B2OL into BD.

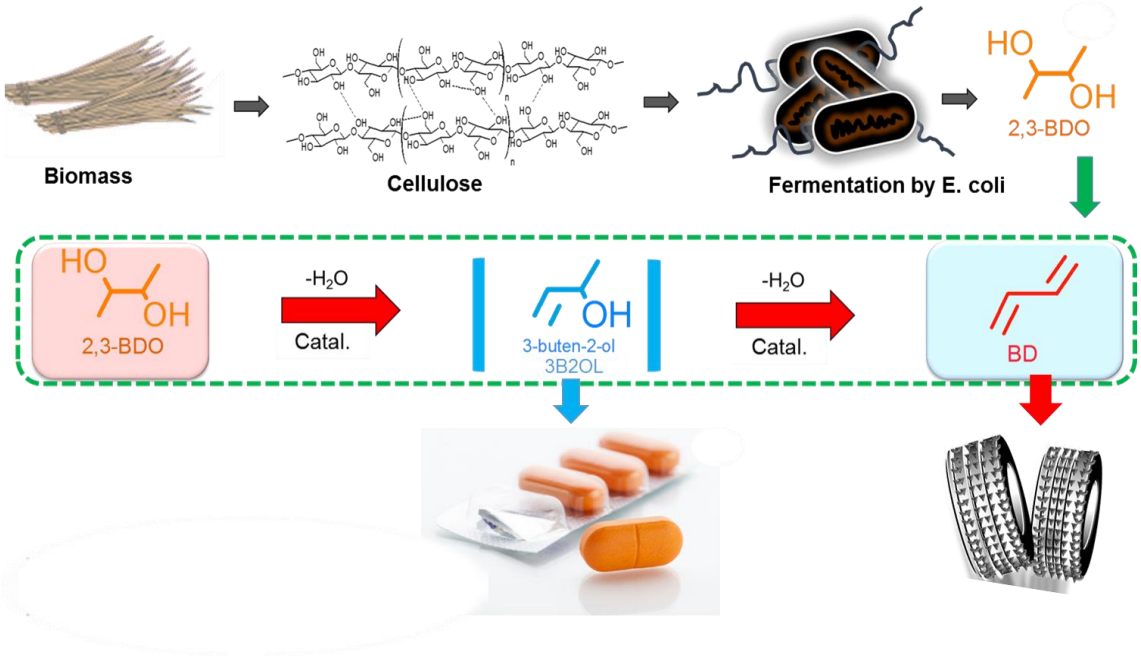

Scheme 1-2 Catalytic production of BD and 3B2OL from biomass-derived 2,3-BDO proposed in this study.

1.8 The current production and synthesis methods of BD

BD is one of important industrial compounds, as the raw material of a wide amount of synthetic rubbers such as styrene-butadiene rubbers, polybutadiene rubbers, acrylonitrile-butadiene-styrene polymers, nitrile rubbers, adiponitrile, butyl rubbers, and etc.[37] In 2012, the global demand for BD was approximately 10 million metric tons and is still growing with a growth of 1-2% per year.[38] Higher than 95% of the total BD production was supplied as a by-product of ethylene plant through the naphtha steam cracking at temperatures around 800°C.

In the distillation process of petroleum, as showed in **Figure 1-10**, the crude oil refined by temperature from 30 to 180°C including the alkanes from C_5H_{12} ~ C_8H_{18} are used as gasoline, the ones refined from 170 ~ 350°C and also from C_9H_{20} to $C_{16}H_{34}$ can be divided into diesel fuel, jet fuel and kerosene. The large ones with higher than 16 carbon atoms are used as fuel oil or lubricating oil. The last group with approximately 25 carbon atoms (>350°C), is paraffin wax. Besides, asphalt has 35 or more, are usually further cracked and converted into more valuable chemical products. Contrastly, the shortest ones with C_4 or smaller compounds, are gaseos at room temperature. They are used as oil gases.

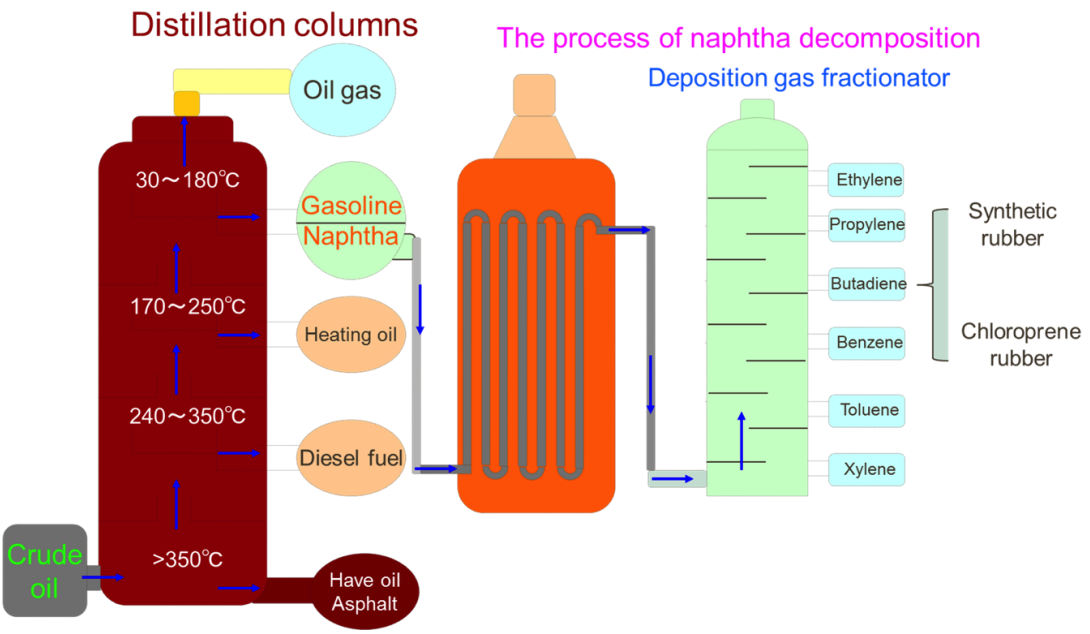

Figure 1-10 The processes of crude oi distillation and naphtha decomposition.

Most part of crude oil are mainly used as fuel. The decomposition of heavier oil into smaller molecular proceeds only under high temperatures and pressures. Only a small part of petroleum is used as the raw material for bulk industry chemical compounds by the process of naphtha decomposition. Naphtha is a mixture of alkane, cycloalkanes, and aromatic hydrocarbons depending on the oil from which the naphtha was derived. The boiling range of a full range naphtha changes from 30 to 240°C, with the compounds commonly including 4~12 carbon atoms. The steam cracking of naphtha yields various products, ranging from hydrogen to heavy liquid fractions. Yield of ethylene (20~30%) as well as propylene and some other by-products such as BD, C_5 and the heavier are for industry usage. However, here BD yield is only up to 4%, as shown in **Table 1-1**.[39-42]

Furthermore, shale gas has been recently utilized as a new resource for ethylene production. It is expected that the shale gas can meet a great part of the global demand for natural gas for the future usage.[43] In the petrochemical industries in Japan, three of 15 ethylene production plants have been shut down in the last 3 years at June, 2016. Herein, there is a prospect that the production of naphtha-based ethylene would greatly decrease together with its by-product, BD. Comparing with the naphtha cracking, the cracking of ethane, which is contained 20% in shale gas, illustrates that the ethylene can be yielded up to 80%, but the by-products such as BD (1%) and $>C_4$ molecules are reduced greatly.[42, 43] In addition, the cost of BD has fluctuated violently and resulted in its price increasing greatly recent years. It indicates that BD supply is not stable in the long run for the major those BD users.[43,44] Thereafter, the synthetic process of BD without depending on petroleum should be developed urgently

to meet the demand for synthetic rubbers indurstry.

Recently, BD production has been reviewed by several groups.[38, 46, 47] Makshina et al. have reviewed from old to new chemistry of the production of BD.[38] They focused on the BD production from ethanol and C_4 alcohols. In addition, BD production from coal, naphtha, natural gas, shale oil and gas is summarized in the previous review.[38] Besides, there are many possibilities of the production of BD from different feedstocks, as described in **Scheme 1-3**. Coal, biomass, shale oil and gas can be an alternative to petroleum.

Table 1-1 The main products yield from the cracking of fossil resources.[42]

Product	Feedstocks				
yield/%	Ethane	Propane	Butane	Naphtha	Gas Oil
Ethylene	80	40	36	23	18
Propylene	3	18	20	13	14
Butylene	2	2	5	15	6
Butadiene	1	1	3	4	4
Fuel Gas	13	38	31	26	18
Gasoline	1	1	5	18	18
Gas Oil	0	0	0	1	12
Pitch	0	0	0	0	10

1.8.1 Researches on Coal- and shale gas-derived BD

In the past years, Korosi et al. tried some efforts to transfer the feedstock from petroleum to coal in order to obtain olefins from some potential resources. The group experimented the hydrogenated coal liquid (HCL), light gas oil petroleum distillate (LGO) and the decahydronaphthalene (DHN) processes. As the results, BD yield was as 4.68%, 4.82% and 4.65% in weight percent respectively, at extremely high reaction temperatures and pressures[45]. Comparing with the only 4% yield of BD from the naphtha steam cracking process, 14% yield of BD can be also industrially available from the ethane feedstock[38]. Some other feedstock such as propane and butane can also be the choices. But these processes are not practicable now for its several conditions such as high reaction temperatures and pressures.

Kyriakou et al. also reported that in the acetylene trimerism to benzene process, and Cu (111) face yielded BD in their work[46]. Besides, Yang et al. reported their mechanistic study on BD formation from acetylene hydrogenation catalyzed by Pd-based catalysts with the method of density functional calculation (DFT), and found that the pathway to BD from acetylene should be suitable over the active sites on the flat Pd (111) surface.[47] In other words, the formation of BD from shale gas-derived acetylene should be also an alternative process in the future.

$C_2H_2+C_2H_2+2H \rightarrow C_4H_4+2H \rightarrow C_4H_5+H \rightarrow C_4H_6$

Scheme 1-4 Synthesis of BD from acetylene[47].

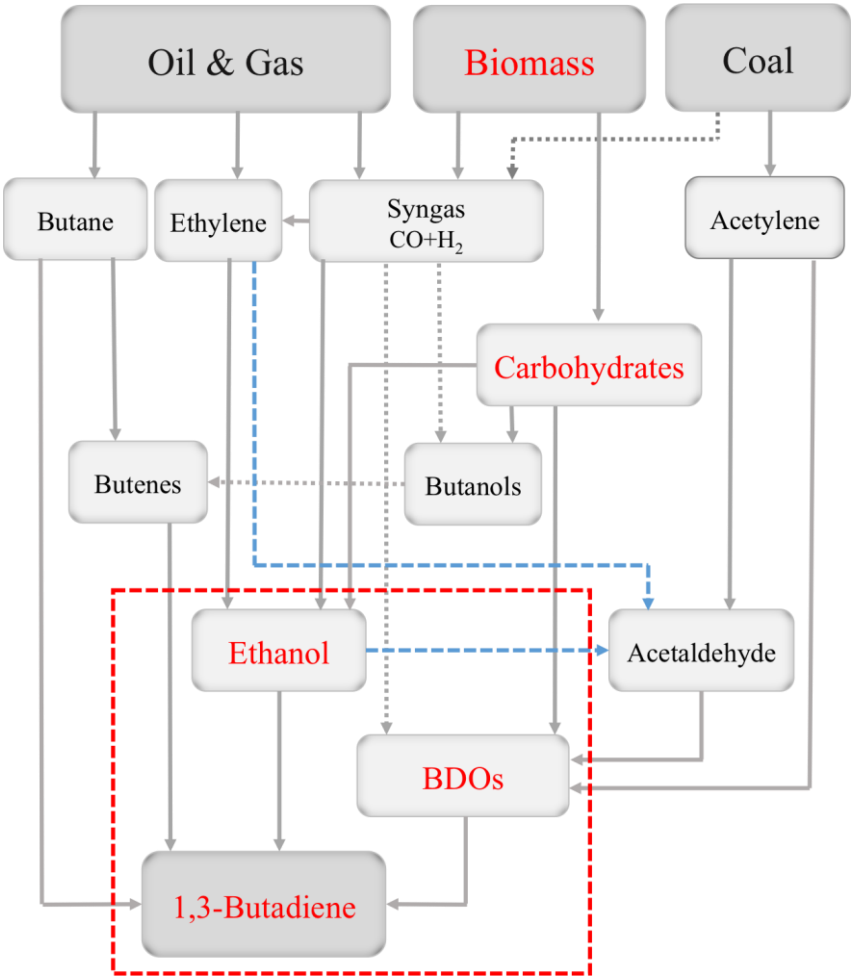

Scheme 1-3 Possible 1,3-butadiene (BD) synthesis routes from various feedstocks, which is proposed by Makshina et al.[38] The area shown in the red broken line indicates the present focused interest. I added the blue broken arrows to acetaldehyde because the routes are readily available.[37]

1.8.2 Ethanol-derived BD

Since ethanol can be used for the production of a lot of chemical compounds it is also applicated as a chemical feedstock. Plants for the ethanol production competing especially in USA and Brazil.[46, 48] Studies on the synthesis of BD from ethanol can be dated back to early 1900's, and details are introduced in the recent review.[38] Among the pioneering research, Lebedev proposed a one-step dehydration process to convert ethanol into BD (Lebedev process) over ZnO-Al_2O_3 catalyst but with very low yield of BD.[49] In 1946, it is also disclosed that a 70% of BD yielded from ethanol at 350°C

and an atmospheric pressure.[50] Ever after, the process was improved and examined a lot over ZnO, Al_2O_3, MgO, ZrO_2 and SiO_2 and even their mixtures.[51] Even after the latest review[38] which introduced many research works,[50-70] a lot of research papers have been published on the BD formation from ethanol in the last 3 years.[71-92]

Table 1-2 summaries major active catalysts reported on the synthesis of BD from ethanol. This indicates that MgO-SiO_2 catalysts as well as ZnO-SiO_2 and ZnO-Al_2O_3 show the specific catalytic abilities to convert ethanol into BD. Among them, CuO-ZrO_2-ZnO-SiO_2 prepared by Matthew et al..[65] and the Al_2O_3-ZnO catalysts prepared by Bhattacharyya and Avasthi[53] showed the very high BD formation rate for higher than 10 mmol/h per gram of catalyst, whereas the conversion and BD selectivity were much lower than those of Ohnishi's work.[56] This could be caused by different space velocity (WHSV): Ohnishi adopted slow WHSV of only 0.15 h^{-1} while the WHSV values are 2.04[53] and 4.73 h^{-1}.[65] Enough ethanol should be fed to achieve the high BD productivity over efficient catalysts. In the research works for a century, the highest BD formation rate of 19 mmol/g_{cat} h, i.e. 1.0 g_{BD}/g_{cat} h, has been reported.[77]

Furthermore, in order to elucidate the BD formation mechanism from ethanol, several possible BD formation proposals are debated among some research groups.[49,50,54,57,59,60,63,64,72,76,82,90] Some of them have believed that the reaction starts from the dehydrogenation of ethanol to the primary product acetaldehyde which needs a good balance of basic and acidic propriety[72,73,82,85,86] and the active defective MgO surfaces (**Scheme 1-5**).[87] Then, the second step consists of the aldol condensation from acetaldehyde to acetaldol, which is dehydrated to 2-butenal. Then, 2-butenal is hydrogenated to 2B1OL via Meerwein-Ponndorf-Verley (MPV) reduction with ethanol as a hydrogen donor followed by the final dehydration of 2B1OL to BD.

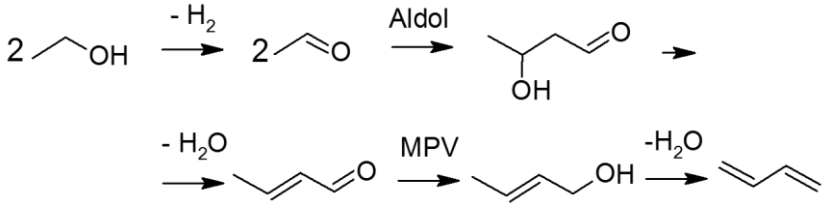

Scheme 1-5 Production of BD from ethanol.[45,55,63,70,71,87]

Table 1-2 Synthesis of BD from ethanol over various active catalysts.

Catalyst	Reaction temp.(°C)	Conversion (mol%)	BD selec. (mol%)	BD formation rate (mmol/g_{cat} h)	Ref.
$Cr_2O_3MgOSiO_2$	400	68	56	1.5	51
$Sb_2O_3Al_2O_3$	425	-	14 yield	1.3	51
Al_2O_3ZnO	425	100	72.8	16.1	53
$MgOSiO_2$	380	46	62	1.3	55
$Na_2OMgOSiO_2$	350	100	87.0	1.4	56
$MgOSiO_2$	400	53	27.5	3.6	90
ZnO-Sepiolite	260	0.1	63.5	0.1	58
$NiOMgOSiO_2$	280	59	90	-	61
$MgOAl_2O_3$	402	15	20	0.1	64
$CuOZrO_2ZnOSiO_2$	375	39	50	10.0	65
$AgMgOSiO_2$	350	97.7	63	1.3	66
$ZnOAl_2O_3$	395	44.5	55	9.2	68
$MgOSiO_2$-ZrZn	325	30	68.7	0.7	69
$ZnOMgOSiO_2$	375	62.6	64.5	2.0	75
$ZrO_2ZnOMgOSiO_2$	375	>80	>60	>4.6	76
$ZnOMgOSiO_2$	400	43.2	49.1	19.0	77
AgZr-BEA(100)	320	47.9	55.6	0.9	78, 81
CrBaAl-MCM-41	450	80	28	8.3	79
$CuOHfO_2ZnO$	360	99	72	1.6	84
Na-$Zn_1Zr_{10}O_z$-H	350	54.4	26	9.0	89
$Ta_2O_3SiO_2$	400	49 [a]	69	2.5	51
$MgOSiO_2$	350	48 [a]	68	0.1	57
$CuZrO_2ZnOSiO_2$	375	44.6 [a]	67.4	15.5	65
$AgZrO_2SiO_2$	320	88 [a]	73.9	0.3	74
$Ta_2O_3SiO_2$	350	46.9 [a]	76.8	2.9	67, 83
ZrO_2SiO_2	320	45.4 [a]	69.7	5.3	88
MgO/K-BEA	300	35 [a]	72	0.6	91
Ta-BEA zeolite	325	30.7 [a]	90.3	2.4	92

[a] Acetaldehyde was co-fed with ethanol.

Gao et al. have confirmed the reaction route over MgO/SiO_2 with IR spectroscopy, and they observed the increment and reduction of intensity in absorption bands of acetaldehyde, 2-butenal temporally and the following growth of C=C bonds for BD.[71] All the mechanisms, however, are

speculated on the basis of the products detected during the reaction. But the fact that acetaldehyde is always one of the primary products facilitates the examination of a two-step pathway with the mixture of acetaldehyde and ethanol (Ostromisslensky process).[52] The first step in **Scheme 1-5** can be eliminated, and the following steps consists of the aldol condensation from acetaldehyde to acetaldol. The Ostromisslensky process performed with better BD selectivity than the Lebedev process using pure ethanol.[51,57,65,67,74,83,88,91,92] They have considered that the condensation step of acetaldehyde should be a rate-limiting reaction.[52,57] It is suggested that 2B1OL, 2-butenal, 1,3-BDO and acetaldol should be the possible intermediates related to the formation of BD.[63,64] In addition, acetaldehyde can be used as a reactant instead of ethanol. Recently, Cespi et al. have proposed a multi-criteria approach based on a online cycle analysis in the synthesis of BD from ethanol: the direct conversion into BD would be more suitable than the two-step process in U.S.[93]

There still needs a lot of work to do even with the two-step process for the BD production with a yield higher than 90 %. In the overall catalysis (**Table 1-2**), catalytic functions can be summarized as follows: basic species such as MgO and ZnO catalyze the aldol coupling, and metallic species such as Ag and CuO assist the dehydrogenation step. Weak acidic sites such as surface hydroxyls of SiO_2 and Al_2O_3 work on catalyzing the dehydration step, while the amount and strength have to be limited to prohibit the dehydration of ethanol to ethylene. The active sites for the MPV reduction is resulted from Lewis acid sites, and a ZrO_2 additive enhances the ability of aldol condensation and MPV hydrogen transfer. Thus, no simple metal oxide catalyst could act for all those complicated reactions,[74] as shown in **Scheme 1-5**. The technology of BD synthesis via multifunctional catalysts seems very difficult and still low BD yield was obtained in several patents being conducted in several countries such as U.S. and Brazil. The processes from C_2 hydrocarbons to BD have been studied for more than 100 years, but an effective process is still unestablished. Here, I am seeking some other possibilities for the production of BD. The biomass-derived C_4 alcohols such as 1-butanol, 2-butanol, 1,2-, 1,3-, 1,4-, and 2,3-BDOs (1,2-butanediol, 1,3-butanediol, 1,4-butanediol and 2,3-butanediol,) etc. should be considered as an alternative.

In this study, I highlighted recent advances in the BD production, especially from C_4 alcohols. I introduced not only how to convert BDOs (butanediols) into BD directly, but also how to dehydrate BDOs into UOLs (unsaturated alcohols) in connection with their further dehydration into BD.

1.8.3 Biomass-derived C_4 alcohols

Catalytic conversion of some C_4 alcohols, such as 1-butanol, 2-butanol, 1,3-, 2,3-, 1,4- and 1,2-BDOs, demonstrated some possible alternative paths in the production of BD. These alcohols have C_4 skeleton, which do not need C-C bond formation such as dimerization of ethanol, and could be the most suitable raw materials for the synthesis of BD. They are all produced possibly from biomass via microbial processes (**Scheme 1-6**), as summarized in **Table 1-3**.[94-109]

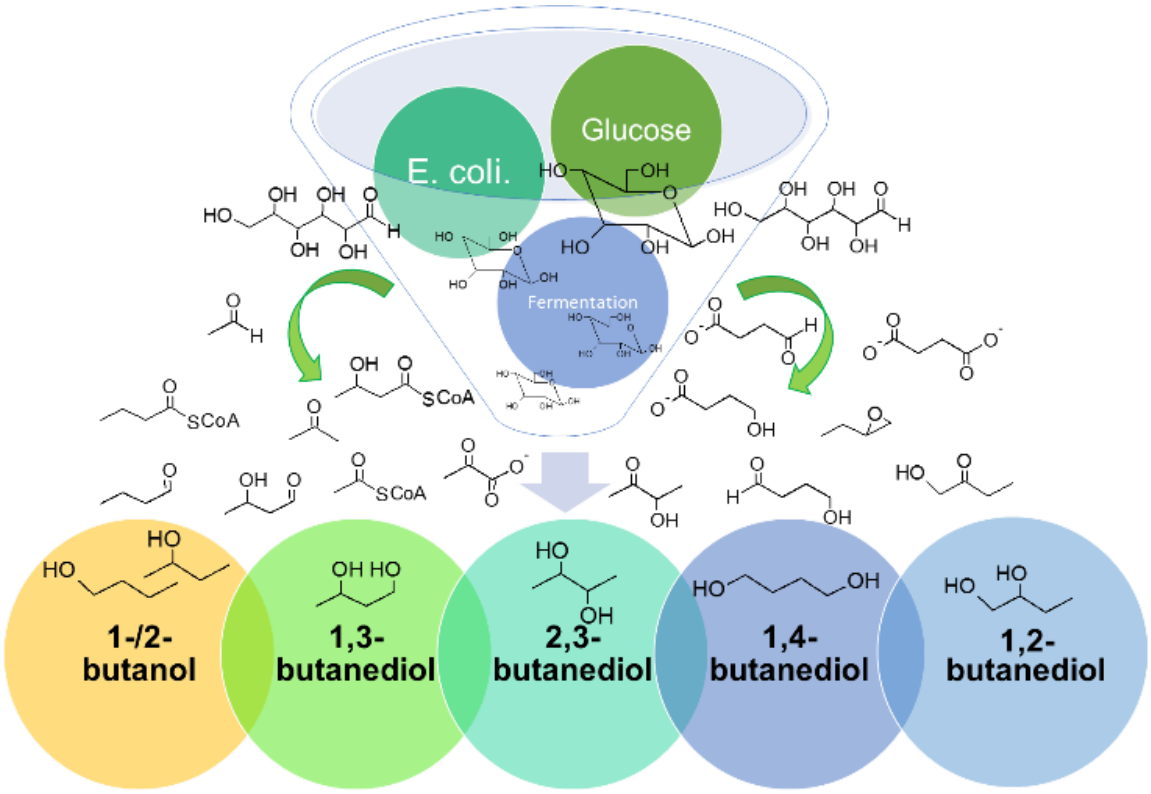

Scheme 1-6 Microbial synthesis of C_4 alcohols from glucose using bacteria.[94-109]

Butanols such as 1-/2-butanols can be obtained from biomass readily just as ethanol production in a large scale. 1-Butanol production from carbohydrates has been carried out using Clostridium by the famous acetone-butanol-ethanol (ABE) fermentation process. In recent years Tsuchida et al.[63] and several other groups[62,80,110-113] also disclosed their efforts on the catalytic production of 1-butanol from ethanol over hydroxyapatite or Mg-Al oxide catalysts: the high butanol productivity even reached to 1.78 mmol /$cm^3_{cat.}$ h over hydroxyapatite,[63] and 4 mmol /$g_{cat.}$ h over Mg-Al mixed oxides (Mg:Al = 3) in a work of Carvalho et al..[111] Butanols are considered as the next-generation gasoline substitute because of its higher energy density and lower vapor pressure when compared with ethanol.[114] Among all the C_4 alcohols, 1-/2-butanol would be the cheapest one. Cobalt Technologies (a company), which has developed a fermentation platform for bio-process 1-butanol, claimed that 1-butanol became natural fit to pursue BD as a product platform.[44] Thus, there is a great prospect to produce BD from butanols.[43]

Table 1-3 Microbial C_4 alcohols production using bacteria species.

Substrate	Alcoholic product	Strains	Yield of alcohol (%)	Ref.
Glucose	1-Butanol	C. B. BA101	76	94
Sugar and starch	1-Butanol	C. B. BA101	0.30 [a]	95
Glycerol	1-Butanol	C. P. ATCC 6013	0.36 [a]	96
MEK	2-Butanol	Gordonia	66	97
4H2B	(R)-1,3-BDO	K. L. IFO 1267	99	98
4H2B	(R)-1,3-BDO	E. coli JM 109	95	98
4H2B	(S)-1,3-BDO	A. A. IFO 10124	68	98
4H2B	(R)-1,3-BDO	E. coli (LSADH)	99	99
Glucose	(meso-/L)-2,3-BDO	Klebsiella pneumonia	0.43 [a]	100
Corncob	(meso-/L)-2,3-BDO	Klebsiella oxytoca	0.50 [a]	101
Glucose	(meso-/L)-2,3-BDO	Klebsiella oxytoca	0.50 [a]	102
Sucrose	(meso-)-2,3-BDO	Serratia marcescens	0.47 [a]	103
Artichoke tuber	(D-)-2,3-BDO	Paenibacillus polymyxa	0.50 [a]	104
Glucose	2,3-BDO	Geobacillus XT15	0.22 [a]	105
1H2B	(R)-1,2-BDO	GDH	70	106
1H2B	(S-/R-)-1,2-BDO	C.p.IFO 0708	62	107
Glucose	1,4-BDO	E. coli	0.6 mM/20g l^{-1} [b]	108
L-homoserine	1,4-BDO	E. coli.	90 [c]	109

[a] Alcohol yield was calculated as diol (g) / substrate (g).

[b] Alcohol yield was calculated as diol (mM) / substrate (g l^{-1}).

[c] Alcohol yield was calculated as diol (mol) / glucose (mol).

4H2B, 4-hydroxy-2-butanone; 1H2B, 1-hydroxy-2-butanone.

C.B.BA101, Clostridium beijerinckii BA101; *C. P. ATCC 6013*, Candida parapsilosis ATCC 6013; *K. L. IFO 1267*, Kluyveromyces lactis IFO 1267; *E. coli JM 109*, Escherichia coli JM 109 modified with CpSADH (pKK-CpA1); *E. coli (LSADH)*, Escherichia coli JM 109 modified with LSADH; *GDH*, glycerol dehydrogenase from Enterobacter aerogenes or Cellulomonas sp.); *C.p.IFO 0708*, C. parapsilosis IFO 0708.

1,3-BDO is also a notable chemical for industrial usages. Approaches to produce 1,3-BDO are always performed via bio-catalytic hydrogenation of 4-hydroxy-2-butanone (4H2B). 4H2B can be prepared from acetone and formaldehyde by the improvement of Hays's method.[115] Dumesic et al. also showed that 4H2B is available from levulinic acid.[116] Besides, the production of 1,3-BDO from 4H2B is also available without the bio-catalytic process. Murakami et al. reported that a modified Raney Ni catalyst showed the best enantio-differentiating hydrogenation activities for the formation

of 1,3-BDO from 4H2B with an optical yield of 70.2%.[117] Schurig et al. also showed the possibilities of the production of 1,2-BDO and 1,3-BDO from ethyl lactate, ethyl 3-hydroxybutanoate, threonine and allothreonine by synthetic processes.[118]

Currently, 1,4-BDO is produced from the fossil-based feedstocks such as acetylene and BD, the present target product, and it is manufactured over 2.5 million tons annually for valuable polymers.[108] According to the report of Yim et al., they engineered the Escherichia coli host with proper genes to enhance its anaerobic operation for the oxidative tricarboxylic acid cycle, and then generated reduction ability to drive the organism synthesized BDO from glucose, xylose, sucrose and some other biomass-derived sugar streams (**Scheme 1-6**).[108]

Recently, microbial production of 2,3-BDO is remarkably increasing because it has a large number of industrial applications (also as described in the part of 1.7). Microbial production of 2,3-BDO has more than 100 years' history.[105] The bacterium employed in those early studies is Klebsiella pneumonia. Then, 2,3-BDO accumulation in cultures of Paenibacillus polymyxa (the modified Bacillus polymyxa) is initially observed. World war II intensed the research efforts on 2,3-BDO fermentation process, and culminated in the technologies for both manufacture and conversion to BD.[119] Recently, microbial production of 2,3-BDO has attracted the worldwide attention for its promising low carbon economy future. High yield and purity of 2,3-BDO even can be also optically obtained from glucose (**Scheme 1-6**).[103-105] Both Genomatica and LanzaTech have announced their plans for bio-BD production based on their successes in biochemical process for fermentation to 2,3-BDO in 2013.[44] Thus, the BD production from 2,3-BDO would be discussed deeply in this study.

Even though rare papers about the synthesis of 1,2-BDO are reported, 1,2-BDO could still be prepared by reduction of 1-hydroxyl-2-butanone (1H2B) enzymatically. Witesides et al. succeeded in the reduction of 1H2B to 1,2-BDO by utilizing a commercially available glycerol dehydrogenase.[106]

1.8.3.1 Dehydration of 1,3-BDO into BD

Dehydration of BDOs into BD seems another perfect process and there have been several papers demonstrating the great efforts throughout the entire century. Wellman reported that 1,3-BDO was contacted with a complex aluminum phosphate catalyst at around 285°C. The gaseous products such as BD were collected and the liquid products containing 3B1OL were separated and then recycled into the 1,3-BDO raw material. In such a process, BD conversion was improved up to 90%.[120] 1,3-BDO was also reported as an intermediate in the above-mentioned BD synthesis process using ethanol as the starting substrate.[52] Over the solid acid metal oxides such as SiO_2-Al_2O_3, Al_2O_3, and TiO_2, a wide variety of products from C_1 to C_5 compounds were formed (**Scheme 1-7**).[121] The dissociation of 1,3-BDO readily occurred: 1,3-BDO was firstly dehydrogenated into 3-hydroxybutanal and 4H2B. The former could be decomposed into two molecules of acetaldehyde via retro-aldol addition and then reduced to ethanol while the latter could be decomposed into formaldehyde and acetone. Coincidently

from the composition of the by-products, C_3 oxygenates and methanol are produced as a constant molar ratio of 1:1.

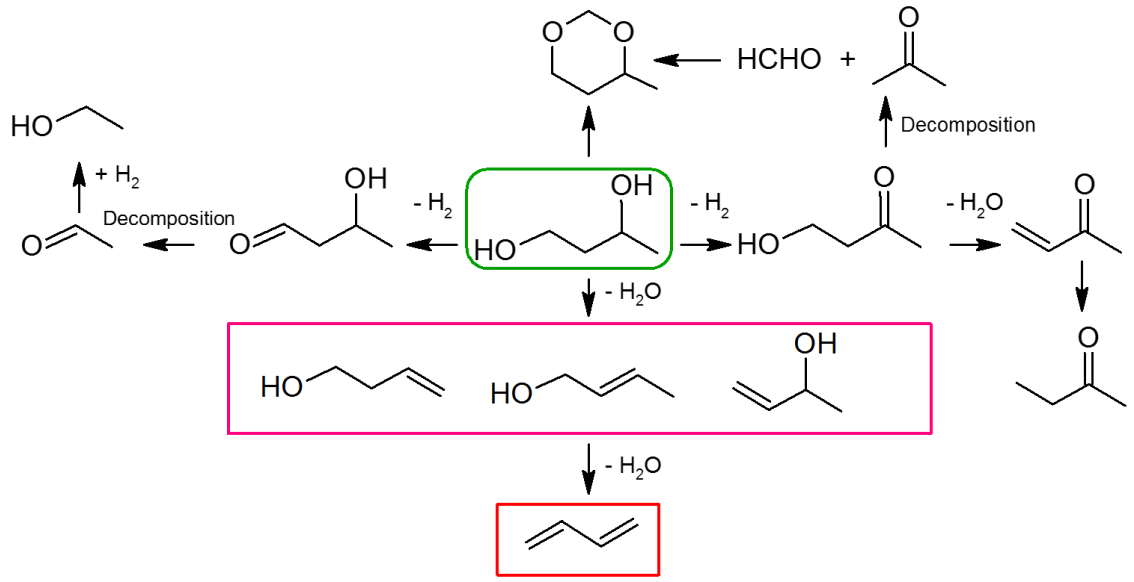

Scheme 1-7 Main products from 1,3-BDO.[121]

1.8.3.2 Dehydration of 1,2-BDO into BD

Researches on the dehydration of 1,2-BDO for the purpose of BD production are still rare. As Vogel reported that via the dehydration of 1,2-BDO products such as MEK (2-butanone), butanal, 2B1OL (2-buten-1-ol), 3B2OL (3-buten-2-ol), 3B1OL (3-buten-1-ol), and BD are available.[122] I also conducted the reaction (**Table 1-4**[123] and **Scheme 1-8**). The main products are in good accordance with Vogel's conclusion except that I could detect neither 3B2OL nor 3B1OL, whereas many unknown by-products are detected. Over the same catalysts such as Yb_2O_3, 1,2-BDO with vicinal hydroxyl groups is dehydrogenated into 1-hydroxyl-2-butanone (**Table 1-4**) in a similar way to 2,3-BDO, which is dehydrogenated to 3-hydroxyl-2-butanone (acetoin) in my present study. On the other hand, 2,3-BDO can be readily converted to MEK over acid-catalysts while Vogel et al. also disclosed that the conversion of 1,2-BDO into 1-butanal and MEK is also very easy.[122] The most active catalysts ZrO_2, CaO/ZrO_2, and Sc_2O_3 tested in my present work for the dehydration of 2,3-BDO into 3B2OL and BD were also tested here, but the highest total selectivity to the UOLs from 1,2-BDO was only 17% over ZrO_2. Most of the conversions summarized in **Table 1-4** are very low. This is a significant difference in the reactivity between 1,2-BDO and 2,3-BDO over these catalysts. Thus, further work should be conducted to find out a special catalyst for the 1,2-BDO dehydration to BD and 2B1OL.

Table 1-4 Dehydration of 1,2-BDO catalyzed by several catalysts.[123]

Catalyst	Reaction temp. (°C)	Conv. (mol%)	Selectivity (mol%)					
			2B1OL	BA	MEK	1H2BO	BOLs	Others
Al_2O_3[a]	285	88	11	4	8	6	16	55
ZrO_2[a,b]	300	6	17	2	2	44	15	20
TiO_2[a,c]	325	97	3	4	10	4	7	72
CaO/ZrO_2[b]	325	8	7	3	2	31	14	43
Sc_2O_3[d]	325	20	4	4	2	32	21	37
CeO_2[d]	395	22	1	1	4	22	8	64
Y_2O_3[d]	395	40	1	2	1	9	9	78
Yb_2O_3[d]	395	30	0	1	1	25	5	68

Reaction conditions: carrier gas, H_2, 80 cm^3 min^{-1}; catalyst weight, 1.0 g; average conversion and selectivity in the initial 5 h.

2B1OL, cis-/trans-2-buten-1-ol; BA, butanal; MEK, 2-butanone; 1H2BO, 1-hydroxyl-2-butanone; BOLs, 2-butanol and 1-butanol.

[a] The sample is supplied by the Catalysis Society of Japan.

[b] Monoclinic ZrO_2 calcined at 800°C.

[c] Anatase TiO_2.

[d] The sample calcined at 800°C.

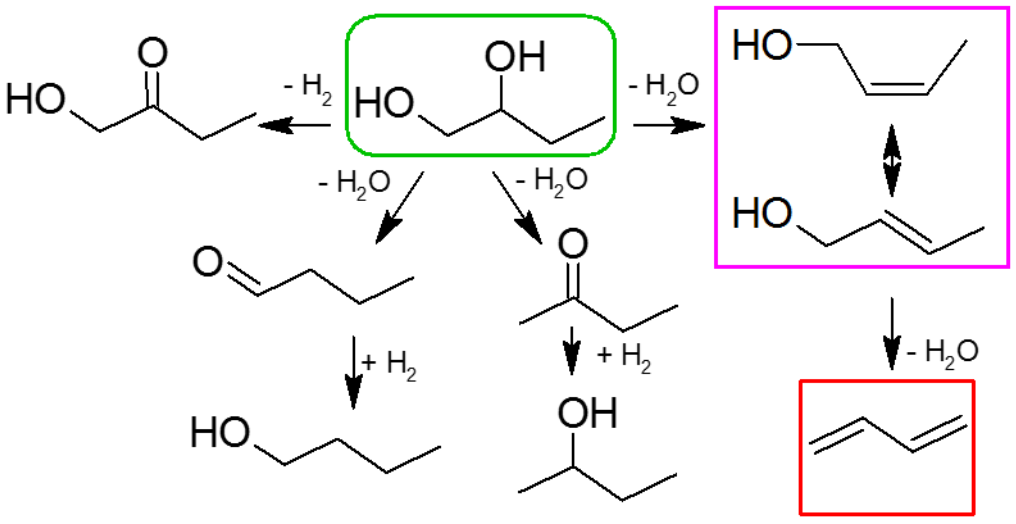

Scheme 1-8 Possible products from 1,2-BDO.

1.8.3.3 Dehydration of 1,4-BDO into BD

In the dehydration of 1,4-BDO, tetrahydrofuran (THF) formation is well known as a famous route (**Scheme 1-9**). Since THF is an important solvent for many polymers and also used as a monomer in the manufacture of polytetramethylene glycol,[124] and the demand of THF is still increasing recent years. The cyclodehydration of 1,4-BDO into THF has been greatly investigated.[125-128] Vaidya et al. claimed that a high yield of THF from 1,4-BDO was obtained with a strong acid cation-exchanged resin catalyst.[127] Aghaziarati et al. studied the performance of zeolites on the dehydration of 1,4-BDO to THF and they succeeded with the THF selectivity of ca. 100%.[125] Hunter et al. disclosed the THF synthesis from 1,4-BDO dehydration in high-temperatured water: THF was produced with an equilibrium yield of 84% at 200°C and 94% at 350°C and acidified conditions accelerate the reaction rate.[126] Vogel and Richter reported that the THF selectivity is nearly 100% by the use of pure supercritical water as the reaction media.[128] Besides, several papers also described that THF as the primary product from 1,4-BDO could be dehydrated into BD even through the process needs strict conditions.[129]

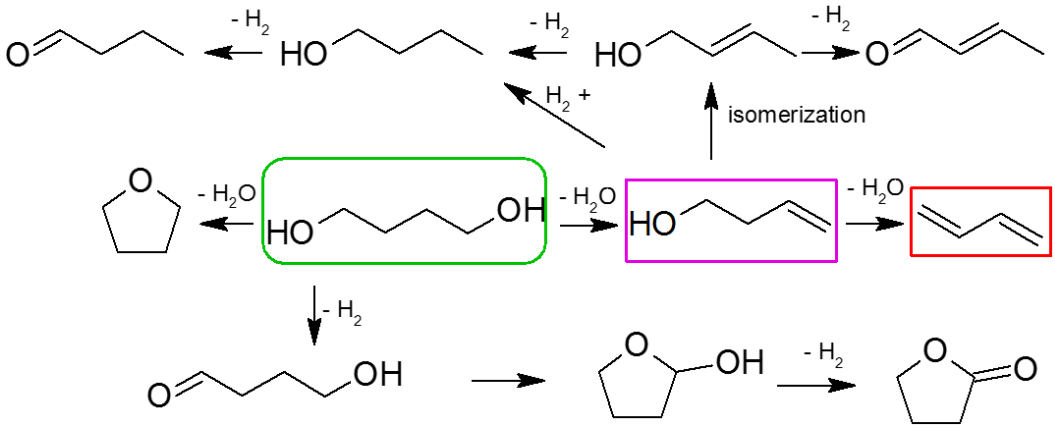

Scheme 1-9 Main products from 1,4-BDO.[130]

1.8.3.4 Dehydration of 2,3-BDO into BD

Dehydration of 2,3-BDO into BD has been investigated since 1940s. But most of the process resulted in good yields of 2-butanone (MEK),[131-138] as summarized in **Table 1-5**. However, 2,3-BDO with vicinal hydroxyl groups is difficult to be dehydrated into BD directly. In the dehydration of 2,3-BDO, some important chemical compounds, such as butenes, 3B2OL, MEK, and MPA (2-methyl-propanal) as well as BD, can be produced. 3B2OL is also one of the important intermediate chemicals in the production of medicines, perfume, and agrochemicals.[33, 139] Zhang et al. have reported Boron-modified HZSM-5 catalysts effectively work in the dehydration of 2,3-BDO to produce mainly MEK along with the formation of MPA.[133] Although the dehydration of 2,3-dimethyl-2,3-BDO, pinacol, is

known as a famous pinacol rearrangement reaction, I can observe that each methyl group always shifts to the carbocation after the OH^- dissociating to produce 3,3-dimethyl-2-butanone. Since the dimethyl groups of pinacol are changed with two hydrogens in 2,3-BDO, not only methyl group but also H^+ on the α-position can shift to the carbocation after the dissociation of OH^-, to produce MPA and MEK can be formed (**Scheme 1-10**).

Table 1-5 Dehydration of 2,3-BDO over several catalysts.

Catalysts	Reaction temp.(°C)	Conversion (mol%)	Selectivity (mol%)			Ref.
			BD	3B2OL	MEK	
H_2SO_4	180	99	-	-	96	131
Bentonite	225	-	-	-	86 [a]	132
Bentonite	700	-	7 [a]	-	10 [a]	132
Bentonite [b]	700	-	19 [a]	-	-	132
B/HZSM-5	200	100	1.4	-	70	133
HZSM-5	200	13	-	-	≥90	134
HZSM-5	250	99	14.5	-	51.5 [a]	135
Cs/SiO_2	400	6	-	17	11	136
Al-MCM-41	300	58	-	0	46	136
$AlPO_4$	250	12	1.4	3.8	64.7	137
$Na\text{-}P/SiO_2$ [b]	400	100	66.4	0	22.1	138
Acetic acid	≥500	100	≥80	-	-	140-142
Formic/acetic acid	500	100	70	-	-	143
ThO_2	350	100	3	70	8	119
ThO_2	500	100	62	1	26	119

BD, 1,3-butadiene; 3B2OL, 3-buten-2-ol; MEK, 2-butanone.

[a] Yield of products.

[b] Dehydration of 2,3-BDO in the present of water vapor as diluents.

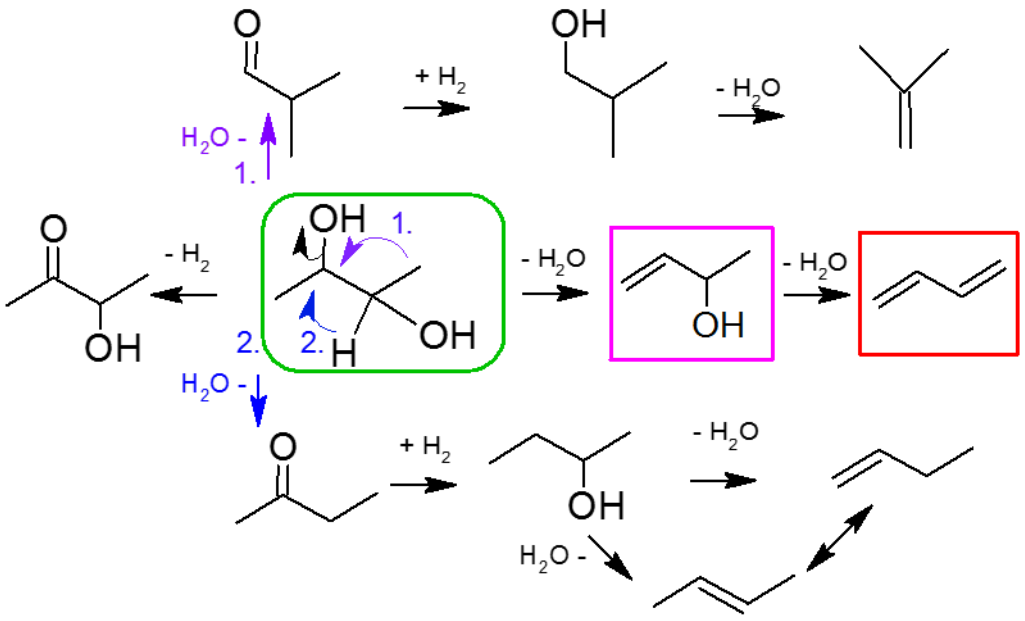

Scheme 1-10 Main products from 2,3-BDO.[119, 131-143]

Table 1-5 indicates that 2,3-BDO dehydration mostly showed high yield of MEK with rare BD over the acid catalysts. In addition, Bourns et al. also reported that MEK could be converted into 20% yield of BD at high reaction temperature of 700°C.[142] Winfield disclosed 62% BD yield over ThO_2 catalyst at 500°C from 2,3-BDO directly.[119] ThO_2 also catalyzed the formation of 3B2OL with a yield of 70.3% from 2,3-BDO at 350°C.[119] The trend is that: the complete dehydration product, BD, can be obtained at high reaction temperature, the primary dehydration product, 3B2OL, is obtained at low reaction temperature. Thus, in the BD production, it is significant to inhibit the formation of MEK and to promote the generation of 3B2OL and then further for BD.

1.8.4 Production of BD from UOLs

BD production from the UOLs, such as 3B1OL, 2B1OL, and 3B2OL over TiO_2, SiO_2-Al_2O_3, and Al_2O_3 catalysts (**Scheme 1-11**) was also examined. In comparison with the direct BD production from BDOs, it is found that the dehydration of UOLs into BD is much easier at temperatures lower than that of 2,3-BDO (**Table 1-6**).

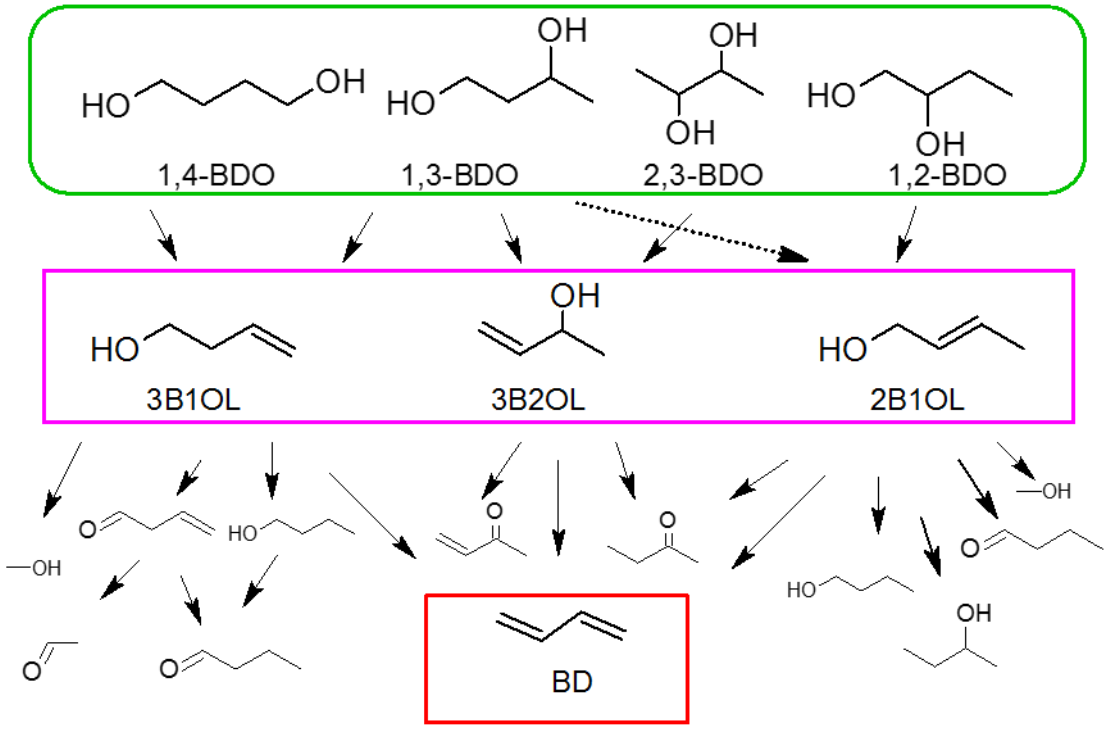

Scheme 1-11 Two-step dehydration from BDOs into BD *via* the corresponding C_4 UOLs.[119, 121, 130]

Table 1-6 indicates that the dehydration of 2B1OL and 3B2OL can be selectively converted to BD even at 250°C over TiO_2, SiO_2-Al_2O_3 and Al_2O_3. It was found that all they are acid type catalysts and the latter two show more and much stronger acid sites than the former one.[117,141] Thus, in **Table 1-6**, it can be understood that higher BD selectivity over 90% can be obtained over SiO_2-Al_2O_3 and Al_2O_3 in the dehydration of 2B1OL and 3B2OL. On the other hand, 3B1OL produces propylene via retro-hydroformylation and some heavier compounds, which well agrees in the report over MgO-SiO_2.[89] Therefore, the most suitable BDOs for the stepwise BD production are 1,3- and 2,3-BDOs, which can be converted into 3B2OL and/or 2B1OL, as being introduced in the following sections. Unfortunately, no good catalysts that can selectively convert THF and 3B1OL into BD have been found although they seem to be a more suitable intermediate to BD than 2B1OL and 3B2OL.

Table 1-6 Dehydration of C_4 UOLs and BDOs into BD.

Reactant	Catalyst	Reaction temp. (°C)	Conv. (mol%)	BD selec. (mol%)	BD yield (mol%)	Ref.
3-buten-1-ol	TiO_2	375	38	50	19	121
	SiO_2-Al_2O_3	250	42	13	5	121
	MgO_2-SiO_2	400	95	14	13	89
2-buten-1-ol	TiO_2	375	53	71	38	121
	SiO_2-Al_2O_3	250	77	93	72	121
	MgO_2-SiO_2	400	100	86	86	89
3B2OL	TiO_2	375	70	70	49	121
	SiO_2-Al_2O_3	250	71	93	66	121
	MgO_2-SiO_2	400	100	68	68	89
1,3-BDO	TiO_2	375	84	0	0	121
	SiO_2-Al_2O_3	250	73	36	26	121
	Al_2O_3	250	49	0	0	121
2,3-BDO	TiO_2	325	97	26	25	this study
	Al_2O_3	325	100	42	42	this study
1,4-BDO	SiO_2-Al_2O_3	200	27	67	18	130
	SiO_2-Al_2O_3	275	100	5	5	130
	Al_2O_3	200	17	70	12	130
	Al_2O_3	275	100	rare	rare	130

1.8.5 Formation of UOLs from BDOs

Besides the dehydration of BDOs, there are some other methods to produce UOLs, such as the addition of formaldehyde to propene[144] and the reduction of 3,4-epoxy-1-butene with formic acid[145] to produce 3B1OL; hydrogenation of 3,4-epoxy-1-butene with Raney Ni catalyst to produce 2B1OL and 3B1OL.[146] There is another method such as the reduction unsaturated carbonyl compounds etc. In the present study, the solvent free and direct catalytic dehydration of BDOs over metal oxides catalysts will be introduced in the following sections.

1.8.5.1 Dehydration of 1,3-BDO into UOLs

My research group have found that UOLs such as 3B2OL and 2B1OL can be selectively yielded from the dehydration of 1,3-BDO at 325°C over CeO_2 catalysts (**Scheme 4**).[147-149] The important issue is that BD was scarcely formed over the catalysts at 325°C.[147,150] Dehydration of 1,3-BDO into UOLs such as 3B1OL, 2B1OL, and 3B2OL have been investigated over ZrO_2,[121] solid acid metal oxides,[121] CeO_2-ZrO_2,[151] and all of the rare earth metal oxide catalysts.[152,153] Among all the rare

earth oxides, CeO_2 is the most active and selective catalyst. CeO_2 with weak basic sites shows the highest 1,3-BDO conversion at 375°C as well as the sum of selectivity of 2B1OL and 3B2OL over 99%.[149] CeO_2 worked as a redox catalyst for the formation of 3B2OL and 2B1OL, as described in **Scheme 1-12** (Figure. 4 of Ref.[154]). A 1,3-BDO molecule adsorbed on CeO_2 surface to form a tridentate coordination between OH groups and Ce cation as well as between the 2-position hydrogen and Ce cation. After the adsorption, the 2-position hydrogen atom is eliminated along with the elimination of an OH group to produce a UOL.

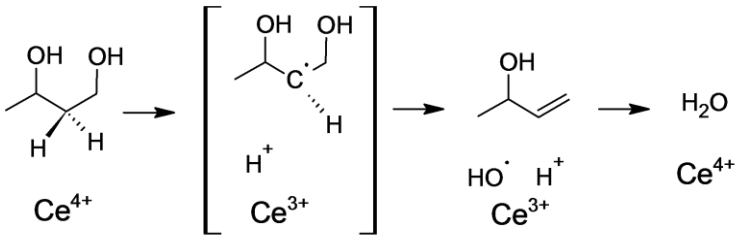

Scheme 1-12 Possible mechanism of dehydration of 1,3-diol via Ce^{4+}-Ce^{3+} redox cycle.[154]

Our group also investigated the dehydration of 1,3-BDO over CeO_2 different in particle size. The catalyst particle size was controlled by calcination temperature during the pretreatment. The reaction results showed that selectivities to 3B2OL and 2B1OL increased with increasing the particle size of catalyst while the further conversion of 3B2OL into 3-buten-2-one (MVK) and MEK decreased. In addition, from the XRD profiles and the TEM images of CeO_2 calcined at different temperatures, it was found that the faster growth of CeO_2 (111) facets can be observed than the other facets with increasing the calcination temperature.[148] The adsorption center is composed of three Ce cations, which are exposed on the O^{2-} point defect of CeO_2 (111) facet (**Figure 1-11**).

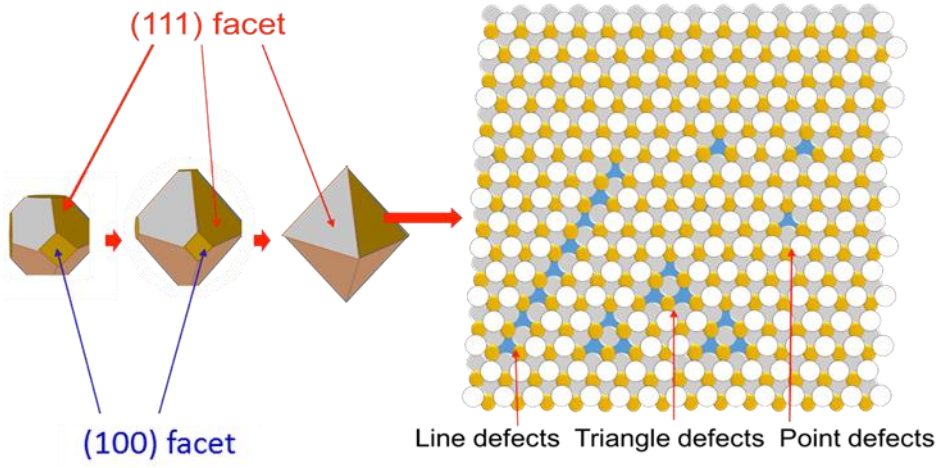

Figure 1-11 Illustration of CeO_2 (111) surface growing with crystal growth and the oxygen defects on it.[153]

The density functional theory (DFT) and paired interacting orbital (PIO) calculations are performed to monitor the tridentate coordinated adsorption model of 1,3-BDO on the CeO_2 (111) surface. The energy for 1,3-BDO adsorption on the O^{2-} defected surface of the CeO_2 (111) is -102.7 kJ mol^{-1} while that on the non-defected surface is -82.7 kJ mol^{-1}.[155] The O^{2-} defect sites of the CeO_2 (111) surface are suitable for the adsorption of 1,3-BDO. The most reasonable mechanism for 1,3-BDO dehydration was also imaged as **Scheme 1-13** (Figure. 10 of Ref. [155]). In a stable structure for adsorption, the 2-position hydrogen interacts with one Ce^{3+} and the 1- and 3-position oxygen atoms interact with another two Ce^{4+}.

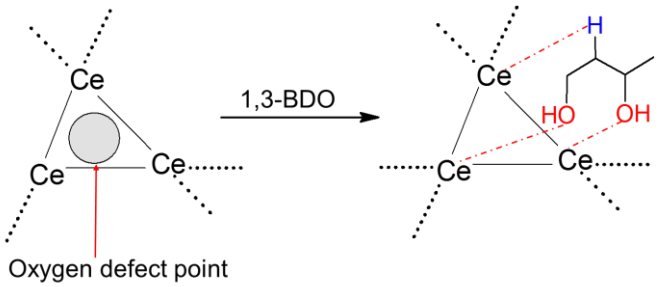

Scheme 1-13 Image of the adsorption structures of 1,3-BDO on an oxygen-defect of CeO_2.[155]

In a similar way to the cubic CeO_2 (111) facet, on the (222) facet of the cubic bixbyite rare earth metal oxides (Ln_2O_3; Ln, rare earth cation) such as Er_2O_3 and Yb_2O_3, oxygen defect sites are also generated intrinsically. Similar to the CeO_2 (111) facet, (222) facet of Ln_2O_3 also grows with increasing calcinations temperature. In_2O_3 and some of Ln_2O_3 catalysts especially Er_2O_3 and Yb_2O_3 also showed high total selectivity to 3B2OL and 2B1OL, as summarized in Table 1 of Ref. [152].[152,153] In_2O_3, which has the same crystal structure of Ln_2O_3 with cubic bixbyite, resembled CeO_2 for its redox property to capture the 2-position hydrogen atom.[156] However, the cation Ln^{3+} of Ln_2O_3 shows no redox activity, which is different from CeO_2. Thus, the mechanism of the UOLs formation from 1,3-BDO over those Ln_2O_3 catalysts is different from that of CeO_2 and In_2O_3. On the other hand, the formation rate showed a specific correlation with the ionic radius of Ln cation (**Figure 1-12**). CeO_2 is exceptionally active for 1,3-BDO dehydration among the Ln_2O_3 catalysts.

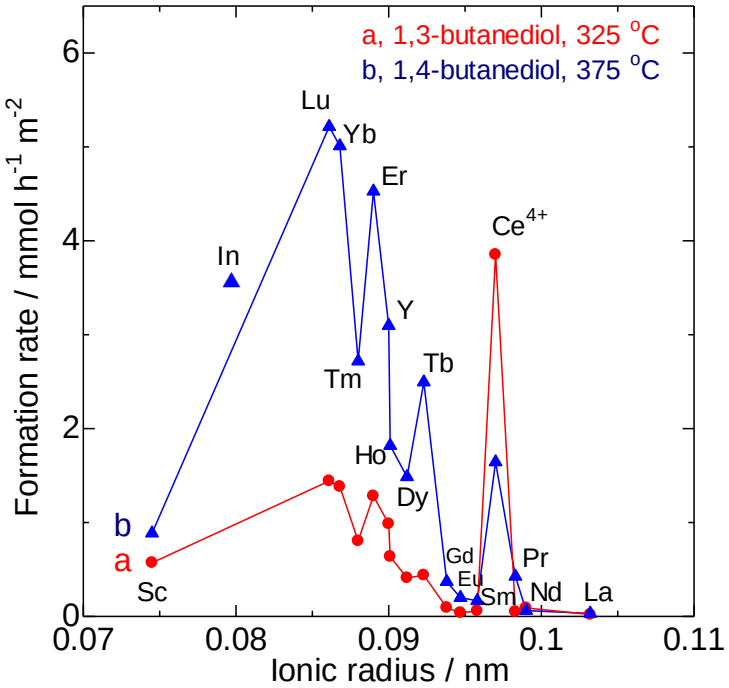

Figure 1-12 Formation rate of the corresponding UOLs with the ionic radii of Ln cations.[153]

Both CeO_2 and Er_2O_3 were poisoned by CO_2 and NH_3 carrier gases in contrast to H_2 carrier gas used as a reference. Carrier gases efficiently enhanced their catalytic activity in the increasing order: $CO_2 < NH_3 < N_2 < H_2$.[156] Thus, it indicates that both basic and acid sites work concertedly in the dehydration of 1,3-BDO over Ln_2O_3.

1.8.5.2 Dehydration of 1,4-BDO into 3B1OL

In the dehydration of 1,4-BDO over some specific catalysts, 3B1OL can be also produced as a dehydration product not to form THF (**Scheme 1-9**). 3B1OL is widely applied as a useful chemical for the synthesis of some important medicines, perfume, and agrochemicals.[157,158] It has been found that the dehydration of 1,4-BDO into 3B1OL is catalyzed by several catalysts, such as CeO_2,[147] In_2O_3,[156,159] Ln_2O_3,[150,160-162] ZrO_2,[163] and the modified ZrO_2.[164-167] Zhang et al. also modified ZrO_2 catalyst with alkaline-earth metal such as CaO, which enhanced the conversion of 1,4-BDO of 94.6% with 3B1OL selectivity of 68.9%.[166,167]

The DFT and PIO calculations were conducted by using the 1,4-BDO dehydration over Er_2O_3 catalyst as a model.[168] The adsorption model of 1,4-BDO on Ln_2O_3 (222) facet is imaged as **Figure 1-13** (Figure 2 of Ref. [168]), in which 1,4-BDO was absorbed on three sites of Ln_2O_3: 2-positon hydrogen atom onto a basic type site (oxygen anion), and the oxygen atoms of 1- and 4-position hydroxyl groups onto two acidic type sites (oxygen vacancies). Among several models, the model shows a reasonable adsorption energy change in the catalytic activity, indicating that the model is the

most probable adsorption model. Then, the 2-position hydrogen atom is firstly captured by the oxygen anion and then the 1-position hydroxyl group is deleted by an oxygen vacancy to form a C-C double bond. The adsorption energy needed for the reactant is -1.52 eV while that for the product 3B1OL is -0.32 eV. Thus, the adsorption of 1,4-BDO is preferable to that of 3B1OL. The high selectivity to 3B1OL over Er_2O_3 is explained by the energy values.

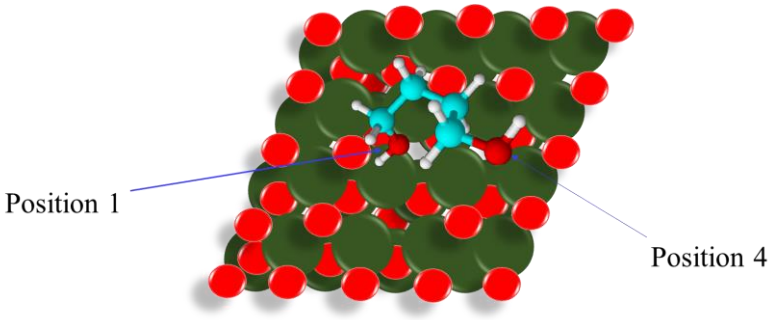

Figure 1-13 An adsorption model of 1,4-BDO on the Ln_2O_3 (222) face for DFT calculation. Ln^{3+}, the large green ball; O^{2-}, the small red ball.[168]

1.8.5.3 Dehydration of 2,3-BDO into 3B2OL

2,3-BDO can be dehydrated into MEK easily over acid type catalysts such as bentonite[132], zeolites,[133,134] aluminum phosphate,[137] and silica-supported sodium phosphate[138] (the details will be discussed in the letter chapter 3.0). However, ThO_2 was reported as an acid-base solid,[169] and it yields the 3B2OL from 2,3-BDO at low reaction temperatures of 300~350°C.[119] In these cases, one molecular water leads to 3B2OL and then further to BD formation should be possible

Therefore, in this thesis I will try to produce 3B2OL as well as BD from 2,3-BDO over some no-acid and the acid-base bifunctional catalysts, and also discuss their catalytic mechanisms.

Chapter II: Experimental

2.1 Catalyst preparation

Monoclinic ZrO_2 (JRC-ZRO-4), anatase TiO_2 (JRC-TIO-4), rutile TiO_2 (JRC-TIO-3), and Al_2O_3 (JRC-ALO-6) were supplied by the Reference Catalyst Division (former Committee), the Catalysis Society of Japan. CeO_2 was offered by Daiichi Kigenso Kagaku Kogyo Co., Ltd., Japan. Here, these catalysts above were used for the reaction without further heat treatment. ZnO, La_2O_3, and all the Ln_2O_3 were purchased from Kanto Chemical Co. Inc. Japan. All the Ln_2O_3 were anealed at 800°C before reaction unless some special case. $Ni(NO_3)_2$ and $Cr(NO_3)_3$ were purchased from Wako Pure Chemical Industry Ltd. Japan. Iron(III) acetate was purchased from Sigma-Aldrich. Fe_2O_3, NiO, and Cr_2O_3 were obtained by calcining the corresponding nitrate at 400 °C for 8 h.

Basic modifiers such as $LiOH{\cdot}H_2O$, $NaNO_3$, KNO_3, $Mg(NO_3)_2{\cdot}6H_2O$, $Ca(NO_3)_2{\cdot}4H_2O$, $Sr(NO_3)_2$, $Ba(NO_3)_2$, $Zn(NO_3)_2{\cdot}6H_2O$, and $La(NO_3)_3{\cdot}6H_2O$ were purchased from Wako Pure Chemical Industries, Ltd. Loading metal oxides on monoclinic ZrO_2 (m-ZrO_2) was performed by using incipient wetness impregnation. In this study, the support m-ZrO_2 was pre-heated in air at 800 °C for 3 h prior to impregnation. Each aqueous solution of the corresponding nitrate or hydroxide with the theoretically prescribed percentages of metal was impregnated little by little onto the m-ZrO_2 support. The resulting samples were dried at 110°C for 12 h before being calcined in air at a prescribed temperature for 3 h, as shown in **Figure 2-1**. As a reference, CaO was obtained from $Ca(NO_3)_2{\cdot}4H_2O$ calcined at 800°C for 3 h. Hereafter, CaO/ZrO_2 catalysts in the section of 3.1.3 are expressed as CaO-*X*-*T*, where *X* presents the CaO loading (wt.%), and *T* is the calcination temperature (°C) after impregnation. And also, the alkaline-earth metal oxides ZrO_2 catalysts in the section of 3.1.4 are expressed as MO-*X*-*T*, where M is the loaded alkaline-earth metal element (Ca, Sr, Ba and Mg), *X* is the expected loading molar ratio as MO:ZrO_2, and *T* is the calcination temperature (°C) after impregnation.

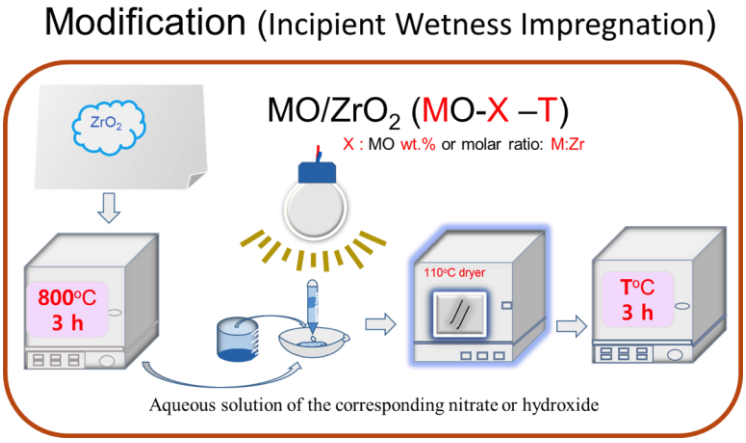

Figure 2-1 Modification of m-ZrO_2 with alkaline-earth metal oxides via incipient wetness

impregnation.

In addition, the aimed perovskites compounds $MZrO_3$ (M=Ca, Sr, Ba and also Mg) were prepared by mixing their nitrates and citric acid together with their molar ratio as M: Zr: citric acid=1:1:3 at 100°C for 2 h in a vacuum and then heated at 230°C for 3 h and at last calcined in air at 800°C for 3 h.

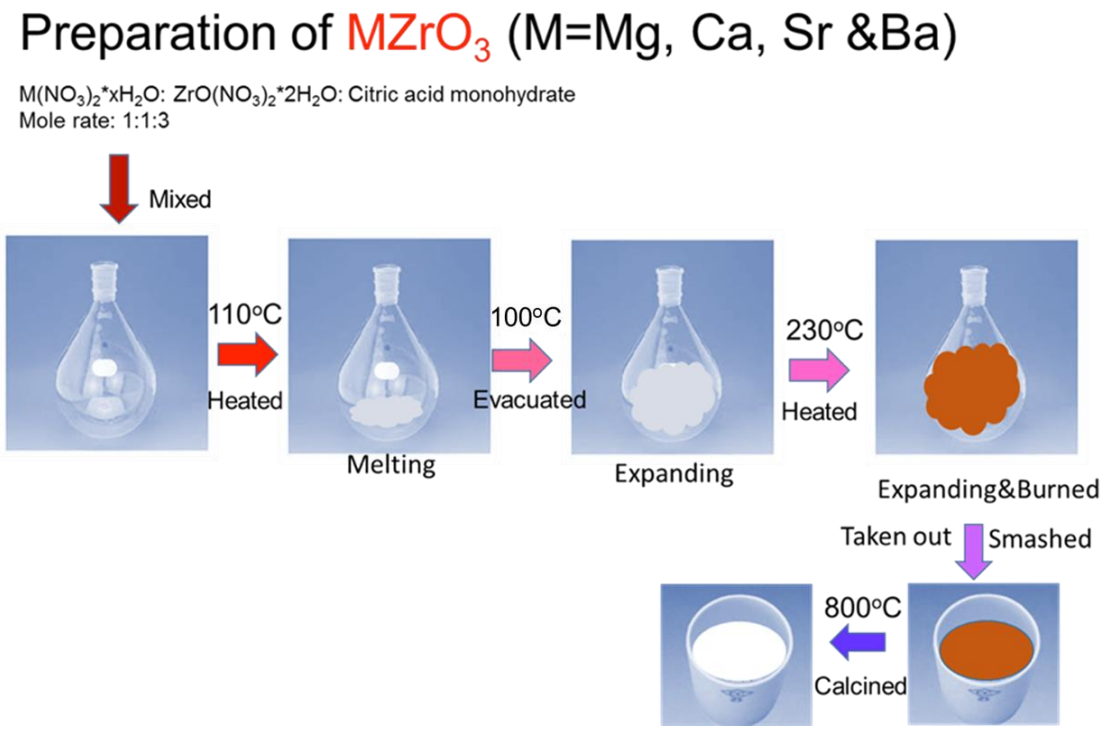

Figure 2-2 Preparation of the aimed perovskites compounds.

2.2 Catalytic reaction

2.2.1 The normal catalytic reaction

The reaction was conducted in a fixed-bed glass flow reactorat 300-400°C (**Figure 2-3**). The catalyst (1.0 g) was set on a small amount of glass wool as the fixed-bed, and then after the catalyst bed had kept stable at the prescribed reaction temperature for 1 h, the reactant 2,3-BDO was fed into the reactor at a feed rate of 11.8 mmol h^{-1} (1.06 g per hour) under the atmospheric pressure of H_2 carrier gas with a flow rate of 45-80 cm^3 min^{-1}.

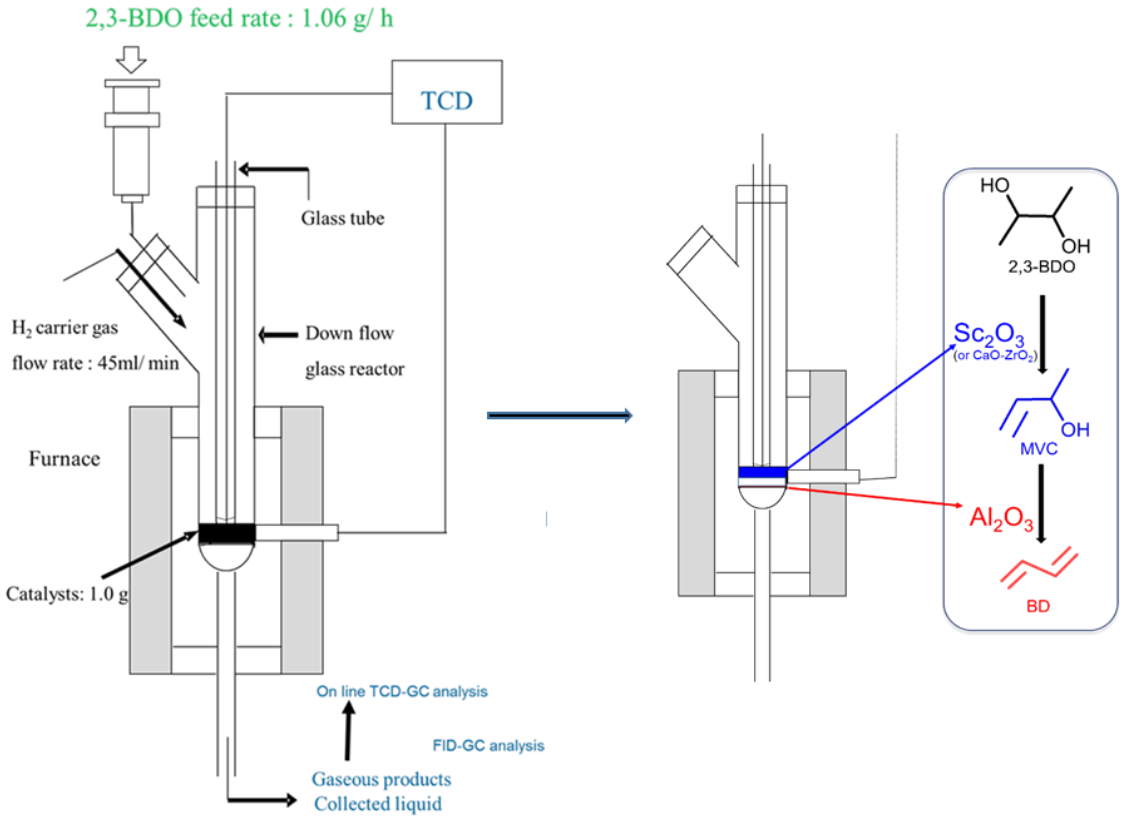

Figure 2-3 Catalytic reaction of 2,3-BDO over the fixed-bed flow reactor (left) and the two-layer fixed-bed (right).

2.2.2 The catalyst poisoning reaction

In order to confirm the effects of poisoning on the basic and acidic sites of the catalyst surface during the reaction, the carrier gas was changed to a mixture of either CO_2/H_2 or NH_3/H_2 with the volume ratio of 24/56 in the total flow rate of 80 cm^3 min^{-1}.

2.2.3 The catalytic reaction of intermediates

The dehydration of MEK and 3B2OL was also examined in the same way as the 2,3-BDO dehydration in order to confirm an intermediate product in the dehydration from 2,3-BDO to BD.

2.2.4 The two-layer catalytic dehydration process

The catalytic reaction of 2,3-BDO was also investigated over a two-layer catalyst, which consisted of 1 g of Al_2O_3 placed as a bottom layer and 1 g of Sc_2O_3 or CaO/ZrO_2 placed as an upper layer, to establish the efficient BD formation as shown in **Figure 2-3** (right).

2.3 Products analytical method and devices

The liquid effluent was collected every 60 minutes and analyzed by gas chromatography (FID-GC-8A, Shimadzu, Japan) with a 60-m capillary column (InertCapWAX-HT). The products were identified by gas chromatography with a mass spectrometer (GCMS-QP5050A, Shimadzu) and a 30-m capillary column (DB-WAX). Gaseous products such as BD and butene isomers were analyzed by on-line gas chromatography (TCD-GC-8A, Shimadzu) with a 6-m packed column (VZ-7).

GC-MS Measurement (identification analysis):

Column:	DB-WAX
Column length:	30 m
Column internal diameter:	0.25 mm
Column film thickness:	0.25 μm
Carrier gas:	helium (Japan Helium Center Corporation)
Column flow rate:	2.00 mL min^{-1}
Linear velocity:	51.6 cm s^{-1}
Injection temperature:	230°C
Split ratio:	9
Detection temperature:	230°C
Measurement method:	scanning
Detector voltage:	0.7 V (absolute value)
Threshold:	1000
Solvent elution time:	0 min (neat)
Interval:	0.5 s
Measurement period:	1.50 - 20.00 min
m/z measurement range:	10.00-450.00
Scanning rate:	1000

Liquid GC Measurement (quantitative analysis by FID):

Apparatus:	GC-8A
Column:	InertCapWAX-HT
Column length:	30 m
Column internal diameter:	0.53 mm
Column film thickness:	1.0 μm
Carrier gas:	Nitrogen (Chiba Nisan Corporation)
Column flow rate:	2.00 mL min^{-1}
Linear velocity:	20.0 cm s^{-1}
Injection temperature:	230°C
Injection pressure:	145.0 kPa
Split ratio:	10
Detection temperature:	230°C

Gaseous GC Measurement (quantitative analysis by TCD):

Apparatus:	GC-8A
Column:	VZ-7
Column length:	6 m
Column internal diameter:	0.4 mm
Column film thickness:	0.3 mm
Carrier gas:	Hydrogen (Keiyou Hydrogen Corporation)
Column flow rate:	0.5 mL min^{-1}
Linear velocity:	20.0 cm s^{-1}
Injection temperature:	60°C
Injection pressure:	145.0 kPa
Split ratio:	10
Detection temperature:	60°C

The catalytic activity was evaluated by averaging the conversion and selectivity data in the initial 5 h. Both the conversion of 2,3-BDO and the selectivity to each product were defined as mol%.
The selectivity to a product (S_i) was calculated as the following equation:

$$S_i = \frac{M_i}{\sum M_i}$$

where M_i is the mole of a product i in the collected effluent or a gas product detected on-line, was calibrated with the carbon number in the product as: M_i = (the mole of the product estimated with GC) × (carbon number in the product).

2.4 Catalysts Characterization

2.4.1 XRD (X-ray diffraction)

XRD patterns were measured on New D8 ADVANCE (Bruker) using Cu Ka radiation to detect the catalysts crystal structure:

Radiation source: Cu Kα (λ = 1.54 Å)

Measuring mode: continuous scanning

Measuring range: 10-80 degree

X-ray tube voltage: 40.0 kV

X-ray tube current: 40.0 mA

2.4.2 XPS (X-ray photoelectron spectroscopy)

Structural features of CaO/ZrO_2 catalysts were also characterized by XPS (Axis Ultra DLD, Shimadzu Corp.) using the X-ray gun of Mg (10 mA and 10 kV and the pass energy was 40 eV). The peak tops of C1s spectra for each sample were 282.8 -282.9 eV. The peak top of C1s has been utilized as a reference to adjust binding energies of other orbitals. It indicates that the binding energies of peak tops of other orbitals such as O1s, Ca2p, and Zr3d can be fairly compared.

2.4.3 Specific surface area

The specific surface area (SA) of catalysts was measured with home-made apparatus in the Brunauer-Emmett-Teller (BET) theory using the N_2 isotherm at -196◦C. Firstly, the sample (0.15 g) was dried at 110°C overnight. The dried sample was loaded into sample tube and heated at 300°C under vacuum. Then, the dead volume (volume of the tube except the sample and the other related parts) was calculated by the pressure change of He gas, which cannot enter into the sample, and written as V_{dead}. Next, the whole volume was calculated by the pressure change of N_2 gas, which can enter into the sample and be adsorbed on the surface of the sample, and written as V_{whole}. Lastly, the SA of catalyst can be obtained as:

$V = (V_{whole} - V_{dead})/W$, where W is the weight of the catalyst.

On the other hand, when the first layer was full, from the second layer the adsorption rate should be considered as the same:

$$a_{i+1} \times \theta_i \times P = b_{i+1} \times \theta_{i+1} \times e^{-Q_{i+1}/RT}$$

where a and b are the constant, P presents the pressure and Q_{i+1} is the adsorption energy for the layer of I, here Q_{i+1} also almost keeps the same.

$$\frac{a_1}{b_1} \neq \frac{a_2}{b_2} = \frac{a_3}{b_3} = \ldots \frac{a_i}{b_i} = \ldots$$

If here we let: $x = \frac{a_i}{b_i} \times P \times e^{Q_i / RT}$, and $y = \frac{a_1}{b_1} \times P \times e^{Q_1 / RT}$, $C = \frac{y}{x}$

thus it will be: $\theta_i = x \times \theta_{i-1} = x^{i-1} \times \theta_1 = y \times x^{i-1} \times \theta_0 = C \times x^i \times \theta_0$

and V can be also written as:

$$V = V_m \times \sum_{i=1}^{\infty} i \bullet \theta_i$$

here V_m is the volume absorbed onto the first layer, and then it can be transferred as:

$$\frac{V}{V_m} = \theta_0 C \times \sum_{i=1}^{\infty} i \bullet x^i \qquad \theta_0 = 1 - \theta_0 \times C \times \sum_{i=1}^{\infty} x^i$$

the next:

$$\theta_0 = \frac{(1-x)}{(1-x+Cx)} \qquad \frac{V}{V_m} = \frac{x \times C}{(1-x)(1-x+Cx)}$$

When the liquid and the gas of N_2 is under equilibrium state, their pressures are almost the same and can be written as P_o,

$$a_2 P_0 = b_2 e^{-Q_L / RT}$$

and then the relative pressure can be: $x = \frac{P}{P_0}$

$$\frac{P}{V(P_0 - P)} = \frac{1}{V_m C} + \frac{C-1}{V_m C} \times \frac{P}{P_0}$$

Here, if the left is plotted against P/P_o to obtain a straight line, the segment and the slope can be used to calculate V_m. Finally, the surface area SA can be obtained via dividing V_m by the cross-sectional area of the adsorbed molecules.

2.4.4 Basicity and acidity

The temperature-programmed desorption (TPD) of adsorbed CO_2 was measured with a home-made apparatus, to estimate the basic properities of those catalysts. After preheated under vacuum at 500°C, CO_2 was adsorbed onto the surface of catalysts at 25°C for 72 h. The measured temperature was raised from 25 to 850°C at a temperature-rising rate of 10°C min^{-1}. The amount of desorbed CO_2, which was bubbled into an aqueous solution of NaOH, was monitored the change of the solution conductivity. The cumulated amount of desorbed CO_2 was obtained as the functions of its adsorption power and the desorbed temperature, and then differentiated for a TPD profile to display the distribution of its basic strength. The amount of basic sites was estimated via the neutralization-titration curves of diluted NaOH.

The TPD of adsorbed NH_3 was also measured in the similar method as CO_2-TPD. Firstly, the catalyst sample was preheated in vacuum at 500°C for 1 h. After cooled to room temperature, the nitrogen gas with 0.1 MPa was introduced to the sample for 10 second. After that, the desorption temperature range was monitored from 25 to 850°C at a heating rate of 10°C min^{-1} under a N_2 flow of 15 ml min^{-1}. Electric conductivity of the H_2SO_4 aqueous solution (0.5 mmol dm^{-3}, 50 g) was monitered together with the desorbed NH_3 in the N_2 flow being bubbled to the solution of H_2SO_4. The amount of desorbed NH_3 was reflected by the conductivity change of H_2SO_4 solution, and the amount of accumulated NH_3 was differentiated to give a TPD profile of the acid strength distribution.

2.4.5 Thermogravimetry-differential thermal analysis

The thermogravimetry-differential thermal analysis (TG-DTA) was measured with Thermoplus 8120E2 (Rigaku, Japan).

Measured conditions

Samples:	9.5~11.5mg
Standard:	γ-alumina
Rate of temperature increase:	10.0°C min^{-1}
Final temperature:	900°C
Environment:	air
Thermocouple plate:	Pt

2.4.6 DRIFT (Diffuse reflectance infrared Fourier transform)

DRIFT spectra were measured with a triglycine sulfate detector (JASCO Corp., Japan). Firstly, the samples were diluted with KBr for 3 wt.% and then pressed into the cell in vacuum.

Measured conditions

Detectors:	TGS
Wavenumber range:	4000-400 cm^{-1}
Scan:	512 times
Resolution:	8 cm^{-1}

2.5 Abbreviation of compound names

BDOs: butanediols including (1,3-butanediol, 1,2-butanediol, 2,3-butanediol, and 1,4-butanediol)
3B2OL: 3-buten-2-ol
3B1OL: 3-buten-1-ol
2B1OL: 2-buten-1-ol
MEK: 2-butanone

MVK: 3-butne-2-one

Acetoin: 3-hydroxy-2-butanone

MPA: 2-methyl-propanal

MPO: 2-methyl-propanol

BD : 1,3-butadiene

USOL: Unsaturated alcohol

m-ZrO_2: Monoclinic Zirconia

t-ZrO_2: Tetragonal Zirconia

MO-X-T: Monoclinic Zirconia modified with alkaline earth metal oxide: where M is the loaded alkaline-earth metal element (Ca, Sr, Ba and Mg), X is the respected loading molar ratio as MO:ZrO_2, and T is the calcination temperature (^oC) after impregnation.

$MZrO_3$: Perovskites compounds (M=Ca, Sr, Ba and also Mg)

Ln_2O_3: Rare earth oxides

Ln: Rare earth atom

Chapter III: Dehydration of 2,3-BDO into 3B2OL

In order to realize the low-carbon society and also to diminish the usage of fossil sources, the demand for sustainable chemical compounds is growing rapidly. Among them, 2,3-butanediol (2,3-BDO) is one of the prospective biomass-derived chemical compounds and its production has been greatly developed via fermentation with various bacteria from glucose, glycerol, sucrose, xylose and etc. [170-172] 2,3-BDO shows the future prospect for wide bio-based chemicals application via catalytic technologies. Studies on 2,3-BDO dehydration were reported even before 1938,[132] but the products distributed variously over different catalysts relying on their properties, as shown in **Scheme 3-1**.

2-Butanone (MEK) can be produced from 2,3-BDO readily via the hydride rearrangement in acidic aqueous solution,[131,173] or over several acid resins and solid catalysts such as bentonite,[132] alumina,[174,175] silica-alumina,[176] heteropoly acids,[177] and zeolites.[134, 137, 178-180] As described in **Scheme 3-1**, the hydroxyl groups at position 2 can be easily captured by proton or acidic sites, and then dissociated. Therefore, the methyl group or hydride at position 3 moves to the position 2. Thus, MEK and 2-metyl-propanal (MPA) are produced (**Scheme 3-1** group (I)). In the work of Zhang and co-workers, MPA formation competed with MEK at almost a constant ratio (*ca.* 20%:68%) over HZSM-5 zeolites.[179] In addition, the strong acid sites accelerate methyl arrangement for MPA,[180] while alumina or zeolites catalysts always deactivate rapidly due to their strong acidity. Nikitina's group also reported that the existence of BrΘnsted acid sites of zeolites resulted in MEK and MPA, as well as some heavy condensation products, while the Lewis acid sites of alumina acted mainly for MEK formation together with less heavy products. However, when combining the two types of acid sites together, heavy products increased rapidly.[137] Some others also observed that high carbon balance and low coke formation can be expected via diluting the reactant 2,3-BDO with an appropriate amount of water.[174]

Sometimes, 1,3-Butadiene (BD) can be also produced from 2,3-BDO together with MEK over acid catalysts such as γ-Al_2O_3.[174] In this rare case, hydroxyl groups at positions 2 and 3 may be captured by acid sites and then dissociate simultaneously or stepwise. Then, the two terminal hydrogens must also dissociate for the stable BD formation, as shown in **Scheme 3-1** group (I) and (II).

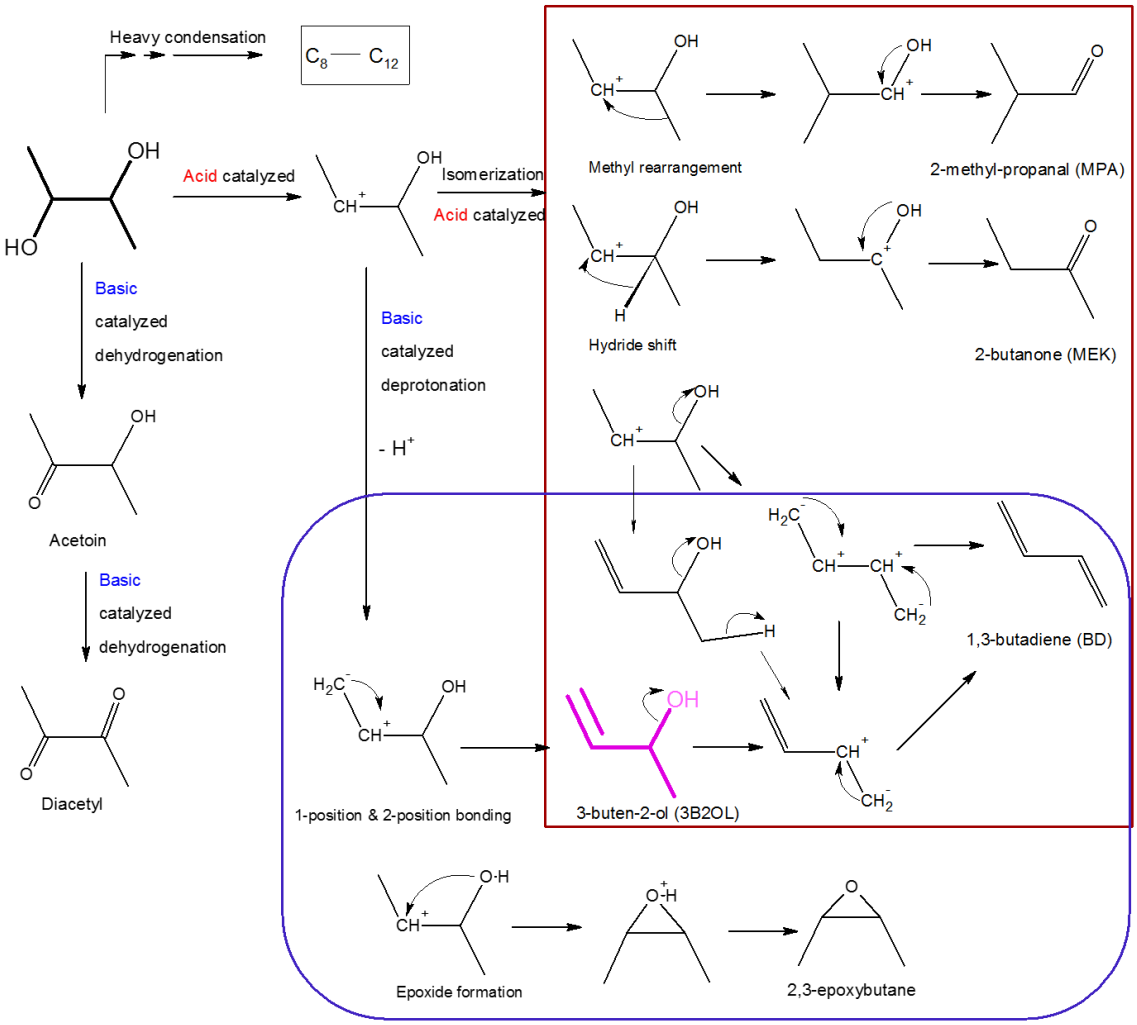

Scheme 3-1 Possible products from 2,3-BDO catalyzed by acid and base catalysts.

Production of BD from 2,3-BDO directly was also reported[119] over ThO_2, which was reported as an acid-base solid.[169] In addition, the intermediate 3-buten-2-ol (3B2OL) can be also yielded from 2,3-BDO at low reaction temperatures of 300-350°C.[119] In these cases, as shown in **Scheme 3-1** group (II), 1,2-elimination of one molecular water leads to 3B2OL and then further to BD formation, as shown in **Scheme 3-1** group (II). Since formations of the two differ in activation energy level, their distribution were successfully controlled by reaction temperature.[119]

On the other hand, 1,2-elimination also occurred over the acid-base bifunctional catalysts such as SiO_2-supported sodium phosphates and cesium dihydrogen phosphate.[181, 182] Over these acid-base bifunctional catalysts, the hydroxyl group at position 2 was captured by an acid site and dissociated for a carbon cation, together with the terminal hydrogen by a basic site for a carbon anion. Thus, an appropriate acid-base balance is significant for the products distribution: the excess acid sites results in MEK, MPA and also the heavy products, while the excess basic sites also lead to dehydrogenate for

acetoin and diacetyl[181] or dehydrate to 2,3-epoxybutane,[183] as shown in **Scheme 3-1** group (Ⅱ) and (Ⅲ). On the other hand, SiO_2-supported sodium phosphates and SiO_2-supported cesium dihydrogen phosphate can produce BD at high reaction temperatures of 400-500°C but cannot stop for a high 3B2OL yield.[181, 182]

Since the further dehydration of 3B2OL into BD with 94% yield proceeds even at 250°C over Al_2O_3 and SiO_2-Al_2O_3 catalysts,[38, 184] 2,3-BDO can be converted into 3B2OL firstly and then further dehydrated into BD by Al_2O_3 at low temperatures. In addition, 3B2OL is also an important chemical compound used as the intermediate for anticancer drugs.[33, 139] In order to synthesize 3B2OL with the cheap and safe catalysts instead of the radioisotope material, ThO_2, in the present study, I also investigated several catalysts and among them the active ones were found out. Both their excellent reaction activities and characters were studied in details.

3.1 Catalytic reaction of 2,3-BDO over various oxide catalysts

Table 3-1 lists the catalytic reaction of 2,3-BDO over typical metal oxide catalysts at 325°C. Over CeO_2, the main products in the dehydration of 2,3-BDO were MEK, MPA, acetoin, 3B2OL, and BD, while 3B2OL was rarely observed. Yb_2O_3 and ZnO showed competitive formation of 3B2OL and acetoin. On the other hand, over anatase TiO_2, rutile TiO_2 and Al_2O_3 catalysts, the main products were BD and MEK but not 3B2OL while the conversion levels were relatively high. In contrast, acetoin was preferentially obtained through dehydrogenation over La_2O_3, NiO, Cr_2O_3, and even under thermal conditions without catalyst. Among the catalysts I tested, only monoclinic ZrO_2 (m-ZrO_2) showed a high selectivity to 3B2OL: ZrO_2 calcined at 800°C showed a selectivity to 3B2OL of 48.6%. In addition, little changes occurred when the carrier gas was changed from H_2 to N_2.

Table 3-1 Dehydration of 2,3-BDO over various metal oxide catalysts at 325°C. [a]

Catalyst	Conversion [b]	Selectivity [b] (mol%)						
	(mol%)	3B2OL	BD	acetoin	MEK	MPA	MPO	Others[c]
blank test	1.7	7.5	0	47.2	12.9	0	0	32.4
CeO_2 [d]	39.1	1.3	0.1	21.5	36.5	3.3	3.7	33.6
La_2O_3 [d]	7.0	5.0	0	47.8	7.3	4.9	3.9	31.1
Yb_2O_3 [d]	17.5	28.1	0	39.5	1.8	0.4	1.0	29.2
ZrO_2 [e]	63.7	37.6	0	17.3	18.2	1.5	11.2	14.2
ZrO_2 [d, e]	62.5	48.6	0	14.9	16.0	1.3	7.8	11.4
ZrO_2 [d, e, j]	76.4	43.8	0	11.4	17.9	1.1	7.4	18.4
ZrO_2 [f]	93.4	1.7	20.1	4.2	34.7	4.4	8.6	26.3
TiO_2 [g]	97.1	13.3	26.4	0.2	30.2	3.7	3.3	23.1
TiO_2 [h]	97.4	0.5	21.9	2.0	38.2	3.2	4.5	29.7
Al_2O_3	100.0	0.2	41.8	1.1	33.1	4.0	0.4	19.4
ZnO	54.5	25.6	0	41.9	1.5	0	0	31.0
Fe_2O_3 [i]	66.4	3.1	0.9	12.6	28.8	2.0	9.9	42.7
NiO [i, j]	50.0	0.4	0	65.6	5.9	3.0	0.2	24.9
Cr_2O_3 [i j]	9.9	7.2	0.3	68.6	4.8	1.2	0	17.9

3B2OL, 3-buten-2-ol; BD, 1,3-butadiene; acetoin, 3-hydroxy-2-butanone; MEK, butanone; MPA, 2-methylpropanal; MPO, 2-methyl-1-propanol.

[a] Catalyst weight: 1 g; feed rate: 1.06 g h^{-1}; flow rate of H_2 carrier gas: 45 cm^3 min^{-1};

[b] Conversion of the reactant and the selectivity of each product were averaged in the initial 5 h;

[c] Others include butene isomers, propylene, ethylene, and 2-butanol.[d] Calcined at 800°C for 3 h; [e] Monoclinic structure; [f] Tetragonal structure; [g] Rutile; [h] Anatase; [i] Calcined at 400°C for 3 h twice; [j] Performed in N_2 flow at a rate of 45 cm^3 min^{-1}.

The reaction products over ThO_2 catalyst are also discussed by Winfield[119]. 3B2OL was the first step dehydration product of 2,3-BDO and then would be followed by the further dehydration to BD at high reaction temperatures. Other products such as MEK, MPA and acetoin were also detected in the previous reports.[131, 185] Acid sites generated on the surface of the catalysts could act as the active sites for 2,3-BDO converting to MPA and MEK via the 2-position methyl and hydrogen atom rearrangement, respectively. The reaction routes to the products are summarized in **Scheme 3-2**. Therefore, only m-ZrO_2 showed the suitable catalytic activities for the 3B2OL formation, but rare BD was obtained.

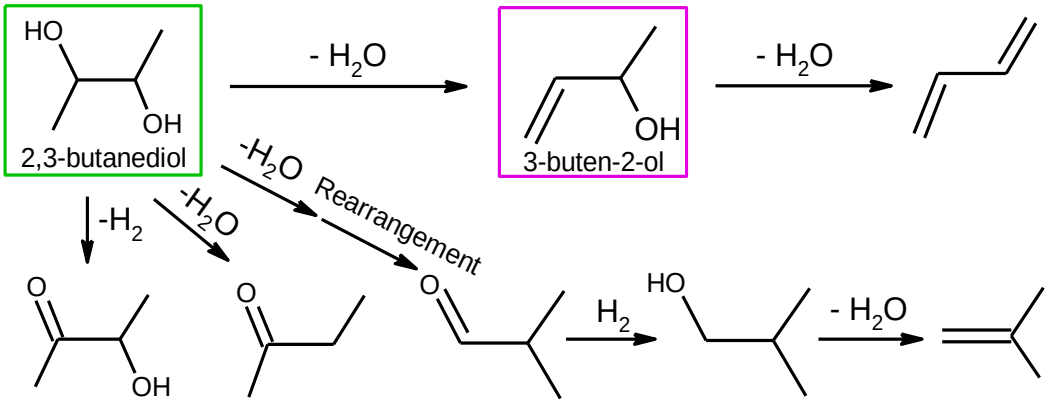

Scheme 3-2 Main products derived in the dehydration of 2,3-BDO.

3.2 Dehydration of 2,3-BDO over ZrO_2

3.2.1 Dehydration of 2,3-BDO over ZrO_2 calcined at different temperatures

Table 3-2 lists the catalytic activity of monoclinic ZrO_2 with different calcination temperatures in the dehydration of 2,3-BDO at 325°C. It is obvious that the conversion of 2,3-BDO does not have much difference at calcination temperatures below 800°C, and it decreased steeply with the calcination temperature over 800°C. However, ZrO_2 calcined at high temperatures prefers to convert 2,3-BDO to 3B2OL rather than to MEK, MPA, and other by-products. The selectivity to 3B2OL reached 57.1% with a conversion of 49.8% over ZrO_2 calcined at 900°C (**Table 3-2**). **Figure 3-1(A)** shows the reaction rate based on per unit surface area of the pure ZrO_2 catalysts, and their surface area was controlled by calcination temperature. Both the consumption rate of 2,3-BDO and the formation rate of 3B2OL were maximized at around 800°C. **Figure 3-1(A)** clearly indicates that ZrO_2 calcined at temperatures of 800-900°C provides active surface for the formation rate of 3B2OL.

Table 3-2 Dehydration of 2,3-BDO over ZrO_2 calcined at different temperatures [a].

Calcination	*SA*	Crystallite size	Conversion	Selectivity (mol%)					
(°C)	(m^2 g^{-1})	*D* [b] (nm)	(mol%)	3B2OL	MEK	acetoin	MPA	MPO	Others[c]
As received	42.8	40.7	63.7	37.7	18.2	17.3	1.5	11.2	14.1
400	35.5	37.0	62.7	34.7	18.9	16.8	1.5	11.5	16.6
600	31.0	38.8	58.0	40.5	18.0	18.3	1.6	10.2	11.4
700	29.9	42.9	67.5	44.4	15.5	15.4	1.5	9.5	13.7
800	26.3	47.9	62.5	48.6	16.0	15.0	1.3	7.8	11.3
850	25.2	47.9	50.0	55.9	13.0	16.1	1.1	6.4	7.5
900	25.1	58.2	49.8	57.1	13.0	15.7	1.1	6.0	7.1
1000	24.7	81.5	22.3	58.5	10.7	21.4	0.9	4.1	4.4

[a] Reaction temperature: 325°C, feed rate:1.06 g h^{-1}, flow rate of H_2: 45 cm^3 min^{-1}, the reactant conversion and the selectivity of each product were averaged in the initial 5 h.

[b] Crystallite size estimated by Scherer's equation was based on the (-1 1 1) peaks of ZrO_2 detected in XRD patterns (**Figure 3-1(B)**).

[c] Others include butene isomers, propylene, ethylene, BD, 2-butanol, and etc.

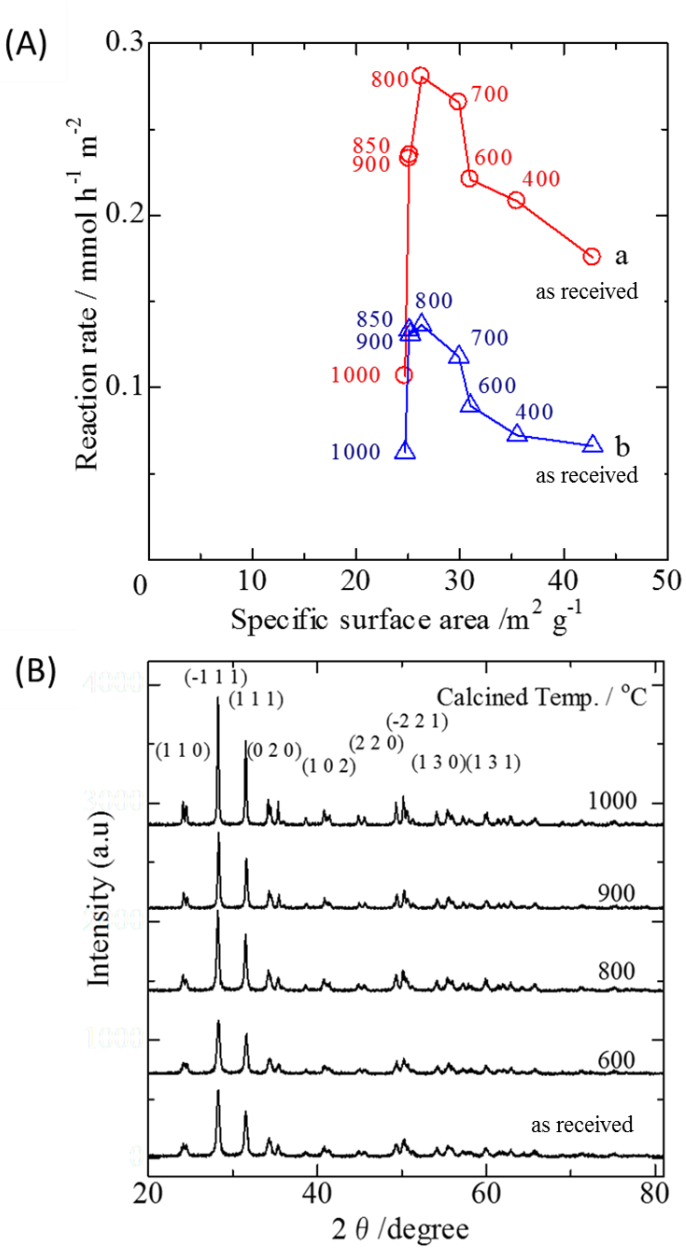

Figure 3-1 (A) The conversion rate of 2,3-BDO and the formation rate of 3B2OL over ZrO_2 with different specific surface area controlled by calcination. a, consumption rate of 2,3-BDO; b, formation rate of 3B2OL. **(B)** The XRD patterns of pure ZrO_2 with different calcination temperatures. Numbers in the Figure represent calcination temperature (°C).

The crystal structures of ZrO_2 calcined at different temperatures were investigated by XRD measurement. All the samples were identified as monoclinic zirconium (IV) oxide even the one calcined at 1000 °C (**Figure 3-1(B)**). **Table 3-2** also lists SA and particle size, D, of ZrO_2. These figures suggest that the primary particle of monoclinic ZrO_2 grew with increasing the calcination temperature.

A higher calcination temperature led to a smaller specific surface area due to agglomeration, whereas the conversion was almost constant up to 850°C and the 3B2OL selectivity increase with rising the calcination temperature. This is a notable issue: low surface area ZrO_2 shows high selectivity to 3B2OL, as I have also observed in the CeO_2 catalyst.[147, 148] The formation rate of 3B2OL is obviously affected by the crystallinity of ZrO_2. This indicates that a highly crystalized surface of monoclinic ZrO_2 would provide a proper adsorption structure for the activation of 2,3-BDO and could select the reaction route to 3B2OL, not to by-products. A similar issue has been discussed previously in the reactive ability of 1,4-BDO catalyzed by rare earth oxides.[153]

3.2.2 Effect of reaction temperature on the catalytic activities of ZrO_2

Figure 3-2 shows the temperature-dependence of the catalystic activity of ZrO_2 calcined at 900°C under an H_2 flow rate of 45 cm^3 min^{-1}. The average conversion value increased as temperature increased and reached to 93.8% at 350°C. It can be found that a higher selectivity to 3B2OL was obtained at a lower reaction temperature. It is obvious that acetoin also prefers to low reaction temperatures. However, the selectivities to BD and MEK were enhanced gradually with increasing the temperature. Similar results are also found in the pioneering work of Winfield.[119]

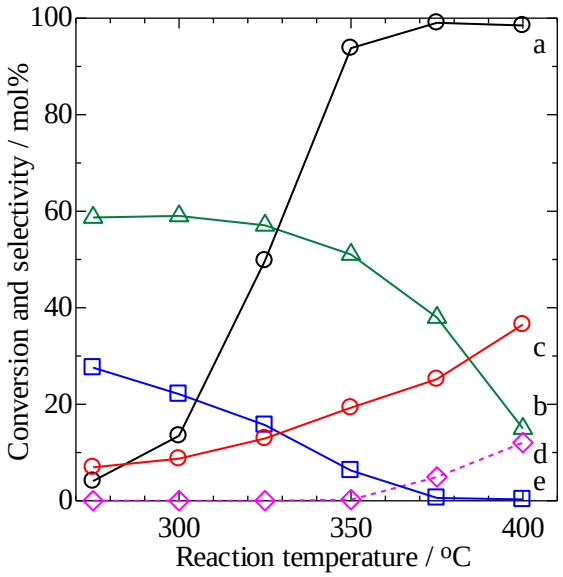

Figure 3-2 The reaction activity of 2,3-BDO over ZrO_2 with reaction temperature increasing: (a) conversion of 2,3-BDO, (b) selectivity to 3B2OL, (c) MEK, (d) BD, and (e) acetoin.

3.2.3 The catalytic stability of ZrO_2 with time on stream

Figure 3-3 shows the catalytic stability of ZrO_2 calcined at 900°C in the dehydration of 2,3-BDO at 350°C and an H_2 flow rate of 80 cm^3 min^{-1}. The selectivity to 3B2OL and other major by-

products kept almost stable in the initial 5 h while the conversion decreased slightly in the initial period.

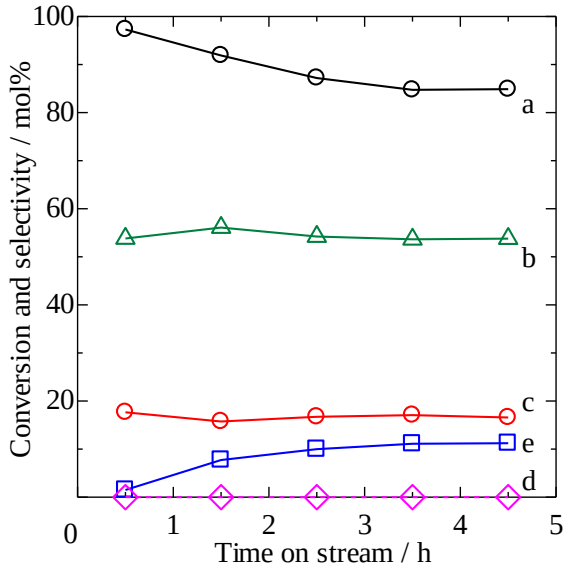

Figure 3-3 Stability with time on stream during the reaction of 2,3-BDO over ZrO_2 at 350°C.
(a) conversion of 2,3-BDO, (b) selectivity to 3B2OL, (c) MEK, (d) BD, (e) acetoin. ZrO_2 was calcined at 900°C; flow rate of H_2 carrier gas was 80 cm^3 min^{-1}.

3.3 Dehydration of 2,3-BDO over modified m-ZrO_2 catalysts.

Table 3-3 lists the results of catalytic reactions of 2,3-BDO over several m-ZrO_2 catalysts modified with basic oxides at 350°C. The conversion of 2,3-BDO decreased by loading metal oxides on the support, while the selectivity to 3B2OL was upgraded by some metal oxides, compared with the pure m-ZrO_2 calcined at 800°C. Li_2O and La_2O_3 decreased the 3B2OL selectivity. Among the metal oxides I tested, alkaline-earth metal oxides such as CaO, SrO, BaO, and also MgO improved the 3B2OL selectivity of m-ZrO_2 together with a moderate 2,3-BDO conversion. The dehydrogenated product, acetoin, also increased because of the alkaline-earth metal oxides loading, while the selectivities to MEK, MPA, and MPO decreased. In particular, the 3B2OL selectivity over CaO/ZrO_2 exceeded 76% at a relatively high 2,3-BDO conversion. Thus, hereafter, CaO/ZrO_2 catalyst that showed the highest 3B2OL selectivity is selected as the aimed catalyst in the following sections.

Table 3-3 Catalytic performance at 350°C of m-ZrO_2 catalysts modified with several metal oxides, MO_n.

MO_n in Catalyst [a]	Molar ratio of C [a]	Conversion[b] (mol%)	Selectivity (mol%) [b]					
			3B2OL	acetoin	MEK	MPA	MPO	Others[c]
pure ZrO_2	0	97.6	43.9	1.7	22.7	8.7	1.6	21.4
Li_2O	0.073	5.8	40.4	40.7	5.0	3.0	0	10.9
MgO	0.031	41.6	65.9	22.5	4.2	2.7	0.3	4.4[f]
MgO	0.068	26.6	65.6	25.1	3.2	0.4	1.7	4.0
CaO	0.068 [d]	55.2	76.8	13.5	4.5	1.5	0.6	3.1
SrO	0.068	55.3	71.0	14.4	3.8	0.5	1.8	8.5
BaO	0.068	41.9	75.8	11.5	3.8	1.9	0.8	6.2
La_2O_3	0.023	47.8	36.5	25.7	9.9	1.4	9.9	16.6

[a] MO_n stands for metal oxides in catalyst; C is the mole ratio of the metal in metal oxides to Zr in m-ZrO_2. The calcination temperature after impregnation is 800°C.

[b] Catalyst weight = 1.0 g; Feed rate of 2,3-BDO = 11.8 mmol h^{-1}; Average conversion and selectivity are for initial 0-5 h.

[c] Ohters included BD, ethylene, propylene, MPA, MPO, 2,3-butanedione and some unknown products.

[d] CaO loading is 3.0 wt.%.

[e] Included 8.7 % MPA and 1.6 % MPO.

[f] Included 2.7 % MPA and 0.3 % MPO.

[g] Included 1.5 % MPA and 0.6 % MPO.

[h] Included 1.9 % MPA and 0.8 % MPO.

3.3.1 Effects of CaO content and the catalyst calcination temperature on the dehydration of 2,3-BDO over CaO/ZrO_2 catalysts

Table 3-4 shows the catalytic activities of CaO/ZrO_2 catalysts with different CaO loadings at 350°C. The addition of CaO onto m-ZrO_2 enhanced the selectivity to 3B2OL greatly up to ≥70%, whereas the 2,3-BDO conversion significantly decreased with increasing CaO loading. **Table 3-4** also shows a summary of the selectivity to by-products. For the dehydrogenated product, i.e. acetoin, the selectivity was increased with increasing CaO content, while the selectivity to MEK was almost constant at 3-5% over the CaO/ZrO_2 catalysts. In addition, the catalytic activity greatly depends upon the calcination temperature over CaO/ZrO_2 with CaO loading of 3 wt.%. It can be also confirmed that both the highest 2,3-BDO conversion and the highest 3B2OL selectivity were obtained at a calcination temperature of 800°C.

Table 3-4 Catalytic performance at 350°C of CaO-ZrO_2 catalysts calcined at different temperatures after impregnation and with different CaO loadings.

Catalyst (CaO-*X*-*T*)[a]	Conversion [b] (mol%)	Selectivity [b] (mol%)			
		3B2OL	acetoin	MEK	Others[c]
CaO-0-800 (ZrO_2)	97.6	43.9	1.7	22.7	31.7
CaO-1-800	81.5	65.8	10.9	5.1	18.2
CaO-1.5-800	61.0	67.3	14.7	3.4	14.6
CaO-2-800	52.8	69.4	15.7	5.3	9.6
CaO-2.5-800	53.7	72.2	15.5	4.8	7.5
CaO-3-800	55.2	76.8	13.5	4.5	5.2
CaO-3.5-800	55.9	73.5	14.4	4.9	7.2
CaO-5-800	34.1	69.9	19.7	4.5	5.9
CaO-7-800	32.8	68.2	19.7	4.2	7.9
CaO-10-800	35.7	72.1	17.8	5.2	4.9
CaO-15-800	30.0	69.4	20.2	5.5	4.9
CaO-30-800	16.4	38.3	32.2	8.5	21.0
CaO-100-800 (CaO)	3.8	7.7	42.2	40.4	9.7
CaO-3-600	18.5	35.8	45.3	3.9	15.0
CaO-3-700	32.1	68.7	20.3	3.3	7.7
CaO-3-900	56.1	72.9	14.1	4.6	8.4

[a] *X* is the weight percentage of CaO in the sample and T is the calcination temperature (°C) after impregnation.

[b] Catalyst weight = 1.0 g; Feed rate of 2,3-BDO = 11.8 mmol h^{-1}; Average conversion and selectivity are for initial 5 h.

[c] Others includes BD, ethylene, propylene, MPA, MPO, 2,3-butanedione and some unknown products.

3.3.2 Effects of reaction temperature on the dehydration of 2,3-BDO.

Figure 3-4 indicates the effects of reaction temperature on the 3B2OL formation from 2,3-BDO over CaO-3-800 catalyst. With increasing reaction temperature, both the conversion of 2,3-BDO and the selectivity to MEK increased, while the acetoin selectivity declined. The selectivity to 3B2OL showed a maximum at 350°C.

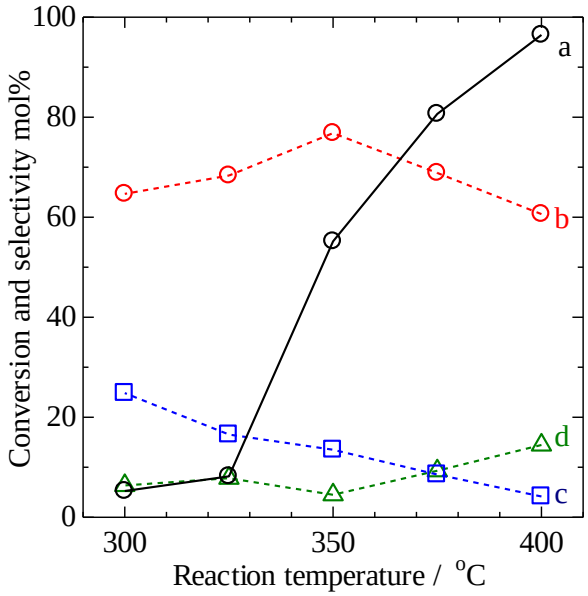

Figure 3-4 Effects of reaction temperature over CaO-3-800 catalyst. (a) 2,3-BDO conversion; (b) Selectivity to 3B2OL; (c) to MEK; (d) to acetoin. W/F =84.7 g_{cat} h mol^{-1}.

3.3.3 Effects of the carrier gas flow rate on the dehydration of 2,3-BDO

Figure 3-5 depicts the changes in the 2,3-BDO conversion and the products selectivities under different contact time (W/F) over CaO-3-800 catalyst at 350°C. Here, W is the catalyst weigh (g) and F is the feed rate of 2,3-BDO (mol/h). The reactant conversion increased with increasing contact time and reached 79.8% at 254 g_{cat} h mol^{-1}, while the selectivity to 3B2OL was almost unchanged at different W/F. Such a result suggests that the excessive side reactions such as the decomposition of 3B2OL rarely proceeds at 350°C even at high 2,3-BDO conversion.

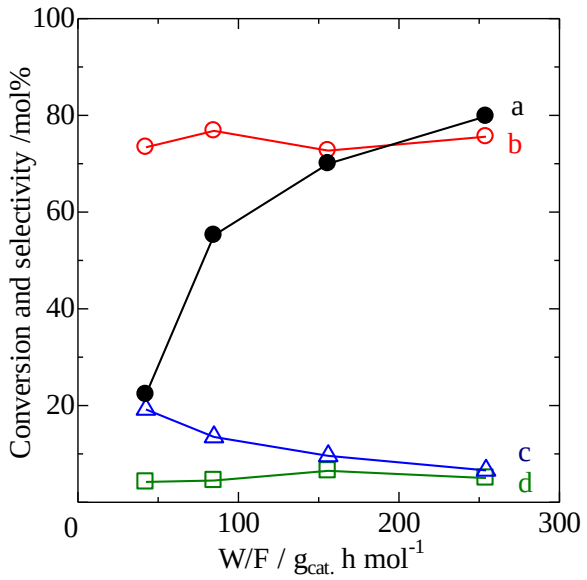

Figure 3-5 Effects of contact time on the catalytic activity of CaO-3-800 at 350°C, where W presents the weight of catalyst (g) and F is the feed rate of reactant (mol/h)
(a) Conversion of 2,3-BDO; (b) Selectivity to 3B2OL; (c) to acetoin; (d) to MEK.

3.3.4 Effects of CO_2 and NH_3 poisoning during the reaction

Judging from the data listed in **Tables 3-3** and **3-4**, it is obvious that the supported alkaline-earth metal oxides such as CaO, SrO, and BaO enhanced 3B2OL selectivity when compared with the pure m-ZrO_2 catalyst. In order to clarify how the acid-base functions of the catalysts work during the reaction, I performed poisoning experiment using NH_3 and CO_2 carrier gases. **Figure 3-6** shows the changes in the catalytic activities with different poisoning carrier gases, i.e. in H_2 carrier gas with 30 vol.% CO_2 or NH_3 over CaO-3-800 catalyst. The 2,3-BDO conversion was significantly reduced in both the CO_2- and NH_3-containing carrier gases. The 3B2OL selectivity was also reduced by CO_2, but slightly increased by NH_3. It is obvious that the formation of 3B2OL from 2,3-BDO is suppressed in the CO_2- and NH_3-containing carrier gases.

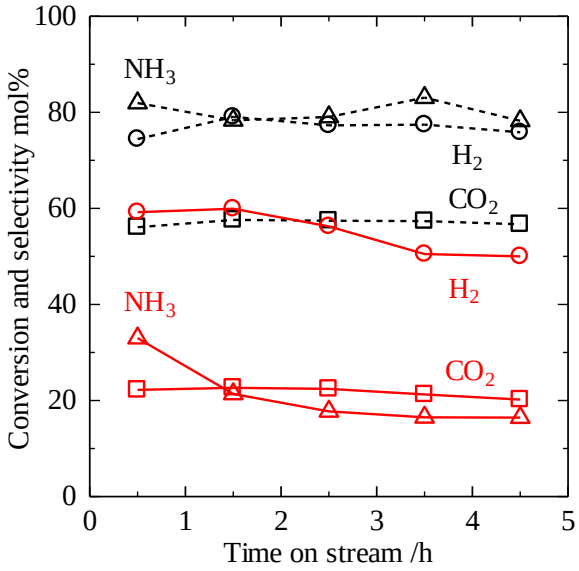

Figure 3-6 Catalytic performance of CaO-3-800 catalyst in different carrier gases.
Solid lines, 2,3-BDO conversion; Dotted lines, 3B2OL selectivity. W/F=84.7 g_{cat} h mol^{-1}.
Total carrier gas flow rate = 80 cm^3 min^{-1}; pure H_2, CO_2-30 vol.%-, and NH_3-30 vol.%-H_2 were used.

Table 3-5 summarizes the poisoning effect over CaO-X-800 catalysts. Over the pure m-ZrO_2 calcined at 800°C, the 2,3-BDO conversion was slightly reduced by CO_2 while the 3B2OL selectivity was almost the same as in H_2 flow. However, NH_3 upgraded the 3B2OL selectivity: the yield of 3B2OL in NH_3 is obviously higher than that in H_2 over pure m-ZrO_2. On the other hand, the 2,3-BDO conversion significantly decreased in both CO_2 and NH_3 over CaO-*X*-800 catalysts at *X*= 1 and 3. However, at *X*= 5, neither CO_2 nor NH_3 gases worked as a poison. In particular, NH_3 gas seems to work as a catalyst to increase the 3B2OL selectivity in a similar way to pure m-ZrO_2. In short, at low CaO loadings of *X*= 1 and 3, the poisoning experiments reveal that both these acidic and basic sites on the modified catalyst could consist of the active centers for the formation of 3B2OL.

Table 3-5 Catalytic performance of $CaO\text{-}ZrO_2$ catalysts under different carrier gases at 350 °C.

Catalyst	2,3-BDO conversion [a] (mol%)		
(CaO-*X*-*T*)	in pure H_2	in 30% CO_2	in 30% NH_3
CaO-0-800 (ZrO_2)	97.6 (43.9)	93.7 (43.4)	89.7 (66.9)
CaO-1-800	81.5 (65.8)	14.1 (50.9)	19.5 (84.1)
CaO-3-800	55.2 (76.8)	21.7 (57.0)	21.0 (80.1)
CaO-5-800	34.1 (69.9)	36.9 (56.0)	38.7 (83.2)

[a] Catalyst weight = 1.0 g; Feed rate of 2,3-BDO = 11.8 mmol h^{-1}; Carrier gas with the total flow rate of 80 cm^3 min^{-1}.

Average conversion and selectivity are for initial 0-5 h. Number in parenthesis is the selectivity to 3B2OL.

3.3.5 Characterization of $CaO/m\text{-}ZrO_2$ catalyst samples

3.3.5.1 Basicity and acidity of $CaO/m\text{-}ZrO_2$ catalyst samples (TPD)

Figure 3-7 illustrates TPD profiles of CO_2 desorbed from the surface of $CaO/m\text{-}ZrO_2$ catalysts. The desorption peaks up to 200 °C (assigned as α) were observed on almost all the samples. Over ZrO_2 supported with alkaline-earth metal oxides (**Figure 3-7A**), a desorption peak appeared at around 300°C (assigned as β), which has also been reported in a mesoporous $CaO\text{-}ZrO_2$.[185] **Figure 3-7B** illustrates CO_2-TPD profiles of CaO-*X*-*T* catalysts. The CaO-3-800 sample had more basic sites β than the other samples. The β peak decreased gradually with increasing CaO loading. At CaO loading of 15 and 30 wt.%, a desorption peak resulted from CaO appeared at 500°C (assigned as γ). In **Figure 3-7C**, the β peak was rarely observed and the strong γ peak appeared when the sample was calcined at temperatures lower than 800°C. At 800°C, the γ peak disappeared and the β peak appeared. It indicates that calcination temperatures of 800°C and higher are needed for the formation of basic sites β. **Figure 3-7D** illustrates NH_3-TPD profiles of CaO-*X*-*T* catalysts, and it indicates that there were really few acidic sites on the surface of ZrO_2 when compared with Al_2O_3 an ordinary solid acidic catalyst which was also used in **Table 3-1**. And it can be also observed that the amount of acidic sites even with different strength declined with *X* increasing. **Table 3-6** summarizes quantitative data for basicity of CaO-*X*-*T* catalysts as well as their specific surface area. Densities of basic sites α and β were calculated as the amount of basic sites based on the unit specific surface area.

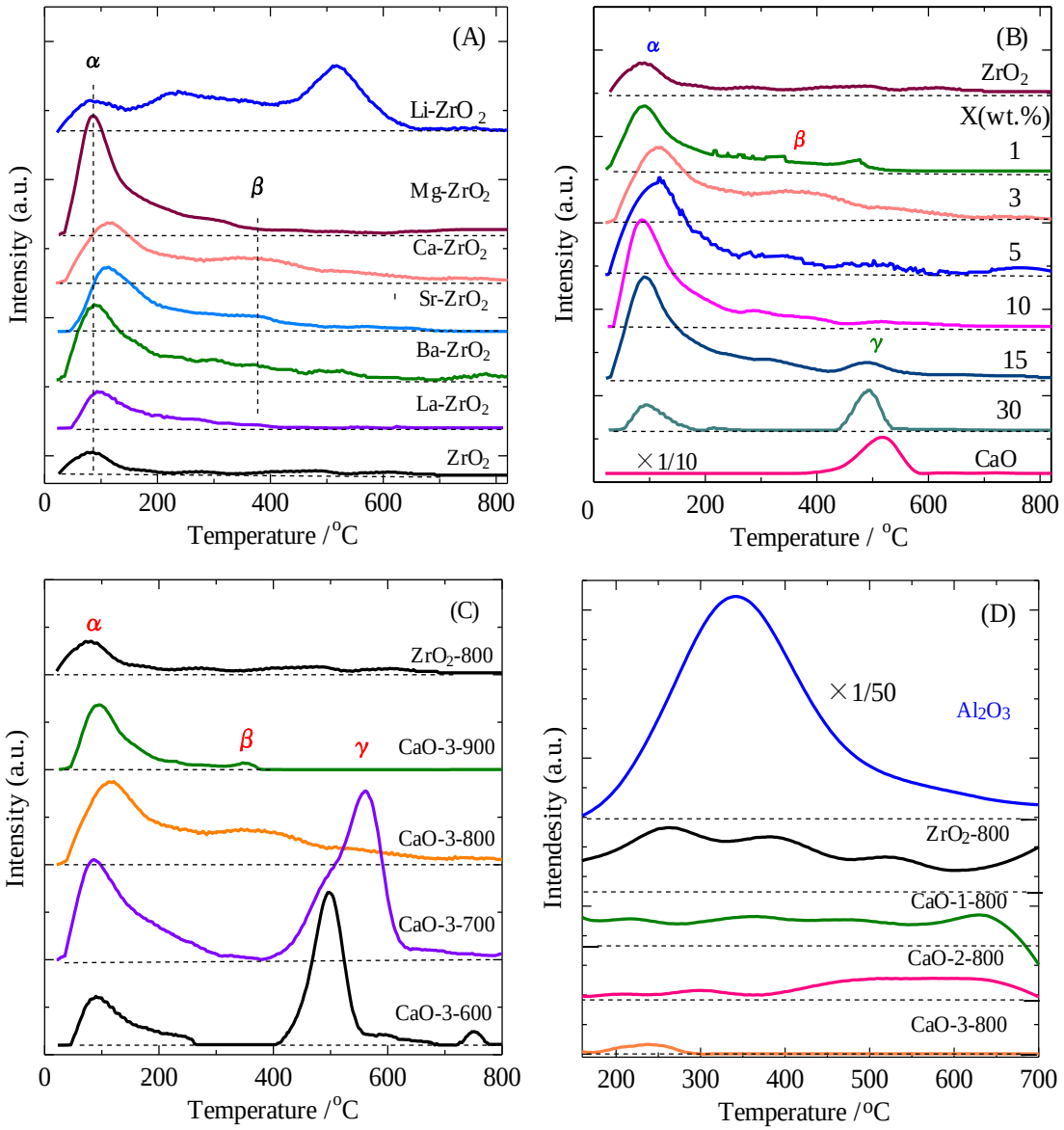

Figure 3-7 CO_2-TPD profiles of (A) m-ZrO_2 modified with different metal oxides, (B) CaO-*X*-800, (C) CaO-3-*T* catalysts and (D) NH_3-TPD profiles of CaO-*X*-800 catalysts.

Table 3-6 Surface properties of CaO-ZrO_2 catalysts changes with calcination and CaO contents.

Catalyst	S.A.	Basicity[a]	Basicity density (μmol m^{-2})	
(CaO-*X*-*T*)	(m^2 g^{-1})	(μmol $g^{-1}_{cata.}$)	Weak (α) [b]	Medium (β) [c]
CaO-0-800 (ZrO_2)	26.3	44.1	1.3	0.4
CaO-1-800	25.9	104.3	2.6	1.5
CaO-3-800	27.4	211.3	3.2	4.0
CaO-10-800	26.6	147.7	4.3	1.3
CaO-15-800	26.7	158.1	4.2	1.7
CaO-30-800	25.4	16.5	0.7	0.0
CaO-100-800 (CaO)	-	356.2	0.0	0.0
CaO-3-600	22.0	211.3	1.9	0.0
CaO-3-900	30.7	63.7	1.8	0.3

[a] Calculated by the method of CO_2-TPD accumulating the amount of CO_2 desorbed up to 800°C.

[b] Calculated by using SA and the amount of CO_2 desorbed up to 200°C.

[c] Calculated by using SA and the amount of CO_2 desorbed from 200°C to 450°C.

3.3.5.2 Crystal structures of CaO/m-ZrO_2 catalyst samples (XRD)

Figure 3-8 shows the XRD patterns of CaO-*X*-*T*, m-ZrO_2, and CaO samples. Pure m-ZrO_2 and all the CaO/ZrO_2 samples could be identified as well-crystallized monoclinic phase. In the CaO-*X*-800 samples (*X*=1.5, 3, 5, 10, 15, 30 wt.%), the intensity of the peaks belonging to m-ZrO_2 became weaker with increasing CaO loading, compared with the pure m-ZrO_2. At CaO loadings of 3 wt.% and higher, the diffraction peaks attributed with $CaZrO_3$ phase with peropskite structure were observed at 2θ = 22.2 and 45.3 degree, which were growing with increasing CaO loading. The $CaZrO_3$-related discussion will be described in the following section of 3.4.5.1. At CaO loadings of 15 wt.% and higher, the peaks attributed to CaO phase were also detected at 2θ = 37.4 and 54.0 degree. In addition, XRD patterns of the CaO-3-*T* samples at *T*= 600, 700 and 900°C were also measured to compare with that of CaO-3-800. No $CaZrO_3$ phase was observed in the samples calcined at 600 and 700°C.

The XRD patterns (**Figure 3-8**) indicate that the excess Ca^{2+} may even aggregate to form CaO phase at high CaO loading over 15 wt.%. **Table 3-4** indicates that, both the reactant conversion and the selectivity to 3B2OL decreased at a high CaO loading or at a low calcination temperature. Excess Ca^{2+} also resulted in much basic sites α (**Figure 3-7B** and **Table 3-6**) and it aggregated to form $CaZrO_3$ and CaO to reduce the dehydration activities. Therefore, it is reasonable that only by loading a proper content of CaO, the active sites can be induced on the surface of m-ZrO_2 to improve the catalytic activities in the dehydration of 2,3-BDO. In my study, the formation of tetragonal ZrO_2 was not

expected because it may preferentially produce BD directly with the competitive by-product MEK rather than 3B2OL, as demonstrated in **Table 3-1**. In the present work, tetragonal ZrO_2 phase was not detected in the XRD patterns of all the CaO-X-T samples.

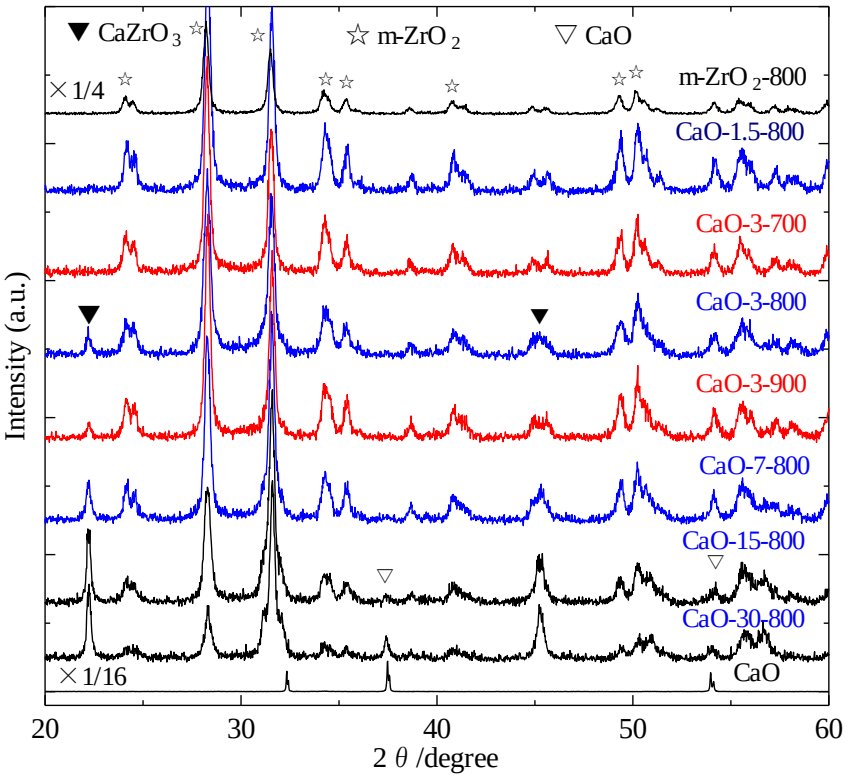

Figure 3-8 XRD patterns of CaO-*X*-*T* samples together with pure ZrO_2 and CaO calcined at 800°C.

3.3.5.3 Structural features of CaO/m-ZrO_2 catalyst samples (DRIFT)

Figure 3-9 shows the DRIFT spectra of the CaO-*X*-800 catalysts. The broad absorption bands from 447 to 556 cm^{-1} can be identified to be characters of the pure CaO phase and the broad bands from 506 to 760 cm^{-1} to be the Zr-O vibration absorption. With increasing CaO loading, the band confirmed as the vibration absorption of Ca-O-Zr shifts gradually from 506 cm^{-1} to higher wavenumber up to 551 cm^{-1}. The changes are well consistent with the samples of ZrO_2 incorporated with Ca cations in the preceding work.[186]

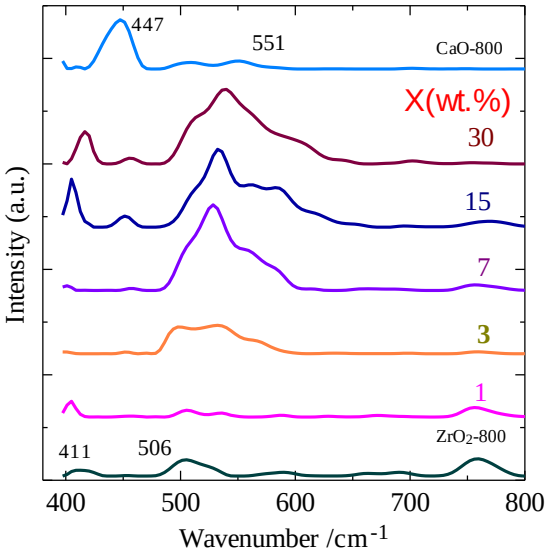

Figure 3-9 DRIFT spectra of CaO-X-800 samples.

3.3.5.4 Confirmation of β basic sites and the new acidic sites over the modified catalysts

In the poisoning experiment of **Figure 3-6** and **Table 3-5**, I can confirm that there are some new acidic and basic sites acting as the active centers for 3B2OL formation from 2,3-BDO on the surface of CaO-3-800 catalyst. It can be also observed that the activities of CaO-*X*-800 catalysts with higher CaO content always showed lower conversion and even got less impaired by the poisoning carrier gases. Thus, it can be concluded that high CaO content also leads fewer active acid-base sites for the dehydration of 2,3-BDO. The CO_2-TPD profiles in **Figure 4A-C** show new basic sites β appeared on all CaO-*X*-800 catalysts when compared with the pure m-ZrO_2 and some other modified samples. As discussed in the work of Zhang et al.,[186] Ca^{2+} replaced with Zr^{4+} of tetragonal ZrO_2 for the new formation of Ca-O-Zr hetero-linkages. Thus, some acid resulted from Zr-O-Zr were removed, and the Ca-O-Zr bond could result in the uneven distributed charges to generate new basic and acidic sites. In the present work, Ca-O-Zr hetero-linkages are also confirmed by DRIFT (**Figure 3-9**). Thus, it is possible that the uneven distribution charges of Ca-O-Zr bonds produce the basic sites β and basic sites α (**Figure 3-7A-C**). But in my present work the acidic sites can be removed greatly by loading CaO and the new acidic sites could not be detected exactly with NH_3-TPD profiles (**Figure 3-7D**). In addition, MgO supported on ZrO_2 (MgO/ZrO_2) which shows the highest intensity of basic site α but the lowest basic site β (**Figure 3-7A**) exhibits lower 2,3-BDO conversion, lower 3B2OL selectivity, and higher acetoin selectivity than those of CaO-3-800 (**Table 3-3**). Both SrO/ZrO_2 and BaO/ZrO_2 with a considerable amount of basic site β show high 3B2OL selectivity. Thus, it is probable that basic

sites β have acted as an effective basic site for the formation of 3B2OL.

In the CaO-3-T samples (**Figure 3-7C** and **Table 3-4**), calcination temperatures clearly affect the basicity and the catalytic activity. The CaO-3-*T* samples are needed to be calcined at a temperature of 800°C and higher to form the basic site β originated from the new Ca-O-Zr bond together with the disappearance of γ peak observed at *T*=600 and 700 °C, which could be originated from CaO dispersed on m-ZrO_2.

3.3.5.5 Relationship between the acid-base properties and their catalytic activities of the modified ZrO_2

In the conversion of 1,4-BDO, it is reported that an appropriate amount of Na_2O[187] or CaO[186] supported on ZrO_2 can improve the production of 3-buten-1-ol (3B1OL). Our research group have demonstrated the dehydration of 1,4-BDO to produce 3B1OL under different carrier gases: both CO_2 and NH_3 act as a poison in the reaction over rare earth oxides such as Er_2O_3.[188] As I demonstrated in **Figure 3-6** and **Table 3-5**, both CO_2 and NH_3 acted as a poison in the reaction over CaO-1-800 and CaO-3-800 catalysts. The results clearly explained that both base and acid generated on the surface of catalysts had enhanced the conversion of 2,3-BDO to 3B2OL. Judging from the stronger poisoning effect of CO_2 than NH_3, the basic sites on the catalyst play the major role on the formation of 3B2OL, while the acidic sites also support the dehydration of 2,3-BDO. In contrast to the basic sites observed in CO_2-TPD (**Figure 3-7**), I observed few acidic sites through the profiles of NH_3-TPD. **Table 3-5** also suggests that the formation of 3B2OL increased in NH_3 over pure m-ZrO_2 and CaO-5-800. I cannot say that acidic sites on ZrO_2 work as active sites for the formation of 3B2OL, but NH_3 adsorbed on the catalyst could act as a catalyst. There is another possibility: there may be some acidic sites on the pure m-ZrO_2 to enhance the formation of some by-products more greatly than 3B2OL from 2,3-BDO. It is obvious that the basic sites are surely poisoned by CO_2 over CaO-5-800 (**Table 3-5**). The major role of the dehydration would be attributed by the basic sites of the abstracting ability of hydrogen of 2,3-BDO in the similar way to the dehydration of 1,4-BDO[188] over Er_2O_3 and tetragonal ZrO_2-supported CaO[186] as well as the dehydration of 1,3-BDO[152] over Er_2O_3.

3.4 Dehydration of 2,3-BDO over m-ZrO_2 modified with alkaline-earth metal oxides.

3.4.1 Effects of the MO content of the modified m-ZrO_2 on the dehydration of 2,3-BDO

In the previous section, I have studied the conversion of 2,3-BDO over CaO/ZrO_2 catalysts in details. In fact, not only CaO/ZrO_2 catalysts but also the other ZrO_2-supported alkaline-earth metal oxide catalysts such as SrO/ZrO_2, BaO/ZrO_2 and MgO/ZrO_2 catalyzed the 2,3-BDO dehydration (**Table 3-3**).

Figure 3-10 shows the effects of alkaline earth metal oxide modifier contents on both 2,3-BDO conversion and 3B2OL selectivity. This indicates that the effects of alkaline earth metal oxide modifier

contents resembled closely with each other over CaO/ZrO_2, SrO/ZrO_2, BaO/ZrO_2, and MgO/ZrO_2: the 2,3-BDO conversion decreased greatly from ZrO_2 support with increasing their modifier contents, while the 3B2OL selectivity increased greatly only at a small amount of these modifiers and almost unchanged at the large amounts. In the MgO/ZrO_2 catalysts, however, only a low content of MgO could act as a modifier in the similar way to the other alkaline earth metal oxides for the 3B2OL formation. Besides, the excess MgO inhibits the catalytic activity of ZrO_2: both the 2,3-BDO conversion and the 3B2OL selectivity decreased at the ratio of MgO/ZrO_2 increased over 0.2. Therefore, due to the high yield of 3B2OL, we choose representative samples with their most proper modifier contents such as CaO-0.0668, SrO-0.0906, BaO-0.0452, and MgO-0.0452 for the further tests.

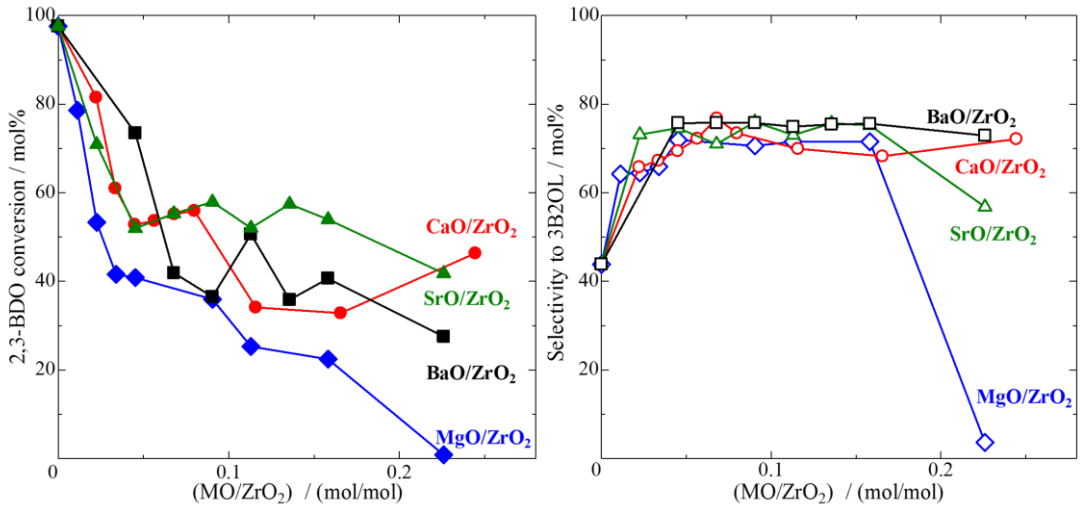

Figure 3-10 Effects of alkaline-earth metal oxide contents on the catalytic activities of ZrO_2-supported catalysts from 2,3-BDO to 3B2OL.

3.4.2 Effects of the modified m-ZrO_2 calcination temperature on the dehydration of 2,3-BDO

Figure 3-11 shows the effects of calcination temperature on the catalytic activities of the modified ZrO_2 catalysts in the dehydration of 2,3-BDO at 350°C. In all the modifiers, the 2,3-BDO conversion was maximized at a calcination temperature of 800°C. In contrast, the 3B2OL selectivity was maintained at high levels and became rarely sensitive to the calcination temperature higher than 600°C.

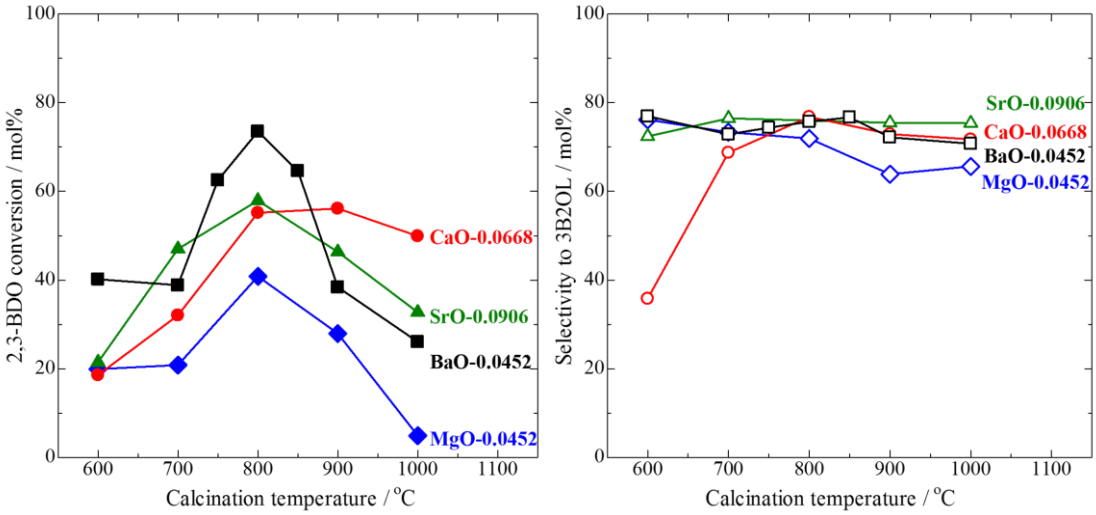

Figure 3-11 Effects of the calcination temperature on the catalytic activities of ZrO_2-supported catalysts for 2,3-BDO conversion and 3B2OL selectivity.

3.4.3 Effects of reaction temperature on the dehydration of 2,3-BDO over modified with alkaline-earth metal oxides.

Figure 3-12 shows the effect of reaction temperature over the samples of CaO-0.0668-800, SrO-0.0906-800, BaO-0.0452-800, and MgO-0.0452-800, which were calcined at 800°C. The 2,3-BDO conversion increased greatly with increasing the reaction temperature while the highest 3B2OL selectivity was obtained at 350°C. At 350°C, BaO-0.0452-800 showed both the highest 2,3-BDO conversion and the highest 3B2OL selectivity among them.

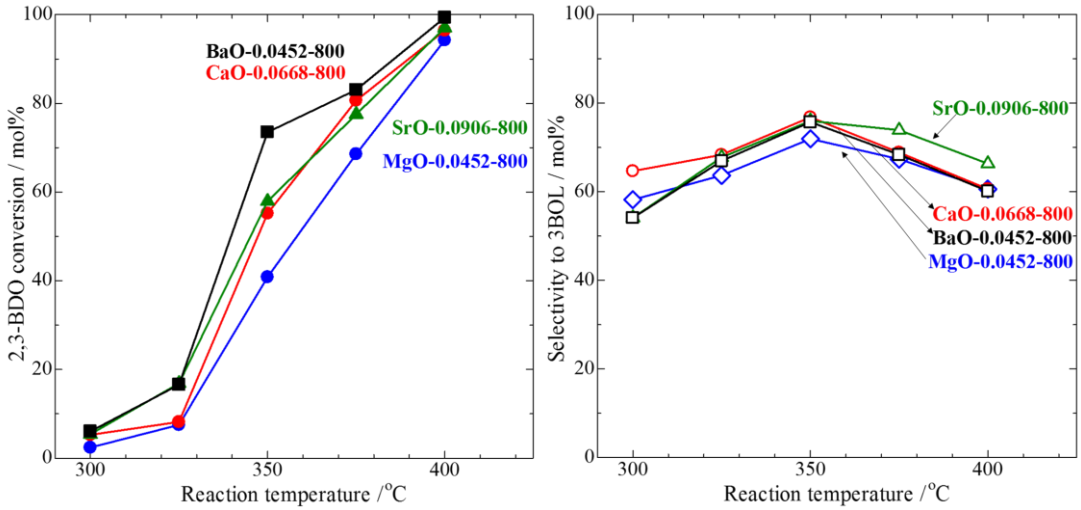

Figure 3-12 The catalytic activities of ZrO_2-supported catalysts for 2,3-BDO dehydration to 3B2OL as a function of reaction temperature.

3.4.4 Catalytic stability with time on stream over ZrO_2 modified with alkaline-earth metal oxides.

As depicted in **Figure 3-13**, the four catalyst samples maintained stable catalytic activities for both the 2,3-BDO conversion and the 3B2OL selectivity in the initial for 5 h with time on stream. Here, BaO-0.0452-800 displayed the highest 2,3-BDO conversion of 75.7% as well as the 3B2OL selectivity of 73.5%.

In the ZrO_2 modified with an appropriate content of alkaline earth metal oxides such as CaO, SrO, BaO, and also MgO, the catalytic activities of ZrO_2 were enhanced efficiently for the 3B2OL formation. Their catalytic activities resembled closely with each other for their loaded contents, calcination temperatures, reaction temperatures, and also stabilities with time on stream (**Figures3-10, 3-11, 3-12, and 3-13**). In addition, among the four modified catalysts, BaO/ZrO_2 acted the best for both 2,3-BDO conversion and 3B2OL selectivity while those of MgO/ZrO_2 were always the lowest. In the following sections, in order to identify the key factors for the enhancement of the present reaction, their structural and basic properties were investigated.

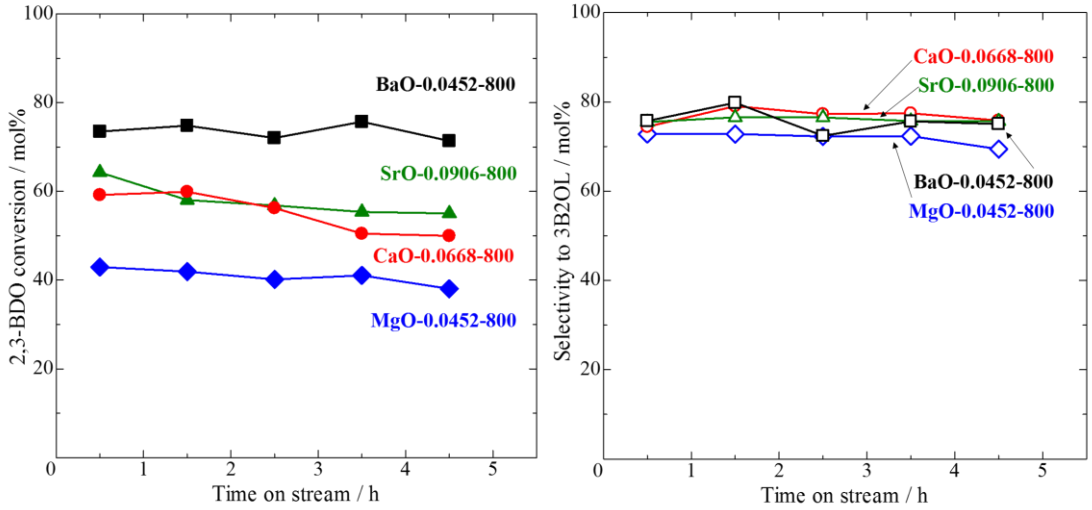

Figure 3-13 Catalytic stability of ZrO_2-supported alkaline-earth metal oxide catalysts with time on stream.

3.4.5 Characterization and discussion

3.4.5.1 Structural properties of ZrO_2-supported alkaline-earth metal oxide catalysts.

Figure 3-14 shows XRD patterns of the typical samples with different calcination temperatures and alkaline earth metal oxide contents. In the samples, main diffraction peaks are attributed from m-ZrO_2 with several additional peaks of perovskite compounds such as $CaZrO_3$, $SrZrO_3$, and $BaZrO_3$. High alkaline earth metal oxide contents and high calcination temperatures enhanced the formation of the new perovskite phases. In addition, both the formation and the crystalline growth of these new perovskite phases can be also observed in the order of $BaZrO_3 > SrZrO_3 > CaZrO_3$. In contrast to

$CaZrO_3$, $BaZrO_3$, and $SrZrO_3$ phases were detected even at low MO contents (M= Ca, Sr and Ba) and low calcination temperatures < 800ºC. However, in MgO/ZrO_2 samples, no peaks assigned to $MgZrO_3$ were detected, and the crystalline of m-ZrO_2 phase grew obviously with increasing both MgO content and calcination temperature. Thus, it is reasonable that the 3B2OL selectivity was enhanced with MgO due to the crystalline growth of m-ZrO_2, which is the most efficient ZrO_2 crystal phase including Mg^{2+} for the 3B2OL formation, as described in the part of 3.1 in detail. However, at high MgO contents and high calcination temperatures, the basic sites generated by the excess MgO and the declined specific surface area resulted in low 2,3-BDO conversion. Here, we have to check the catalytic activity of perovskite compounds such as $CaZrO_3$, $SrZrO_3$, and $BaZrO_3$.

In order to investigate the catalytic activities of the perovskite compounds, we prepared $CaZrO_3$, $SrZrO_3$, and $BaZrO_3$. As listed in **Table 3-7**, we succeeded in preparing these perovskite compounds (XRD patterns in **Figure 3-14 (b)**) but even together with a small amount of $SrCO_3$ and $BaCO_3$, which are difficult to be removed during the preparation and characterization processes in air. The results in the catalytic reaction emphasized that all the perovskite compounds showed no catalytic activity for the formation of 3B2OL from 2,3-BDO: not only the extremely low 2,3-BDO conversion but also the low 3B2OL selectivity were obtained. It can be concluded that these perovskite compounds such as $CaZrO_3$, $SrZrO_3$, and $BaZrO_3$ detected in the modified m-ZrO_2 could not provide the active sites for the 3B2OL production.

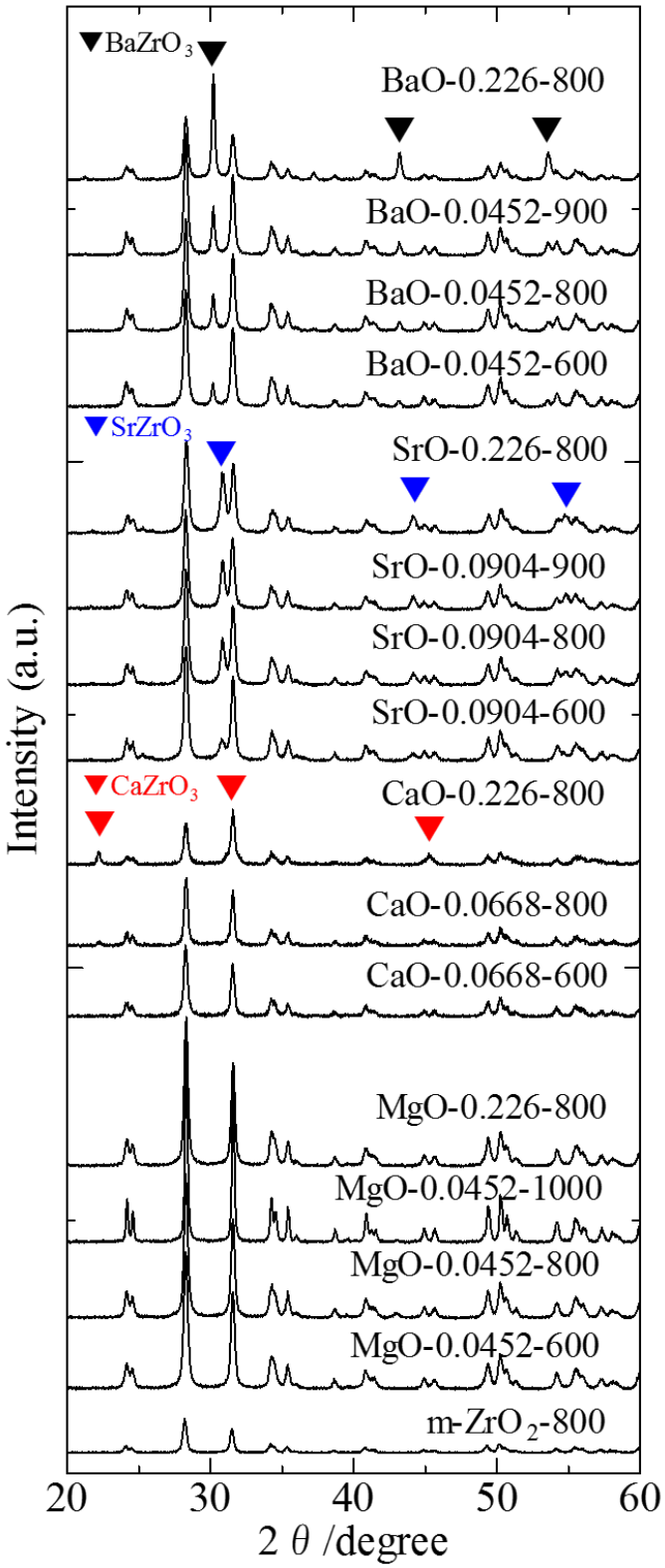

Figure 3-14 (a) XRD patterns of alkaline-earth metal oxide modified ZrO_2 catalysts: effects of calcination temperature and the alkaline-earth metal oxide contents on their crystal structures.

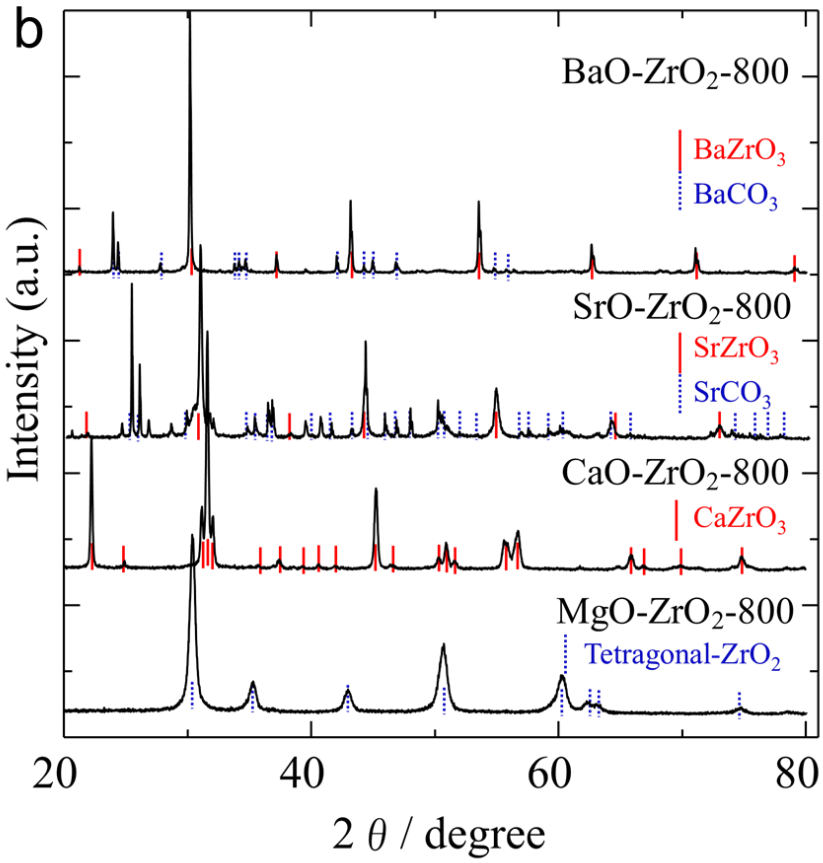

Figure 3-14 (b) XRD patterns of perovskites compounds ($MZrO_3$) aimed samples: the names in black are their aimed compositions, and the words in red and blue are the compounds detected from these samples.

Table 3-7 Reaction activities of perovskites compounds ($MZrO_3$), tetragonal $MgO\text{-}ZrO_2$ and m-ZrO_2 for 2,3-BDO dehydration.

Catalyst (1.0g)	S.A m^2 / g	Crystal composite	Conversion / mol %	Selectivity / mol %			
				3B2OL	MEK	Acetoin	Others
Blank test			1.7	7.5	12.9	47.2	32.4
$MgO\text{-}ZrO_2$	16.5	Tetragonal	16.4	52.6	9.4	20.6	17.4
$CaO\text{-}ZrO_2$	7.4	$CaZrO_3$	4.5	0.0	11.8	64.9	23.3
$SrO\text{-}ZrO_2$	<1	$SrZrO_3$+$SrCO_3$	3.3	7.1	11.0	76.0	5.9
$BaO\text{-}ZrO_2$	<1	$BaZrO_3$+$BaCO_3$	0.9	5.9	13.6	69.8	10.7
ZrO_2	26.3	Monoclinic	97.6	43.9	22.7	1.7	31.8

All the catalysts were calcined at 800°C during the preparation produce, and the reaction temperature was 350°C.

Figure 3-15 shows the O1s, Ca2p, and Zr3d XPS spectra of CaO-0.0668-800, CaO-0.226-800, and CaO-0.0668-600 samples together with CaO-800, ZrO_2-800, and $CaZrO_3$-800. Firstly, from the O1s spectra of the samples, the peak at 527.45 eV, which is different from those of both CaO-800 (529.45 eV) and ZrO_2-800 (527.83 eV), was found to be the same as that from $CaZrO_3$-800. In **Figure 3-9**, Ca-O-Zr hetero-linkages are also confirmed by the DRIFT spectra of CaO-*X*-800 samples. Thus, the new peak at 527.45 eV should be assigned to the O1s peak of Ca-O-Zr hetero-linkages, which would attribute to the base structure of $CaZrO_3$. The results also well agree with some other works.[189-196] In addition, the XPS spectra of Ca2p and Zr3d also support the Ca-O-Zr hetero-linkage formation: $Ca2p_{1/2}$ shifted from 344.92 to 344.31 eV and that of $Ca2p_{3/2}$ from 348.55 to 348.03 eV, together with $Zr3d_{3/2}$ shifting from 182.26 to 181.81 eV and that of $Zr3d_{5/2}$ from 179.92 to 179.47 eV. However, among the CaO/ZrO_2 samples, CaO-0.0668-800 presents the highest percentage of Ca-O-Zr state via its O1s XPS spectra, as well as the spectra of Ca2p and Zr3d. However, in comparison with CaO-0.0668-800, the spectra of CaO-0.226-800 show lower percentages of Ca-O-Zr hetero-linkages. This contradicts with their XRD patterns (**Figure 3-14 (a)**), in which the stronger peaks assigned to $CaZrO_3$ phase were detected from CaO-0.226-800 rather than CaO-0.0668-800. It indicates that, unlike CaO-0.226-800, Ca-O-Zr hetero-linkages were highly dispersed on the surface of CaO-0.0668-800 at the appropriate CaO loading. However, CaO-0.226-800 with excess CaO content aggregated the most Ca-O-Zr hetero-linkages to the highly crystalized $CaZrO_3$ phase, which is not active for the formation of 3B2OL from 2,3-BDO (**Table 3-7**). On the other hand, no proof of the Ca-O-Zr hetero-linkage can be found from the CaO-0.0668-600 sample though its O1s, Ca2p or Zr3d XPS spectra. In addition, the XRD pattern of CaO-0.0668-600 sample (**Figure 3-14 (a)**), as well as the samples calcined at lower than 800°C in **Figure 3-8**, displayed no peaks assigned to $CaZrO_3$ phase. It indicates that high

calcination temperature at 800°C or higher is needed for the formation of Ca-O-Zr hetero-linkage and then for $CaZrO_3$ phase. Furthermore, some groups also reported that they succeeded in preparing $CaZrO_3$ at high temperatures over 800°C. [191-195]

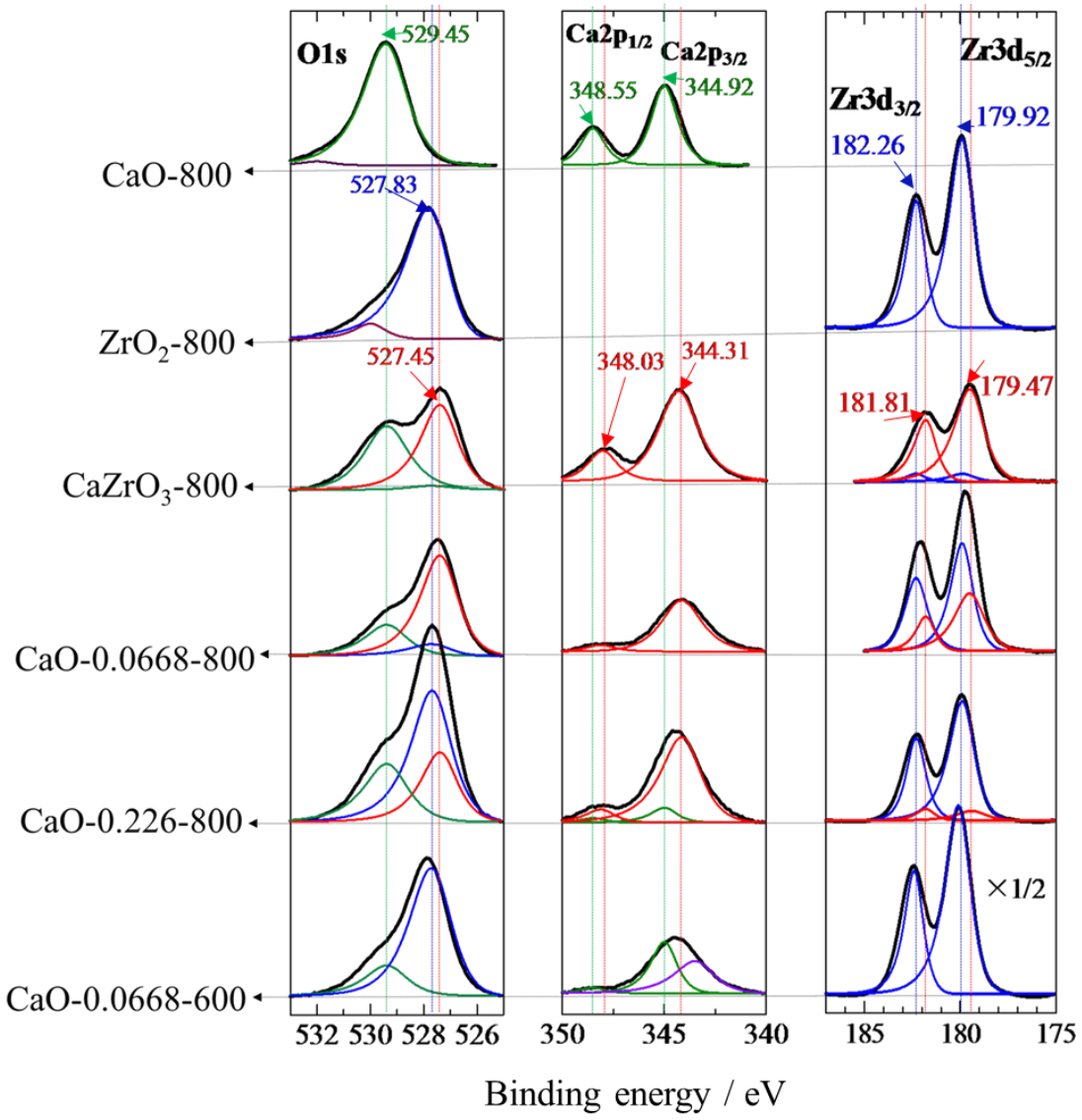

Figure 3-15 O_{1s}, Ca_{2p} and Zr_{3d} XPS spectra of CaO-800, ZrO_2-800, $CaZrO_3$-800, CaO-0.0668-800, CaO-0.226-800 and CaO-0.0668-600.

Figure 3-16 shows TG-DTA profiles of the alkaline earth metal nitrate loaded on m-ZrO_2 samples prior to calcination. These alkaline earth metal nitrates have different difficulties in decomposing metal nitrates with increasing calcination temperature, and they increase in the order of $Mg(NO_3)_2$ < $Ca(NO_3)_2$ < $Sr(NO_3)_2$ < $Ba(NO_3)_2$. They all have almost finished decomposing at lower than 600°C (**Figure 3-16** (a)). The results are also well accordance with the O1s XPS spectra shown in **Figure 3-**

15, in which only the O1s XPS peaks attributed to CaO and ZrO_2 were detected from CaO-0.0668-600 sample and no O1s XPS peak attributed to $Ca(NO_3)_2$ was observed. It can be concluded that these alkaline earth metal nitrate decomposed at temperatures lower than 600°C for the formation of CaO, and then Ca^{2+} of CaO immerged into ZrO_2 for Ca-O-Zr hetero-linkage at around 800°C, and that more Ca-O-Zr hetero-linkages aggregated and transformed to $CaZrO_3$ phase at calcination temperatures higher than 800°C. Judging from the XRD patterns (**Figure 3-14**), it is reasonable that the formation of M-O-Zr hetero-linkage and their aggregation to form perovskite phases over SrO/ZrO_2 and Ba/ZrO_2 samples should have occurred at lower temperatures than that of CaO/ZrO_2. However, even with a small amount, but their weight losses continued even above 600°C, especially the BaO-0.0452 sample seems to be further decomposed totally at higher than 1000°C (**Figure 3-16(b)**). The weight loss after 600°C should be attributed to the decomposition of their carbonates, which form easily in air environment containing CO_2.

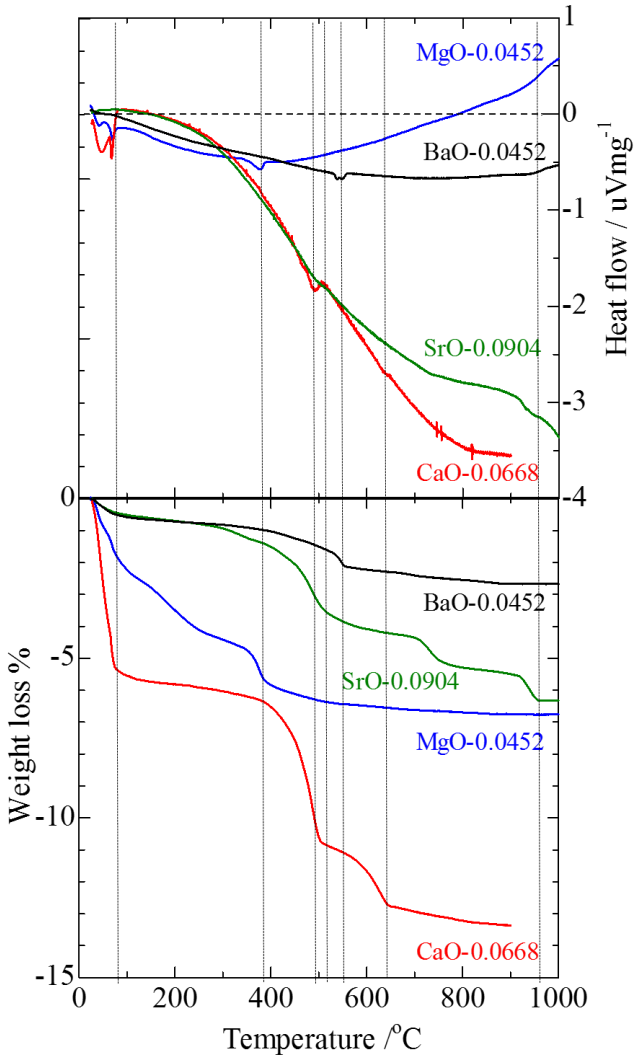

Figure 3-16 TG-DTA profiles of the alkaline-earth metal nitrate loaded ZrO_2 samples.

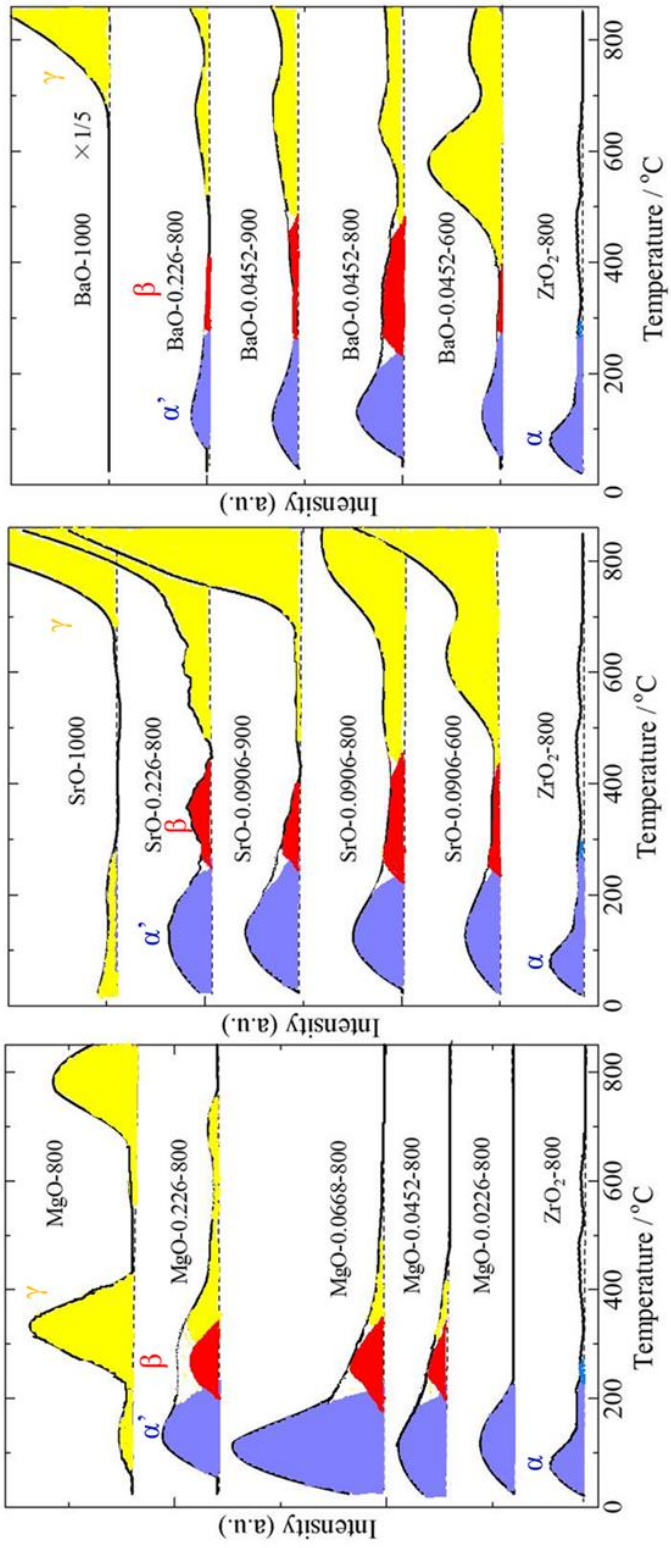

Figure 3-17 Effects of calcination temperature and alkaline-earth metal oxide contents on their basic

properties (CO_2-TPD) of the modified catalysts.

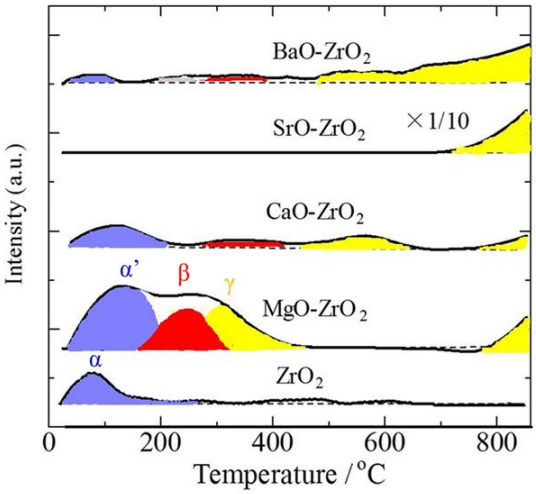

Figure 3-18 CO_2-TPD profiles of the perovskite compounds, tetragonal MgO-ZrO_2 and m-ZrO_2.

3.4.5.2 Basic properties of ZrO_2-supported alkaline-earth metal oxide catalysts

In **Table 3-5**, **Table 3-6**, **Figure 3-6** and **Figure 3-7**, the basic properties of CaO/ZrO_2 have been reported in detail. **Figure 3-17** shows the basic properties of MgO/ZrO_2, SrO/ZrO_2, and BaO/ZrO_2 investigated by CO_2-TPD. Among the samples, the CO_2 desorption peaks attributed to weak basic sites were detected as shifting slightly from 77°C to 115°C (peaks α and α'), and their amount increased properly with increasing the alkaline earth metal oxide contents. Besides, the desorption peak β attributed to new medium basic sites was also found at around 350°C from SrO/ZrO_2 and BaO/ZrO_2 in the same way as CaO/ZrO_2, as shown in **Figure 3-7B**. The peaks γ at temperatures higher than 600°C were detected over SrO/ZrO_2 and BaO/ZrO_2. The similar peak was also detected at around 500°C over CaO/ZrO_2 (**Figure 3-7B**). They could be resulted from the CO_2 desorbed from the rare alkaline earth metal oxides. However, the peaks higher than 800°C could be resulted from the decomposition of their carbonates. In the actual reactions performed at 350 °C, the peak γ of the adsorption sites, which strongly adsorb CO_2, could not be attributed to the reaction.

On the other hand, new peaks generated on MgO/ZrO_2 samples were detected at around 250°C, even few but such changes on its basic property must be related to the structural changes as described in the previous section of XRD (**Figure 3-14 (a)**). The desorption peaks at 335°C were resulted from the excess MgO and it should be the reason for the decrease in the catalytic activity of MgO/ZrO_2 catalysts in **Figure 3-10**. The CO_2-TPD profiles of MgO/ZrO_2 resembled closely to the reports elsewhere. [197-199]

The intensity of peaks β varies with contents of those modifiers respectively. Especially, at molar ratio MgO/ZrO_2 = 0.0226, SrO/ZrO_2 = 0.0906, and BaO/ZrO_2 = 0.0452, as well as CaO/ZrO_2 = 0.0668

(as reported in **Figure 3-7**), the largest amount of basic sites β were detected. The samples calcined at 800°C show the largest amount of basic sites β, but the amount decreased with increasing calcination temperature. Of course, the catalysts, with the largest amount of basic sites β, were also confirmed as the most active ones for the high 2,3-BDO conversion and the high 3B2OL selectivity.

Figure 3-18 shows CO_2-TPD profiles of the MgO-ZrO_2 mainly composed of tetragonal ZrO_2 and the perovskite compounds of $MZrO_3$ (M= Ca, Sr, and Ba), which showed no good catalytic activities for the 3B2OL formation from 2,3-BDO (**Table 3-7**). Over the perovskite compounds of $MZrO_3$, the decomposition peaks resulted from their carbonates were mainly observed but rare basic sites appeared. Over the MgO-ZrO_2 i.e. tetragonal ZrO_2, large desorption peaks attributed to new basic sites with medium strength were observed at around 250°C. As reported in my previous work (**Table 3-1**), tetragonal ZrO_2 was not suitable for the formation of BD and 3B2OL from 2,3-BDO. In the present study, however, the new medium-strength basic sites would have contributed to the formation of 3B2OL even with a low reactant conversion by incorporating Mg^{2+} in the tetragonal ZrO_2.

Although the perovskite compounds of $MZrO_3$ have no active basic sites β, $MZrO_3$ phase was detected in the XRD patterns of modified m-ZrO_2 catalysts which showed catalytic activities for the present reaction. Among the CaO/ZrO_2 catalysts, however, CaO-0.0668-800 has only weak XRD peaks attributed to $CaZrO_3$, but it has the most percentages of O1s XPS peak assigned to the Ca-O-Zr hetero-linkage highly dispersed on its surface. These highly dispersed hetero-linkage could have attributed to the most amount of basic sites β, and also enhanced the 3B2OL formation from 2,3-BDO. Thus, the highly dispersed Ca-O-Zr hetero-linkage on its surface must have generated the basic site β, which acts as the active site for the production of 3B2OL. As discussed in the research of Zhang's group,[186] the uneven distribution in charges of the Ca-O-Zr hetero-linkage generates new acidic and basic sites, which is different from those of the pure CaO and ZrO_2. In the XPS spectra of the samples containing Ca-O-Zr hetero-linkage (**Figure 3-15**), it can be found that not only the O_{1s}, but also their Ca_{2p} and Zr_{3d} spectra shifted to lower energy positions as compared with those of pure CaO and ZrO_2. Thus, it can be concluded that the bond distances of Ca-O-Zr are smaller than those of pure CaO and ZrO_2. Since our research group found that the formation rates of some unsaturated alcohols from diols are very sensitive to the ionic radii of cations in the rare earth metal oxide catalysts, as shown in **Figure 1-12**.[153] Here via the highly dispersed hetero-linkages forming, the distance between these active sites should also be adjusted much more suitably for the present reaction. In addition, the O_{1s} spectra shifting to lower energy positions would contribute to the new medium basic sites β, which I speculated as the O^{2-} from Ca-O-Zr hetero-linkage. Since the O^{2-} of CaO has stronger base than that of ZrO_2, the O^{2-} from Ca-O-Zr distributes more charge to Zr^{4+} and resulted in the basic O^{2-} as the medium basic sites β weaker than the O^{2-} of CaO, but still stronger than that of ZrO_2. On the other hand, their Ca_{2p} and Zr_{3d} spectra shifting to lower energy positions must also adjust the acidic sites balance which should be much more suitable for the present reaction. I propose that the formation of

3-buten-2-ol proceeds via acid-base concerted mechanism. The present MO/m-ZrO_2 catalysts must efficiently work with the basic modifiers in a fine acid-base balance for the formation of 3B2OL from 2,3-BDO. Since Zhang groups detected the changes in acidity of CaO/ZrO_2 via NH_3-TPD,[186] I will perform further work to identify these acid sites of the modified ZrO_2 catalysts.

3.4.6 Speculative reaction mechanism over CaO/ZrO_2 catalyst

In a Similar way to CaO/m-ZrO_2 catalysts, I also found that with a moderate amount content loaded, m-ZrO_2- supported alkaline-earth metal oxides such as SrO, BaO and also MgO can enhance 3B2OL selectivity and maintain the high reactant conversion. Especially, among all the m-ZrO_2 supported alkaline-earth metal oxides, the BaO/m-ZrO_2 samples calcined at 800°C with the lowest content mount of BaO (molar ratio BaO:ZrO_2=0.0452) but the highest reactant conversion of 75.7% and 3B2OL selectivity of 73.5% at 350°C. Not only their reaction results but also their basic properties and their crystal structures resembled greatly with each other. It should be concluded that, by loading these alkaline-earth metal oxides onto m-ZrO_2 with proper contents and also calcined at 800°C, the highly dispersed M-O-Zr hetero-linkage on their surface were formed to adjust the proper distances of these active sites and also to generate the proper acid-base balance for the 3B2OL formation from 2,3-BDO.

On the other hand, our research group has calculated the stable adsorption structure of 1,4-BDO on Er_2O_3 catalyst using theoretical calculations, and proposed a reasonable mechanism in the reaction of 1,4-BDO.[200] Our research group has also demonstrated the acid-base concerted mechanism over Er_2O_3 for the formation of 3-buten-1ol from 1,4-BDO.[188,200] The most reasonable adsorption structure is a tridentate coordination that the position-2 hydrogen atom of 1,4-BDO is placed on the top of an oxygen anion of Er_2O_3, and that two hydroxyl groups of 1,4-BDO fill two oxygen vacancies of the Er_2O_3 surface. The oxygen anion and the oxygen vacancy can be regarded as a basic and an acidic site, respectively. The estimated reaction mechanism is as follows: first, a hydrogen atom at position 2 is abstracted by an oxygen anion; consequently, the hydroxyl group at position 1of 1,4-BDO is abstracted by a Ln cation to form π bond between the carbon at position 1 and position 2; finally, unsaturated alcohol is desorbed. It was concluded that the conversion of 1,4-BDO into 3B1OL over Er_2O_3 proceeds with an acid-base concerted mechanism.[200]

The poisoning experiments in **Figure 3-6** directly indicates that the basic and acidic sites on the modified catalyst cooperatively work as active sites to produce 3B2OL from 2,3-BDO. I succeeded in introducing the acid-base sites, which have acted as the active sites for 2,3-BDO conversion, to the well-crystallized surface of pure m-ZrO_2 through impregnation of CaO. In order to understand how the acid-base sites acting as active center for the formation of 3B2OL from 2,3-BDO, I propose a speculative mechanism described in **Scheme 3-3**. The mechanism is speculated from the mechanism above-mentioned in the dehydration of 1,4-BDO over Er_2O_3 catalyst.[200]

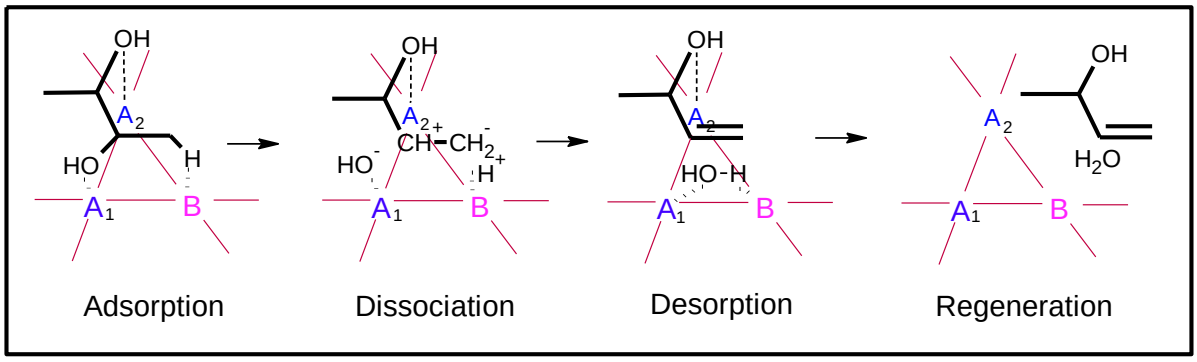

Scheme 3-3 Activation of 2,3-BDO to produce 3B2OL over acid(A)-base(B) concerted active sites.

In **Scheme 3-3**, the active center consists of a basic site (expressed as B) and two acidic sites (expressed as A_1 and A_2). Four reaction steps involve adsorption, abstraction, dissociation, and regeneration. In the first step, an oxygen in OH groups of 2,3-BDO is captured by the acidic sites A_1 when the reactant 2,3-BDO is passing the catalyst. Then, the other OH is also captured by another acidic site A_2. Finally, the adsorptive interaction between a hydrogen of the methyl group and the basic site B on the catalyst appears to form a tridentate coordination with the largest adsorption energy. In the second step, the hydrogen of methyl group is eliminated by the basic site B to form an anion and followed by elimination of HO^- on an acidic site A_1 to form a cation. It is probable that the formation of a pair of C^+ and C^- which could lead to 3B2OL should be produced over a pair of acidic and basic sites. In the third step, the formation of C=C bond occurred by the shortening of C^+-C^- bond and the lengthening of A_1-OH and B-H bonds for the formation of a water molecule. The final step involves the departure of a water molecule from the acid-base pair sites and the oxygen of OH group desorbs from an acidic site A_2 for the departure of 3B2OL.

There is another possibility of the adsorption (**Scheme 3-3**): an active center consists of an acidic site A and a basic site B to form a bidentate adsorption. When the OH groups of 2,3-BDO could be adsorbed on a basic site and an acidic one, a hydrogen of OH group and the other OH group could be eliminated by cooperatively acid-base sites to form CH_3CHO^--C^+HCH_3, which could be readily isomerized to MEK.

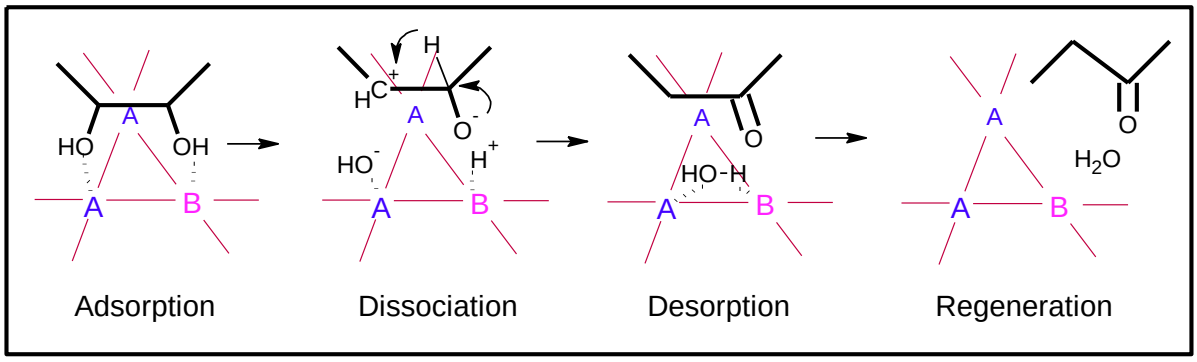

Scheme 3-4 Activation of 2,3-BDO to produce MEK over acid(A)-base(B) concerted active sites.

Over pure m-ZrO_2, considerable amounts of MEK and MPA are produced (**Table 3-1**). It is reasonable that an OH group is eliminated by an acidic site to form $CH_3CH(OH)C^+HCH_3$, which can lead to MPA via pinacol rearrangement. The intermediate $CH_3CH(OH)C^+HCH_3$ could also be deprotonated to produce 3B2OL and MEK. Actually, MEK is a major product in the reaction of 2,3-BDO catalyzed by acidic zeolites.[133] The formation of MEK and MPA over pure m-ZrO_2 can be explained by the acid-catalyzed formation of $CH_3CH(OH)C^+HCH_3$ during the dissociation in **Scheme 3-4**. Actually, the selectivity to 3B2OL is upgraded greatly by the poisoning of acidic sites of pure ZrO_2 in NH_3 (**Table 3-5**). And by loading the Alkaline-earth metal oxides such as CaO on the well-crystallized ZrO_2, not only some acidic sites were poisoned but also some new basic sites β were also generated as the active sites for the formation of 3B2OL.

3.5 Dehydration of 2,3-BDO into 3B2OL over rare earth metal oxides (Ln_2O_3)

It is also well known that, 3B2OL is used as the important intermediates for the synthesis of monomer esters and medicines.[33,202] The production 3B2OL from bio-2,3-BDO is also under great expectation. It seems that the dehydration of 2,3-BDO generally results in good yields of MEK over acidic catalysts.[131-133, 201] In the pioneering work of Winfield, it is reported that ThO_2 catalyzes the dehydration of 2,3-BDO into 3B2OL with a yield of 70.3% at 350°C, and a BD yield of 62.1% was obtained with a 3B2OL yield of only 8.4% at 500°C.[119] ThO_2 was also reported as acid-base solid.[169] Unfortunately, ThO_2 cannot be applied as industrial catalyst for its radio-active property. Thus, in the section of 3.1, I have investigated several possible metal oxide catalysts and found that highly crystallized monoclinic ZrO_2 with acid-base proprieties, exhibits high catalytic activity in the conversion of 2,3-BDO to 3B2OL. I also succeeded in preparing the well-adjusted acid-base catalysts MO/ZrO_2 (M= Ca, Ba, Sr and Mg) to produce 3B2OL from 2,3-BDO to take the place of ThO_2.

However, I have not check the activities of the catalysts without acid sites on the present reaction. In addition, rare earth metal oxides were found without acid proprieties and only a few weak basic sites.[203] I have also reported several examples on the synthesis of unsaturated alcohols from

alkanediols over rare earth oxides (Ln_2O_3).[153] Catalytic activities of these Ln_2O_3 depends on the position of OH groups of reactant diols: 1,3-diols are effectively dehydrated into 3B2OL and 2-buten-1-ol by CeO_2, 1,4-BDO can be dehydrate to 3B1OL by Er_2O_3 Yb_2O_3 and Lu_2O_3,[153] and 1,5-pentanediol to 4-penten-1-ol by $Sc_{0.5}Yb_{1.5}O_3$.[204] Lattice parameter of the cubic rare earth oxides seems to affect the adsorption and activation of alkanediols.[204] Among all the rare earth oxide catalysts, Sc_2O_3 with the smallest cation radius but always shows perfect selective activities especially in the dehydration of terminal diols including 1,6-hexanediol, 1,7-heptanediol, 1,8-octanediol, 1,9-nonanediol, 1,10-decanediol, and 1,12-dodecandediol to their corresponding unsaturated alcohols.[205, 206] In this section, I investigated the reaction of 2,3-BDO over the rare earth oxides and the bixbyite In_2O_3, which has a specially catalytic activity in the conversion of 1,4-BDO to produce 3B1OL.[156, 207]

3.5.1 Dehydration of 2,3-BDO into 3B2OL catalyzed by all the rare earth metal oxides at low reaction temperatures

Table 3-8 Synthesis of 3B2OL from 2,3-BDO over Ln_2O_3.

Catalyst	Conversion	Selectivity / mol%[a]			
(1.0 g)	/ mol%[a]	3B2OL	MEK	acetoin	Others[b]
Sc_2O_3	99.9	85.0	2.8	4.9	7.3
In_2O_3	59.4	65.8	4.0	16.5	12.0
ZrO_2[c]	62.5	48.6	16.0	14.9	20.5
$Sc_{1.5}Yb_{0.5}O_3$	35.1	53.4	3.1	16.7	26.8
$ScYbO_3$	28.4	47.8	3.9	23.7	24.6
$Sc_{0.5}Yb_{1.5}O_3$	22.6	33.6	3.8	34.3	28.3
Lu_2O_3	16.5	19.8	7.6	42.4	30.2
Yb_2O_3[c]	17.5	28.1	1.8	39.5	30.6
Tm_2O_3	1.9	0.0	6.7	40.2	53.1
Er_2O_3	14.3	14.5	2.4	45.9	37.2
Y_2O_3	11.5	7.6	2.7	49.7	40.0
Ho_2O_3	7.3	3.9	17.1	39.8	39.2
Dy_2O_3	11.3	20.3	3.9	40.9	34.9
Tb_4O_7	9.9	3.9	3.2	53.6	39.3
Gd_2O_3	10.0	12.9	4.8	45.4	36.9
Eu_2O_3	10.9	4.3	4.3	43.8	47.6
Sm_2O_3	8.9	5.6	2.8	52.2	39.4
CeO_2	39.1	1.3	36.5	21.5	40.7
Nd_2O_3	7.4	4.8	5.4	49.4	40.4
Pr_6O_{11}	8.2	1.3	6.2	51.8	40.7
La_2O_3[c]	7.0	5.0	7.3	47.8	39.9

[a] Reaction temperature, 325°C; carrier gas, H_2, 45 cm^3 min^{-1}; all the Ln_2O_3 catalysts were purchased from Kanto CHEMICAL CO., INC. and calcined at 800°C for 3 h. The reactant conversion and each selectivity of its products were calculated and averaged in the initial 5 h.

[b] Include MPO, MPA, BD, propylene, ethylene, 1- and 2-butanol.

[c] Cited from **Table 3-1**.

Table 3-8 shows that all the rare earth metal oxides showed their catalytic activities to convert 2,3-BDO into 3B2OL even through being different greatly in yields. The main byproducts obtained were acetoin and MEK but rare BD. It also suggests that, at such low reaction temperature, the Ln_2O_3

catalysts such as Y_2O_3, Pr_6O_{11}, Nd_2O_3, La_2O_3, Sm_2O_3, and Tb_2O_3 showed their higher dehydrogenation abilities to acetoin rather than the dehydration abilities to 3B2OL. On the other hand, the selectivities completed violently between 3B2OL and acetoin over Yb_2O_3 and Dy_2O_3. While the catalysts such as Sc_2O_3, In_2O_3, and ZrO_2 effectively catalyzed the production of 3B2OL from 2,3-BDO. Especially, Sc_2O_3 gave not only the highest 3B2OL selectivity of 85.0 mol% but also a conversion of 99.9 mol% in an average of the initial 5 h. Next to Sc_2O_3, In_2O_3 and ZrO_2 also showed high activities to produce 3B2OL with 65.8% selectivity at 59.4% conversion. I have discussed the properties and the activities of ZrO_2 in the sections of 3.1~3.4. In the present work, I will focus on the catalytic activities of Sc_2O_3 and In_2O_3.

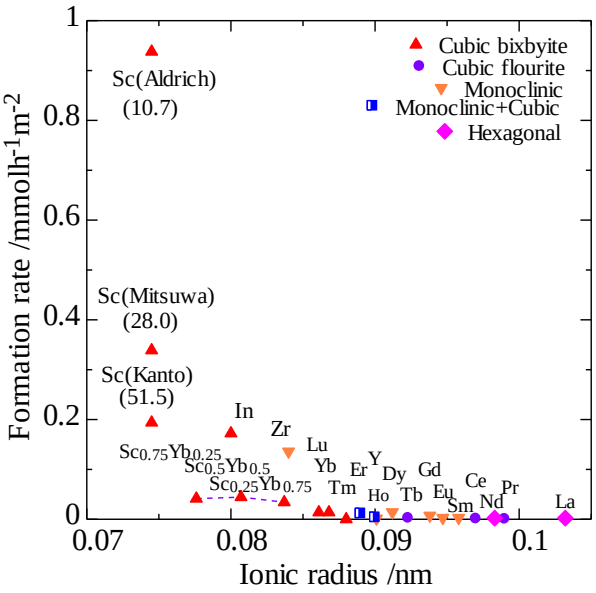

Figure 3-19 The formation rate of 3B2OL (purple) from 2,3-BDO (red) related to the average ionic radius of Ln cations. Reactions were conducted at 325°C, the ionic radii of trivalent Ln cations were based on the coordination of number 6 (Ce^{4+} with coordination number 8) were cited from the work of Shanon et al. ,[208] and the specific surface area of the rare earth oxide catalysts and crystal phase were partly cited from our previous work.[203, 204]

Figure 3-19 also shows the dependence of the catalytic activity of 3B2OL formation from 2,3-BDO on the average ionic radii of In^{3+}, Zr^{4+} and the other rare earth metal cations. In my previous work I found that Ln_2O_3 with small ionic radii are more effective in the formation unsaturated of alcohols from diols.[153] And Sc_2O_3 always shows the highest formation rate of those unsaturated alcohols for its smallest ionic diameter.[206] In the present work the tendency was also observed and the highest formation rate of 3B2OL was also obtained over Sc_2O_3. It also indicates that more active sites may generate on the smaller the specific surface area for faster formation rate over Sc_2O_3 catalyst.

It is really reasonable that In_2O_3 and ZrO_2 also displayed high formation rate of 3B2OL since their ionic diameters are just next to Sc_2O_3.

3.5.2 Dehydration of 2,3-BDO into 3B2OL over Sc_2O_3 and In_2O_3 calcined at different temperatures.

Table 3-9 summaries the reaction of 2,3-BDO over Sc_2O_3 calcined at different temperatures. It indicates that higher calcination temperature enhanced the catalytic activities of Sc_2O_3 for higher 3B2OL selectivity. I also learned that the calcination led Sc_2O_3 catalyst grow to large particles with well-crystallized structure,[203] which might have offered the small but active surface for the dehydration of 2,3-BDO to 3B2OL. And in order to confirm the roles of calcination, Sc_2O_3 catalyst supplied by Mitsuwa Co., Lot. and SIGMA-Aldrich, Co., Lot. were also investigated as comparisons. After being calcined at 800°C they both showed not only higher conversion but also higher 3B2OL selectivity. Those results are well accord with that of the Sc_2O_3 catalyst purchased from Kanto Chemical Co. Inc.

Table 3-9 Dehydration of 2,3-BDO over Sc_2O_3 annealed at different temperatures.

Calcination	SA	Conversion	Selectivity / mol%[a]			
temp. /°C	/ m^2g^{-1}	/ mol%[a]	3B2OL	MEK	Acetoin	Others[b]
As-received	98.4	69.8	52.3	9.2	11.4	27.1
600	72.1	99.0	79.8	4.9	0.3	15.0
700	66.2	97.1	83.1	4.0	0.9	12.0
800	51.5	99.9	85.0	2.8	4.9	7.3
800[c]	---	96.6	72.1	7.5	1.0	19.4
900	45.4	95.8	84.1	4.3	1.1	10.5
1000	31.9	94.7	84.8	4.9	1.2	9.1
As-received[d]	33.0	19.7	71.8	4.5	12.9	10.8
800[d]	28.0	91.0	88.3	2.0	1.3	8.4
As-received[e]	---	10.5	50.6	12.4	21.2	15.8
800[e]	10.7	96.5	88.2	1.4	3.5	6.9

[a] Reaction temperature, 325°C; carrier gas, H_2, 45 cm^3 min^{-1}; catalyst weight, 1.0 g; the reactant conversion and products selectivities were averaged b in the initial 5 h. The specific surface data of the Sc_2O_3 catalyst supplied by Kanto CHEMICAL CO., INC. were cited from ref.[20].

[b] Mainly Include MPA, MPO, BD, propylene, ethylene, 1- and 2-butanol.

[c] Carrier gas, N_2, 45 cm^3 min^{-1}.

[d] Supplied by Mitsuwa Chemical Co., Ltd., carrier gas H_2, 80 cm^3 min^{-1}.

[e] Supplied by SIGMA-Aldrich, Co., Lot., carrier gas H_2, 45 cm^3 min^{-1}.

The catalytic activities of In_2O_3 calcined at different temperatures were also investigated and just as displayed in **Table 3-10**. With the same bixbyite structure[156] as Sc_2O_3, In_2O_3 also showed higher conversion at a higher calcination while the highest selectivity was obtained when it was calcined at 400 °C but not at 800°C.

Table 3-10 Dehydration of 2,3-BDO over In_2O_3 calcined at different temperatures.

Calcination temp. /°C	Conversion / mol%[a]	Selectivity / mol%[a]			
		3B2OL	MEK	Acetoin	Others[b]
As-obtained	66.5	73.6	1.7	7.8	16.9
400	51.9	79.6	1.5	11.6	7.3
400[c]	98.0	75.2	4.9	7.8	12.1
600	55.7	75.2	1.9	14.3	8.6
800	72.9	68.5	1.8	9.2	20.5

[a] Reaction temperature, 305°C; carrier gas, H_2, 45 cm^3 min^{-1}; catalyst weight, 1.0 g; average conversion and selectivity in the initial 5 h.

[b] Mainly include MPA, MPO, BD, propylene, ethylene, 1- and 2-butanol.[c] Carrier gas, N_2, 45 cm^3 min^{-1}.

3.5.3 Effects of reaction temperature on the dehydration of 2,3-BDO into 3B2OL over Sc_2O_3 and In_2O_3.

Figure 3-20 shows that effects of reaction temperature on the dehydration of 2,3-BDO into 3B2OL over Sc_2O_3 and In_2O_3. The dehydration of 2,3-BDO over both Sc_2O_3 and In_2O_3 increases with increasing reaction temperature. Both of them also showed the highest yield to 3B2OL at 325°C. The increasing reaction temperature decreased the selectivity to 3B2OL increased that of BD.

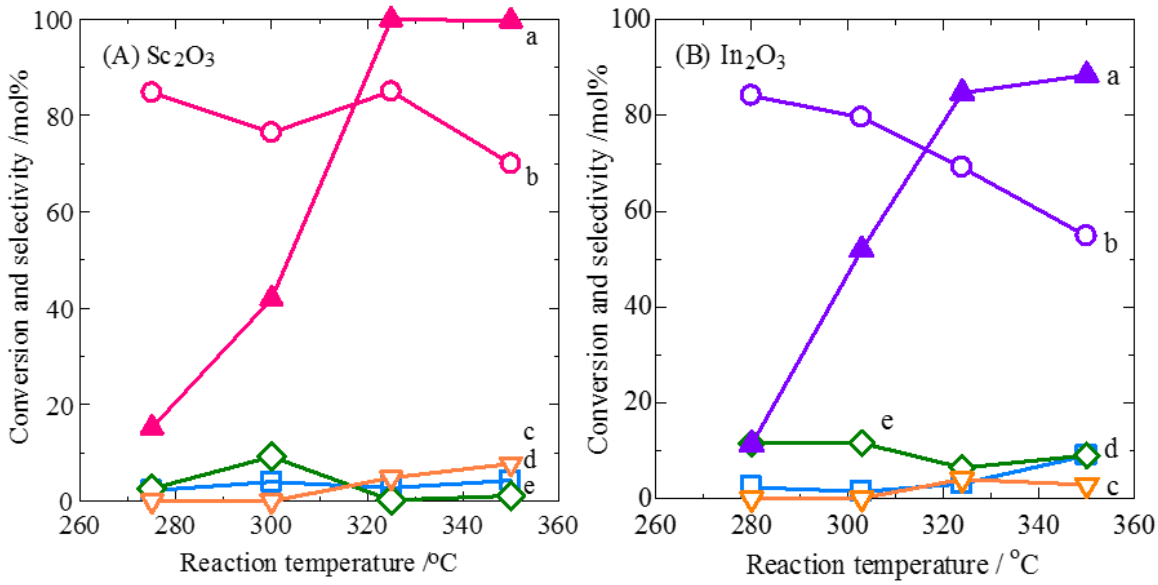

Figure 3-20 Influence of reaction temperature on the dehydration of 2,3-BDO over (A) Sc_2O_3 calcined at 800°C and (B) In_2O_3 calcined at 400°C. (a) Conversion of 2,3-BDO, (b) Selectivity to 3B2OL, (c) Selectivity to BD, (d) Selectivity to MEK, (e) Selectivity to acetoin; The flow rate of H_2, 45 cm^3 min^{-1}; Catalyst weight, 1.0 g, feed rate of 2,3-BDO, 1.06 g h^{-1}.

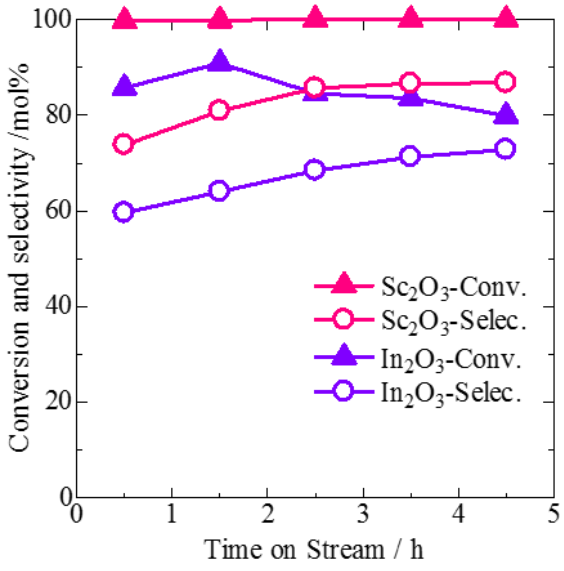

Figure 3-21 The stabilities of Sc_2O_3 calcined at 800°C and In_2O_3 calcined at 400°C in the dehydration of 2,3-BDO at 325°C; The flow rate of H_2, 45 cm^3 min^{-1}; Catalyst weight, 1.0 g; feed rate of 2,3-BDO, 1.06 g h^{-1}.

Figure 3-21 shows the changes in catalytic activities of Sc_2O_3 and In_2O_3. When the reaction temperature was 325°C the stable catalytic activities of Sc_2O_3 catalyst calcined at 800°C can be confirmed. On the other hand, from **Table 3-10**, it is obvious that In_2O_3 calcined at 400°C showed the highest selectivity to 3B2OL. Thus, its stable catalytic activity was also investigated at 325°C. The result showed that In_2O_3 kept stable selectivity just like Sc_2O_3 catalyst did but the conversion of 2,3-BDO decreased slightly with time on stream.

It is concluded that vapor-phase 2,3-BDO conversion to produce 3B2OL can be obtained over Sc_2O_3, In_2O_3, and ZrO_2. Especially at 325°C, Sc_2O_3 calcined at 800°C effectively catalyzed the dehydration with a selectivity of 85.0 mol% to 3B2OL, and also a conversion of 99.9 mol% stably. In_2O_3 calcined at 400°C also showed a good selectivity of 65.8% to 3B2OL and 59.4% conversion at 325°C. Calcination at proper temperatures can make the large Sc_2O_3 (800°C) and In_2O_3 (400°C) particles with better crystallized structure for a higher yield of 3B2OL.

3.5.4 Speculative reaction mechanism for 3B2OL formation over Sc_2O_3 catalyst

I have proposed a probable reaction mechanism in the formation of 3B2OL from 2,3-BDO with a tridentate coordination over the active center consisted of two acidic (A_1, A_2) sites and a basic (B) site (**Scheme 3-2**). The site B is a basic site with medium strength newly generated by such heterolinkage of Ca-O-Zr on the alkaline-earth metal oxides modified monoclinic ZrO_2. Cubic bixbyite-type oxides such as Ln_2O_3 have regular oxygen defects spread over the (222) facets. Over Sc_2O_3, an O^{2-} anion presents a site B, and Ln^{3+} cations and/or oxygen defect sites act acidic site, A_1 and A_2. The site B eliminates the 1-position proton, following the neighboring OH^- group eliminated by the site A_1, to produce 3B2OL, while the site A_2 has a significant function for anchoring the diol molecule (**Scheme 3-5**). Here, A (including A_1 and A_2) and B sites are proposed to be Sc^{3+} and O^{2-}, respectively. That is why the high 3B2OL selectivity is acheived in the dehydration of 2,3-BDO over Sc_2O_3. Monoalcohols such as 1-/2-butanols and 3B2OL, however, are much less reactive than BDOs over the catalysts.

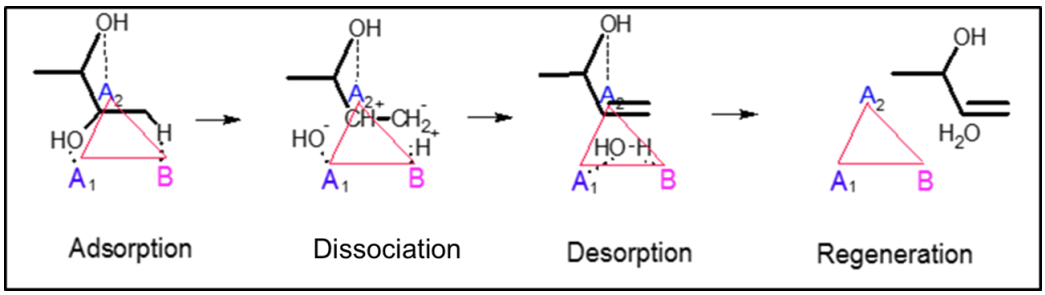

Scheme 3-5 Activation of 2,3-BDO to produce 3B2OL over acid(A)-base(B) concerted active sites.

Among Ln_2O_3 catalysts together with In_2O_3, Sc_2O_3 has the smallest ionic radii and they showed the highest 3B2OL selectivity in 2,3-BDO dehydration. In the surface geometry of Ln_2O_3, distances

between surface cations and anions depend on ionic radii of RE cations. I compare the formation rate of different UOLs such as 1,3-, 2,3-, and 1,4-BDOs over Ln_2O_3 (**Figure 1-12 and Figure 3-19**). The fastest formation rate was shown at 0.0977 nm (Lu^{3+}) for 1,3- and 1,4-BDOs and at 0.0870 nm (Sc^{3+}) for 2,3-BDO. Surface basicity of Ln_2O_3 decreased with decreasing ionic radii of Ln cations, and Sc_2O_3 show no acidity which can be detected by NH_3-TPD but only rare weak basic property. In the dehydration of BDOs, 1,3- and 1,4-BDOs have similar reactivity over Ln_2O_3 at temperatures at a range of 325-375°C.[153] Exceptionally, CeO_2 is active in the formation of unsaturated alcohols from 1,3-BDO: the reactivity of 1,3-BDO is ten times higher than that of 1,4-BDO over CeO_2 at the same temperature. 2,3-BDO is less reactive than the other BDOs even in Sc_2O_3: the reactivity of 2,3-BDO is a third of that of 1,3-BDO over Sc_2O_3 (**Figure 1-12 and Figure 3-19**). It should be agreed that the surface geometry determined by ionic radii of Ln cations has affected their catalytic activities, as well as the activated adsorption structure for BDOs on the surface of Ln_2O_3 catalysts.

Chapter IV: Dehydration of 2,3-BDO into BD

Winfield reported that in the dehydration of 2,3-BDO over ThO_2: 3B2OL was mainly obtained with a selectivity of 70% at 350 °C, and BD was mainly obtained with a selectivity of about 62% together with 3B2OL selectivity of only 8% at 500 °C.[119] This indicates that 3B2OL and BD can be obtained as stepwise dehydration products of 2,3-BDO at low and high reaction temperatures, respectively. In my present work, I have synthesized 3B2OL at high yields from 2,3-BDO over monoclinic ZrO_2, alkaline earth metal oxides-modified monoclinic ZrO_2 at 350 °C and also In_2O_3 and several Ln_2O_3 catalysts, especially Sc_2O_3 at 325 °C. Unfortunately, neither monoclinic ZrO_2 nor the modified ones showed their activities to produce BD even at high reaction temperatures. However, the possibilities of In_2O_3 and rare earth metal oxide Ln_2O_3 catalysts have not been evaluated at high temperatures.

4.1 Dehydration of 2,3-BDO catalyzed by Ln_2O_3 at high reaction temperatures.

Table 4-1 summarizes the catalytic reaction results of 2,3-BDO over the Ln_2O_3 catalysts at 425 °C. In the dehydration of 2,3-BDO, BD was mainly produced only over Sc_2O_3, together with by-products such as 3B2OL, MEK, MPA, MPO, and butene isomers. In particular, Sc_2O_3 calcined at 800 °C showed a high BD yield of 88.3% at 411 °C. Lu_2O_3 showed almost the same ability for the formation of BD and MEK. The other Ln_2O_3 such as Er_2O_3, Yb_2O_3, Y_2O_3, Dy_2O_3, Ho_2O_3, Tb_4O_7, Gd_2O_3, Sm_2O_3 and Nd_2O_3 displayed similar catalytic activities to form 3B2OL and MEK, but BD was not produced.

Figure 4-1 summaries the relationship between the ionic radii of Ln_2O_3 and their formation rate of BD. Sc_2O_3, $Sc_{2-x}Yb_xO_3$, and Lu_2O_3 have the same cubic crystal phase, as shown in **Table 4-1**. Among the Ln_2O_3 catalysts, Sc_2O_3 has the smallest ionic radius and showed the highest BD selectivity. Lu_2O_3 also showed the selectivity to BD while the others with larger ionic radii showed no catalytic abilities to produce BD. In this section, the highest formation of BD is obtained over Sc_2O_3 at 411°C (**Figure 4-1**). Thus, Sc_2O_3 with the smallest ionic radius of Sc^{3+} would provide a suitable surface for the adsorption of 2,3-BDO for the formation of BD. It is the smallest ionic radius Sc^{3+} that made it most possible for the proper distance between the dehydration active sites, which is convenient for the formation of BD.

Relationships between the ionic radii of Ln cations[203,208] and their corresponding catalytic activities to the formation of unsaturated alcohols similar to **Figure 4-1**, have also been observed in the dehydration of other diols.[152, 153, 188, 204-206] Terminal diols such as 1,5-pentanediol,[204, 205] 1,6-hexanediol, 1,7-heptanediol, 1,8-octanediol, 1,9-nonanediol, 1,10-decanediol, and 1,12-dodecanediol[206] were converted into the corresponding unsaturated alcohols with sufficient selectivity over Sc_2O_3 catalyst. In the production of 4-penten-1-ol from 1,5-pentanediol[205], $Sc_{0.5}Yb_{1.5}O_3$ with the average ionic radius of 0.0837 nm shows the highest formation rate, so that there

must be the most proper lattice parameter between that of Sc_2O_3 and Lu_2O_3. As a result, $Sc_{0.5}Yb_{1.5}O_3$ (mole rate Sc:Yb= 0.5:1.5) was confirmed to be more active than Sc_2O_3 and Lu_2O_3. Except CeO_2, Lu_2O_3 is the most active in the dehydration of both 1,3-BDO and 1,4-BDO[153] while CeO_2 is exceptionally the most active in the case of 1,3-BDO.[152]

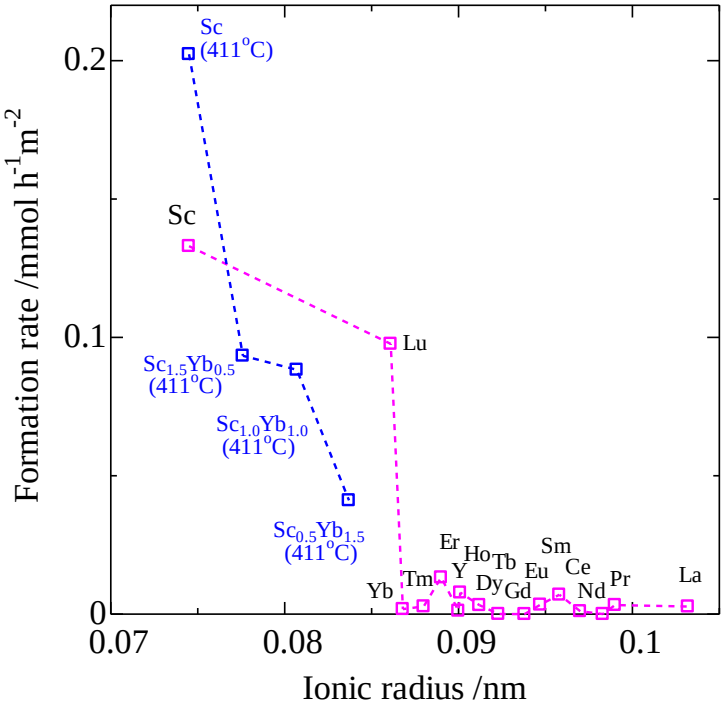

Figure 4-1 Formation rate of BD at 425°C over Ln_2O_3 catalysts with different Ln radii.
Calcination temperature, 800°C; flow rate of H_2, 45 cm^3 min^{-1}. The formation rate was averaged in the initial period between 0 and 5 h. The reaction temperature over $Sc_{2-x}Yb_xO_3$ catalysts was 411°C.

In the dehydration of 2,3-BDO at 325 °C, high selectivities to 3B2OL have also been obtained over In_2O_3 and ZrO_2 catalysts while the ionic radii of In_2O_3 (0.0800 nm) and ZrO_2 (0.0840 nm) are between that of Sc_2O_3 (0.0745 nm) and Lu_2O_3 (0.0861 nm). Sc_2O_3 and Lu_2O_3 show the BD selectivity of 58.2 and 28.2 mol% at 425 °C, respectively (**Table 4-1**), while ZrO_2 shows the 2,3-BDO conversion of 98.6% and the selectivities to BD, 3B2Ol, and MEK of 13.9, 19.6, and 33.3 mol% at 400°C, respectively as shown in **Figure 3-2**. In_2O_3, however, shows at most 4.7% for the BD selectivity (**Figure 3-20B**), because In_2O_3 has an ability of hydrogenation of BD to butene isomers. In_2O_3 actually has redox catalytic property: 1,4-BDO is dehydrogenated into γ-butyrolactone, and 1-butanol can be dehydrogenated to butanal.[156]

Table 4-1 Hydration of 2,3-BDO over Ln_2O_3 calcined at 800 °C[a].

Catalyst	R_i[b]	*SA*[c]	CP[d]	Conv.	Selectivity (mol%)					
	(nm)	(m^2g^{-1})		(mol%)	BD	3B2OL	MEK	MPA	MPO	Others[e]
Sc_2O_3	0.0745	51.5	C	100.0	58.2	1.9	12.8	1.6	1.7	23.8
Sc_2O_3[f]	0.0745	51.5	C	100.0	88.3	0.8	1.1	0.1	0.3	9.4
$Sc_{1.5}Yb_{0.5}O_3$[f]	0.0776	53.2	C	98.8	42.6	10.6	14.9	2.1	4.7	25.1
$Sc_{1.0}Yb_{1.0}O_3$[f]	0.0807	35.9	C	99.1	27.1	10.9	15.3	2.6	6.2	37.9
$Sc_{0.5}Yb_{1.5}O_3$[f]	0.0837	26.2	C	99.2	9.2	35.3	14.9	6.3	5.9	28.4
In_2O_3	0.0800	13.2	C	99.0	2.5	0.6	22.8	1.8	0.6	70.7
Lu_2O_3	0.0861	27.8	C	99.4	23.2	5.0	23.1	1.8	0.8	46.1
Yb_2O_3	0.0868	28.8	C	97.2	0.5	20.5	20.2	5.4	11.2	42.2
Tm_2O_3	0.0880	27.0	C	78.4	0.8	6.5	34.1	17.6	16.2	24.8
Er_2O_3	0.0890	21.5	M+C	100.0	2.4	20.0	21.1	7.2	7.2	42.1
Y_2O_3	0.0900	29.3	M+C	99.3	0.3	19.3	22.8	7.0	7.0	43.6
Ho_2O_3	0.0901	23.7	M	92.3	1.7	24.6	23.9	4.4	8.2	37.2
Dy_2O_3	0.0912	19.1	M	99.1	0.5	13.0	15.7	5.9	9.2	55.7
Tb_4O_7	0.0923	17.7	C_F	83.6	0.0	20.0	19.8	6.1	9.9	44.2
Gd_2O_3	0.0938	20.6	M	96.1	0.0	20.6	18.2	4.6	6.4	50.2
Eu_2O_3	0.0947	19.8	M	99.2	0.6	17.5	32.9	6.1	3.7	39.2
Sm_2O_3	0.0958	20.3	M	99.5	1.2	21.3	21.7	7.1	6.2	42.5
CeO_2	0.0970	53.7	C_F	100.0	0.5	0.5	39.2	2.4	0.6	56.8
Nd_2O_3	0.0983	18.2	H	87.8	0.0	35.2	16.9	4.0	6.0	37.9
Pr_6O_{11}	0.0990	22.7	C_F	95.6	0.7	9.6	34.7	8.6	9.3	37.1
La_2O_3	0.1032	18.0	H	92.5	0.5	8.1	23.2	9.2	11.8	47.2

BD, 1,3-butadiene; 3B2OL, 3-buten-2-ol; MEK, butanone; MPA, 2-methylpropanal; MPO, 2-methyl-1-propanol.

[a] Reaction temperature: 425 °C, catalyst weight: 1 g, the feed rate of 2,3-BDO:1.06 g h^{-1}, the flow rate of H_2: 45 cm^3 min^{-1}, 2,3-BDO conversion and each of the products selectivities were calculated and averaged in the initial 5 h.

[b] Ionic radii of trivalent Ln cation were considered as coordination number 6, except Ce^{4+} , which was 8, and the data were cited from Ref.[208].

[c] The data was cited from Ref.[203].

[d] CP, Crystal phase; C, C-type cubic bixbyite; C_F, cubic fluorite; M, B-type monoclinic; H, A-type hexagonal, The data were cited from Ref.[203].

[e] Others included acetoin, 2,3-butanedione, 2-butanol, *trans*-2-butene, 1-butene, isobutene, propylene,

ethylene, etc.

[f] Reaction temperature, 411 °C.

xIn the previous work of the dehydration of 1,4-BDO over Ln_2O_3 catalysts,[188] our group have reported that a high calcination temperature results in high selectivity to 3-buten-1-ol (3B1OL) in spite of growth of Ln_2O_3 particles with a well crystallized cubic phase. And a proper calcination temperature could lead to the well-crystallized monoclinic ZrO_2 for the adsorption of the reactant 2,3-BDO (as shown in **Table 3-2** and **Figure 3-1**). Besides, Sc_2O_3 was conformed to be better crystallized cubic phase with calcinations temperature increasing.[203] On the other hand, the basic density kept almost the same with only 2.3-2.2 μ mol m^{-2} even with increasing calcination temperature from 500 °C to 1000 °C, and no acidic sites were detected with the method of TPD.[203] Thus, it indicates that Sc_2O_3, the most active catalyst converted 2,3-BDO into BD successfully without the cooperation of those basic-acid sites, even though acid-base sites played important roles in the formation of 3B2OL from 2,3-BDO.

4.2 Dehydration of 2,3-BDO over In_2O_3 and Sc_2O_3 calcined at different temperatures

Table 4-2 Dehydration of 2,3-BDO over In_2O_3 calcined at different temperatures [a].

Reaction	Conv.	Selectivity (mol%)								
temp. (°C)	(mol%)	BD	3B2OL	MEK	MPA	MPO	BEs	PE	EE	Others
280 [b]	11.6	0.0	84.1	2.3	2.7	0.4	0.0	0.1	0.0	9.4
305 [b]	51.9	0.1	79.6	1.5	0.0	0.9	1.4	0.7	0.0	15.8
325 [b]	85.4	4.6	64.8	3.2	0.6	0.1	6.9	0.7	0.0	19.1
325 [c]	59.4	0.3	65.8	4.0	0.3	0.4	2.3	0.5	0.0	26.4
350 [b]	89.9	2.9	58.0	9.0	1.3	0.2	6.7	0.5	0.0	21.4
355 [c]	87.4	1.9	44.3	8.8	0.5	0.3	11.0	1.2	0.0	36.0
375 [b]	90.0	1.3	36.2	22.4	2.0	0.5	5.2	0.3	0.0	32.1
375 [c]	97.0	4.7	32.5	13.6	1.3	0.3	16.2	1.1	0.0	30.3
404 [c]	95.1	0.9	15.9	30.8	1.6	1.1	12.2	1.5	0.1	35.9
425 [c]	99.0	2.5	0.9	20.8	1.8	0.6	49.1 [d]	11.0	1.3	13.1

BD, 1,3-butadiene; 3B2OL, 3-buten-2-ol; MEK, butanone; MPA, 2-methyl-1-propanal; MPO, 2-methyl-1-propanol; BEs included *trans*-2-butene, 1-butene, and isobutene; PE, propylene; EE, ethylene; Others including acetoin, 2,3-butanedione, and 2-butanol, etc.

[a] Catalyst weight: 1 g, feed rate:1.06 g h^{-1}, flow rate of H_2: 45 cm^3 min^{-1}, conversion and selectivities of products were averaged in the initial 5 h.

[b] In_2O_3 calcined at 400 °C.

[c] In_2O_3 calcined at 800 °C.

[d] BEs included *trans*-2-butene (20.8%), 1-butene (14.8%), and isobutene (13.5%).

In_2O_3 calcined at 800 °C in **Table 4-1** shows a quite low selectivity to BD, although it shows a 3B2OL selectivity of 68.5% at a 2,3-BDO conversion of 72.9% at 305 °C (**Table 3-10**). In the case of In_2O_3 catalyst, calcination at 400 °C is preferable to obtain a 3B2OL-selective In_2O_3 catalyst. **Table 4-2** shows the catalytic activity of In_2O_3 calcined at 400 and 800 °C. The 3B2OL selectivity was 84.1% at 280 °C, and it decreased steeply with increasing reaction temperature due to the accumulated coke. At 425 °C, BD and 3B2OL were hardly obtained over In_2O_3. It was also found that 2,3-BDO was converted into MEK and some gaseous by-products such as *trans*-2-butene, 1-butene, isobutene, and propylene over In_2O_3 but not BD at high temperatures.

Table 4-3 shows the dehydration ability of Sc_2O_3 calcined at different temperatures, in the dehydration of 2,3-BDO at 411 °C. Under the conditions, the conversion of 2,3-BDO reached ca. 100%. It is obvious that when calcined at 800 °C, Sc_2O_3 displayed the highest BD selectivity, which exceeded 88%. The change in the selectivity had no correlation with the specific surface area, which in fact decreased with increasing calcination temperature.

Table 4-3 Dehydration of 2,3-BDO over Sc_2O_3 calcined at different temperatures [a].

Calcination	SA[b]	Conv.	Selectivity (mol%)								
(°C)	(m^2g^{-1})	(mol%)	BD	3B2OL	MEK	MPA	MPO	BEs	PE	EE	Others
As-received	98.4	99.9	50.4	4.4	11.9	1.8	4.0	3.9	6.1	2.2	15.3
600	72.1	99.9	66.5	0.8	8.3	1.2	2.0	4.6	7.5	2.2	6.9
700	66.2	100.0	83.0	0.9	1.9	0.1	0.6	3.8	4.5	2.8	2.4
800	51.5	100.0	88.3	0.8	1.1	0.1	0.3	2.8	2.9	1.6	2.1
900	45.4	100.0	62.4	1.9	11.8	1.7	3.1	6.2	4.8	1.5	6.6
1000	30.9	100.0	62.6	2.5	7.6	0.9	1.5	4.1	8.7	4.2	7.9

Abbreviations are the same as those listed in **Table 4-2**.

[a] Reaction temperature: 411 °C, catalyst weight: 1 g, feed rate:1.06 g h^{-1}, flow rate of H_2: 45 cm^3 min^{-1}, reactant conversion and selectivity of each product were averaged in the initial 5 h.

[b] The data were cited from Ref.[203].

4.3 Effects of high reaction temperature on the dehydration of 2,3-BDO over Sc_2O_3

In the previous part, the dehydration activities of Sc_2O_3 have been already investigated at reaction temperatures up to 350 °C in the formation of 3B2OL from 2,3-BDO. Over Sc_2O_3 calcined at 800 °C, the highest yield of 3B2OL was obtained at 325 °C with a selectivity of 85% and the selectivity

declined rapidly at 350 °C with only a little BD detected, as shown in **Table 3-8** and **Table 3-9**. In the present section, the catalytic activity of Sc_2O_3 calcined at 800 °C was further investigated at higher reaction temperatures. **Figure 4-2** shows that 3B2OL was mainly obtained at low reaction temperatures, while the formation of BD increased at high temperatures. Sc_2O_3 showed the maximum BD yield of 88.3% at 411 °C. However, the selectivity to BD declined rapidly at 425 °C. At 425 °C, dimerized BD such as octenes was also detected along with MEK. It indicates that the appropriate reaction temperature is 411 °C for a high yield of BD.

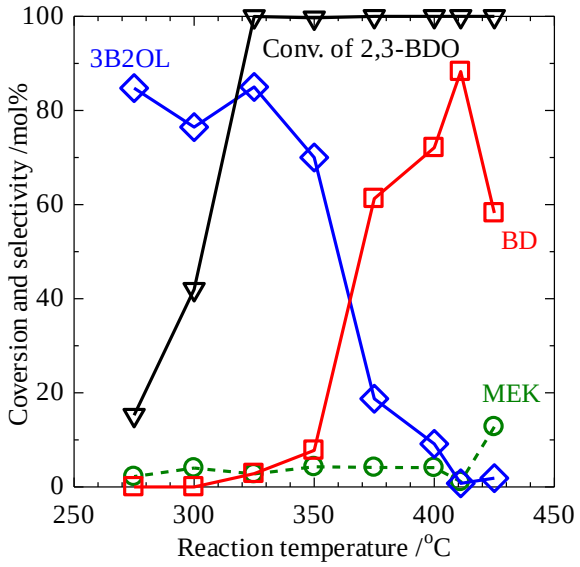

Figure 4-2 Changes in the dehydration ability of Sc_2O_3 for BD, 3B2OL, and MEK from 2,3-BDO with increasing reaction temperature. Calcination temperature of Sc_2O_3, 800 °C; Carrier gas of H_2, 45 cm^3 min^{-1}; catalyst, 1 g.

4.4 Catalytic stability with time on stream of the 2,3-BDO dehydration of over Sc_2O_3

Figure 4-3 shows the changes in catalytic activities of Sc_2O_3 calcined at 800 °C in the dehydration of 2,3-BDO with time on stream. Stable catalytic activity was obtained in the initial 5 h: 2,3-BDO conversion kept 100% with BD selectivity of 88% in H_2 flow at 411 °C. The selectivity to propylene was ca. 3% while selectivities to the sum percentage of butene isomers such as *trans*-2-butene, 1-butene, and isobutene was ca. 3%. Both the selectivities of 3B2OL and MEK were as low as 1%.

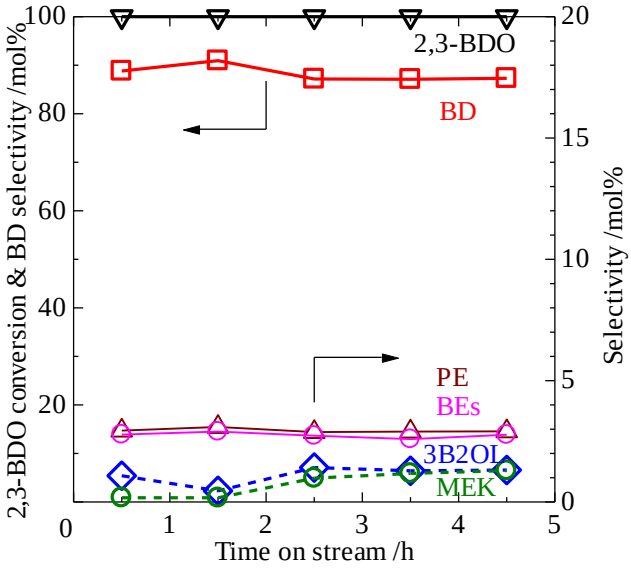

Figure 4-3 Changes in conversion and selectivities to BD, 3B2OL and MEK over Sc_2O_3 with time on stream. Calcination temperature of Sc_2O_3, 800 °C; Reaction temperature, 411°C; catalyst weight, 1 g; feed rate of 2,3-BDO, 1.06 g h^{-1}; flow rate of H_2, 45 cm^3 min^{-1}.

4.5 Effects of carrier gas on the dehydration of 2,3-BDO over Sc_2O_3 calcined at 800 °C

4.5.1 Dehydration of 2,3-BDO under the N_2 carrier gas

Figure 4-4 shows the catalytic activity of Sc_2O_3 in different carrier gases. The trend in the catalytic activity of Sc_2O_3 in N_2 flow resembled that in H_2 flow (**Figure 4-2**). However, even at the same reaction temperature, the selectivities to both 3B2OL and BD in N_2 flow were always lower than those in H_2 flow, as being compared with **Figure 4-2**. Besides, comparing to the used catalyst in N_2 flow I also found that less coke was accumulated on the one in H_2 flow. Thus, H_2 carrier gas may be effective to decrease coke so that to enhance the formation of BD.

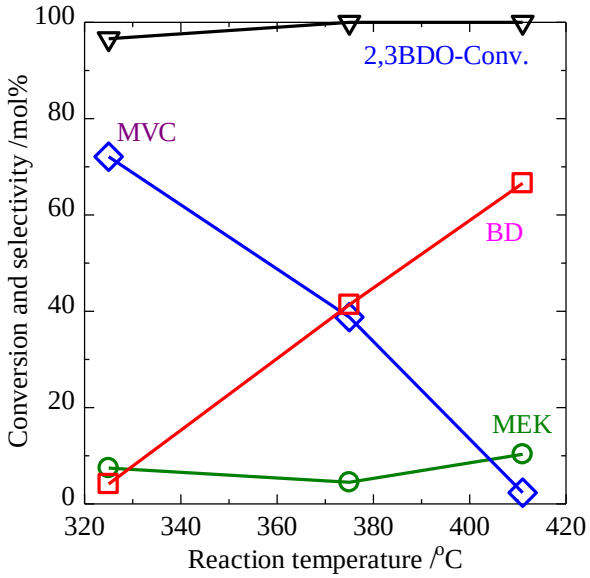

Figure 4-4. Dehydration ability of Sc_2O_3 in the dehydration of 2,3-BDO in N_2 flow. Calcination temperature of Sc_2O_3, 800 °C; Carrier gas of N_2, 45 cm^3 min^{-1}; catalyst, 1 g.

4.5.2 Effects of the H_2 carrier gas flow rate on 2,3-BDO dehydration

Figure 4-5 shows the changes of the selectivities to BD, 3B2OL, and MEK in the dehydration of 2,3-BDO catalyzed by Sc_2O_3 with different H_2 flow rate. Under a slow H_2 flow rate of 20 cm^3 min^{-1}, the selectivities to 3B2OL and MEK were higher than those at high H_2 flow rates while the selectivity to BD was lower. Under a H_2 flow rate of 80 cm^3 min^{-1}, a stable BD selectivity over 90% was obtained, while under that of 100 cm^3 min^{-1}, by-products such as butene isomers increased so that resulted in a decreased BD selectivity. Therefore, the proper flow rate of H_2 carrier gas can be considered as 80 cm^3 min^{-1}.

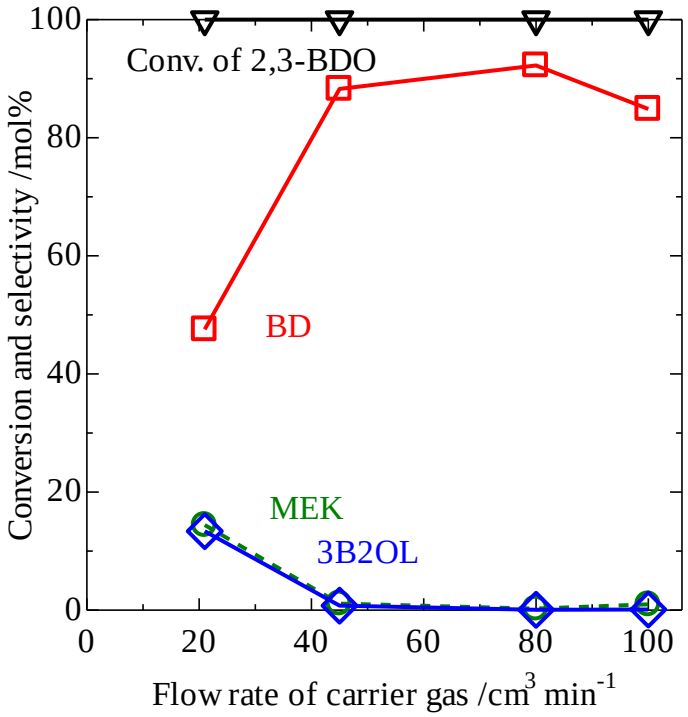

Figure 4-5 Changes in the dehydration of 2,3-BDO at different flow rates of H_2 carrier gas over Sc_2O_3. Calcination temperature of Sc_2O_3, 800 °C; Reaction temperature, 411°C; catalyst, 1 g.

Chapter V: Efficient formation of BD from 2,3-BDO dehydration step by step

5.1 Dehydration of MEK

MEK is one of the products in the dehydration of 2,3-BDO, so that it could be an intermediate in the BD formation. **Table 5-1** summaries the dehydration of MEK over Sc_2O_3 and Al_2O_3 catalysts. However, the reactant MEK was rarely reacted at 325°C over Al_2O_3 catalyst. Even at 550°C, the decomposition of MEK proceeded mainly to produce butene isomers, propylene, and ethylene, and BD with a selectivity of 8.6% was detected. Contrastly, the reaction proceeded at 425°C over Sc_2O_3, but no BD was detected from MEK. Therefore, MEK would not be a major intermediate in the BD formation from 2,3-BDO over Sc_2O_3.

Table 5-1 Dehydration of MEK over Sc_2O_3 and Al_2O_3[a].

Catalyst	React.temp.	Conv.	Selectivity (mol%)							
(1g)	(°C)	(mol%)	BD	3B2OL	MPA	MPO	BEs	PE	EE	Others
Al_2O_3	325	2.7	0.0	0.0	4.2	0.0	22.9	23.4	1.6	47.9
Al_2O_3	550	39.7	8.6	0.0	7.2	0.0	34.3	12.5	21.0	16.4
Sc_2O_3 [b]	425	40.2	0.0	0.0	2.2	6.9	15.7	18.5	4.6	52.1

[a] Feed rate:1.06 g h^{-1}, flow rate of H_2: 45 cm^3 min^{-1}, conversion and each selectivity of these were averaged in the initial 5 h.

[b] Sc_2O_3 was calcined at 800 °C

5.2 Dehydration of 3B2OL

3B2OL could also be an intermediate in the BD formation from 2,3-BDO. **Figure 5-1** shows the dehydration of 3B2OL over Sc_2O_3 and Al_2O_3 catalysts as well as a blank test without using catalysts. It is obvious that even at 425 °C the thermal decomposition of 3B2OL hardly proceeded without the catalysts. Sc_2O_3 showed the dehydration ability at temperatures between 300 and 400°C. Over Sc_2O_3, both the conversion of 3B2OL and the BD selectivity increased with increasing reaction temperature, and they reached the highest at 372°C. In addition, the BD selectivity from 3B2OL (91.5%) is higher than that directly from 2,3-BDO even at the same reaction temperature in comparison with **Figure 4-2**. This indicates that the formation of BD from 3B2OL is much easier than that from 2,3-BDO.

Figure 5-1 also indicates that Al_2O_3 is more active than Sc_2O_3 on the formation from 3B2OL to BD. Although their catalytic activities showed a similar trend over the reaction temperature, the highest BD yield was obtained over Al_2O_3 at 250 °C: 3B2OL conversion, 95.4%; BD selectivity, 91.2%. Al_2O_3 showed the similar trend to Sc_2O_3 in the catalytic performance at a temperature which is 127°C lower than Sc_2O_3 did. It is reasonable that the dehydration of 3B2OL into BD can be easily catalyzed by an ordinary dehydration type solid acid catalyst such as Al_2O_3 at a low temperature. The detail

researches were also conducted somewhere by our group.[209]

In the pioneering work of Winfield, 3B2OL is mainly obtained at 350°C while the main product shifts to BD at high reaction temperatures around 500°C over ThO_2 in the dehydration of 2,3-BDO.[119] However, other research groups also disclosed their results with high MEK selectivities but rare or no 3B2OL.[103, 131, 133] Some researchers believed that MEK was the intermediate from the dehydration of 2,3-BDO.[132] Bourns et al. reported that MEK was obtained with a yield of 86% at 225 °C over mineral acids such as bentonite, and it was converted into BD of 20% at 700°C with water as a diluent.[132] It seems that both MEK and 3B2OL can be considered as the intermediates for the formation of BD from 2,3-BDO.

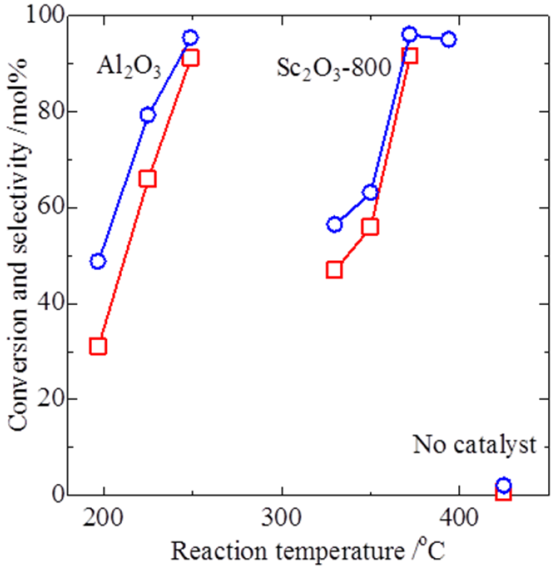

Figure 5-1 Changes in the conversion of 3B2OL into BD with increasing reaction temperature over Al_2O_3, Sc_2O_3 calcined at 800°C, and in blank test in H_2 flow (45 cm^3 min^{-1}).

In this work (**Table 5-1** and **Figure 5-1**), it is obvious that 3B2OL is the intermediate from 2,3-BDO to BD over Sc_2O_3, whereas MEK is not appropriate to be the intermediate to BD. In addition, butene isomers could come from butanols via dehydration. 2-Butanol and MPO are actually detected in the products. It is speculated that propylene could be formed via the dehydration of 1-propanol through propanal, which can be produced via pinacol rearrangement with the elimination of methanol instead of water.

Winfield has also pointed out that the equilibrium constant for the conversion of 2,3-BDO to MEK is 10^5 times greater than that for the reaction to 3B2OL at 500 °C, while the equilibrium constant for the dehydration of 3B2OL to BD is 10^4 times greater than that for the reaction of MEK to BD at

500 °C.[119] Thus, it is really considerable that the formation of MEK from 2,3-BDO readily proceeds but the formation of BD from MEK is difficult. The BD formation from MEK needs a high reaction temperature. Here from the results of **Table 5-1** and **Figure 5-1**, these points could be well confirmed again.

5.3 Efficient formation of BD on the dehydration of 2,3-BDO over the two-layer catalysts

Al_2O_3 catalyzes the dehydration of 3B2OL at 250 °C (**Figure 5-1**), and 3B2OL has been obtained with a yield of 85% from 2,3-BDO over Sc_2O_3 at 325 °C (**Table 3-8**). Thus, 2,3-BDO could be effectively converted to BD using Al_2O_3 as a dehydration catalyst for 3B2OL, the intermediate, at a low temperature. In order to obtain BD directly from 2,3-BDO at a low temperature, the dehydration was investigated over two-layer catalysts, which composed of Sc_2O_3 calcined at 800 °C loaded as an upper layer to convert 2,3-BDO into 3B2OL and Al_2O_3 placed as a bottom layer to convert 3B2OL into BD. **Figure 5-2** shows the catalytic activities at 318 °C with time on stream. The flow rate of H_2 carrier gas was 80 cm^3 min^{-1}, and all the other conditions were the same as the dehydration of 2,3-BDO over the single-layer Sc_2O_3 catalyst (**Figure 4-3**). The average of the 3B2OL selectivity was 94% with the complete conversion of 2,3-BDO at 318 °C during the initial 5 h. Butene isomers with the total selectivity less than 5 % and propylene with less than 1 % were observed whereas little MEK and 3B2OL were detected. In contrast, MEK and 3B2OL were observed over the single-layer Sc_2O_3 catalyst at 411 °C (**Figure 4-3**). It is obvious that the two-layer catalysts have stable catalytic activity, and the selectivity to BD is also higher than that of the single-layer Sc_2O_3 catalyst tested at 411 °C. The two-layer catalytic process was also conducted with long time on stream to confirm its catalytic stability. **Figure 5-3** (left) shows that the two-layer reaction keep stable for 50 h. Therefore, the two-layer catalysts consist of Sc_2O_3 and Al_2O_3 catalysts efficiently work to produce BD directly from 2,3-BDO. In addition, CaO/ZrO_2 (CaO-0.0668-800) was also used as the upper layer catalyst, to take the place of Sc_2O_3. As **Figure 5-3** (right) shows that he two-layer catalysts consisted of CaO/ZrO_2 and Al_2O_3 catalysts can also efficiently produce BD directly from 2,3-BDO at low reaction temperatures for a long time of 50 h.

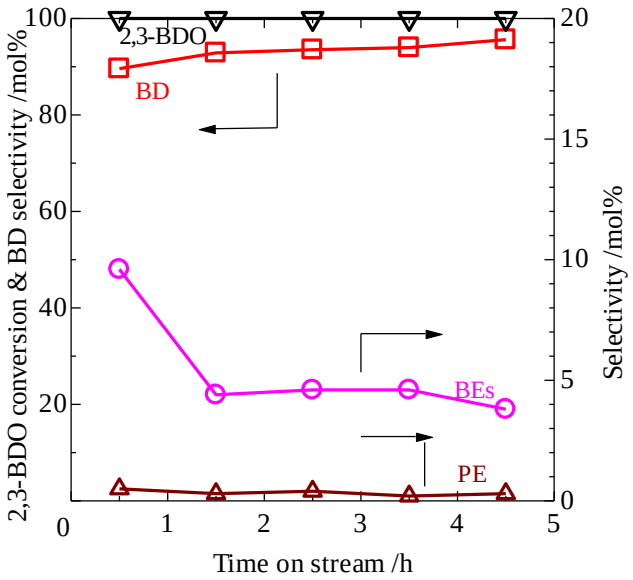

Figure 5-2 Changes in conversion and selectivities to BD, BEs, and PE in the dehydration of 2,3-BDO at 318°C over the two-layer catalysts of Sc_2O_3 and Al_2O_3 with time on stream.

Reaction conditions: catalyst weight: Sc_2O_3 (calcined at 800°C) placed in the upper layer, 1 g; Al_2O_3 located in the bottom layer, 1 g; feed rate of 2,3-BDO, 1.06 g h-1; flow rate of H_2 carrier gas, 80 cm^3 min^{-1}. BEs including trans-2-butene, 1-butene, and isobutene; PE, propylene.

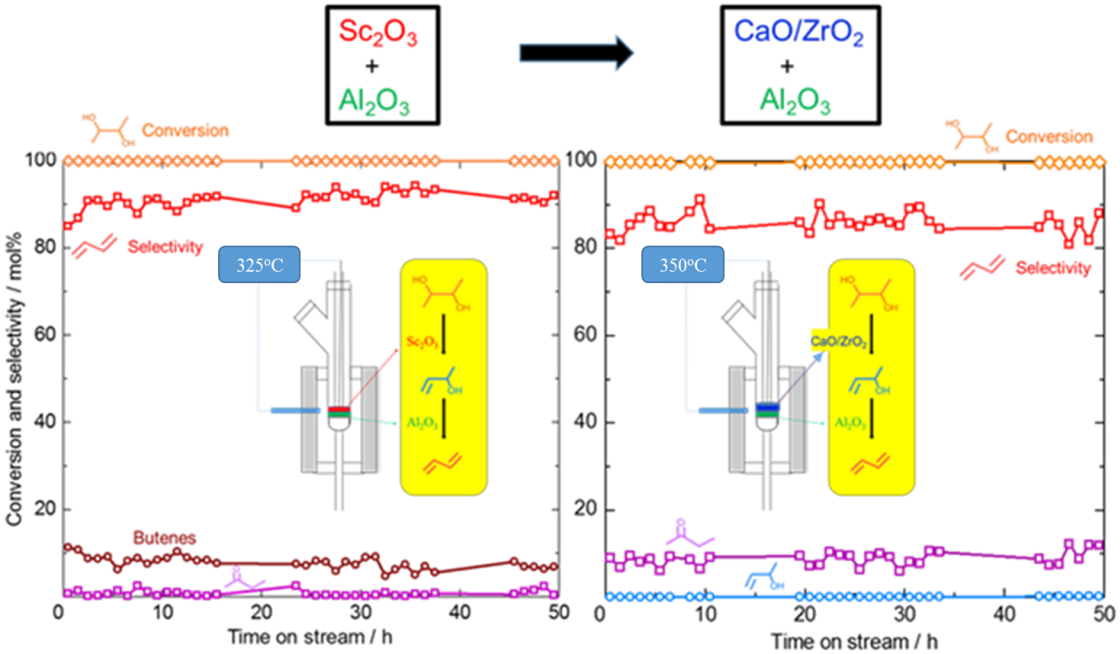

Figure 5-3 Catalytic stability with time on stream over the two-layer catalysts of Sc_2O_3 and Al_2O_3 (left); CaO-0.0668-800 and Al_2O_3 (right). Reaction conditions: catalyst weight: Sc_2O_3 (calcined at 800 °C) placed in the upper layer, 1 g (left); CaO/ZrO_2 (CaO-0.0668-800) placed in the upper layer, 1 g (right); Al_2O_3 located in the bottom layer, 1 g; feed rate of 2,3-BDO, 1.06 g h^{-1}; flow rate of H_2 carrier gas, 80 cm^3 min^{-1}; Reaction temperature, 350°C. BEs including *trans*-2-butene, 1-butene, and isobutene; PE, propylene.

I have demonstrated that BD production from 2,3-BDO proceeds over the two-layer catalysts at 318 °C in **Figure 5-2** and 325°C in **Figure 5-3** in order to overcome the decomposition of the intermediates. The main by-products such as MEK and propylene observed in **Figure 4-3** are greatly reduced in the two-layer catalysts. BD is obtained with selectivity higher than 94%. This is probably because Al_2O_3 catalyst in the bottom layer not only converted 3B2OL into BD efficiently but also cooperated with upper-layer Sc_2O_3 or CaO/ZrO_2 catalysts to promote the formation of BD directly from 2,3-BDO. The two-layer catalyst system consisting of Sc_2O_3 (or CaO/ZrO_2) and Al_2O_3 would be a candidate in the manufacture of BD from bio-based 2,3-BDO.

Chapter VI: Summary and future perspects

In the present work, among the investigated catalysts, only monoclinic ZrO_2 catalyst catalytically dehydrated 2,3-BDO to 3B2OL along with the by-products such as MEK and acetoin. More acidic tetragonal ZrO_2 than monoclinic one reduced the selectivity to 3B2OL because it produced more MEK. Decrease in the acid sites of monoclinic ZrO_2 is effective for decrease in the selectivity to MEK by the modification with loading some basic metal oxides such as Li_2O, La_2O_3, and CaO. However, strong basic Li_2O- and La_2O_3-modified monoclinic ZrO_2 catalysts increased the dehydrogenation product, acetoin. In contrast, the modification of monoclinic ZrO_2 with basic alkaline-earth metal oxides such as CaO, SrO, and BaO were efficient for the production of 3B2OL. The catalytic activity was strongly dependent on the calcination temperature of catalyst. Especially, the sample calcined at 800°C gave the highest 2,3-BDO conversion and 3B2OL selectivity. New basic sites with medium strength named as β, which belong neither to ZrO_2 nor to the alkaline-earth metal oxides, were detected in the active catalysts modified with alkaline-earth metal oxides.

Sc_2O_3 also catalyzed the formation of 3B2Ol from 2,3-BDO. Although it was rarely used as a catalyst itself because of its high cost. After calcination of Sc_2O_3 at temperatures higher than 800°C, Sc_2O_3 showed an excellent activity not only for the formation of 3B2OL from 2,3-BDO but also for the corresponding UOLs from the terminal diols, such as 1,6-hexanediol and then 1,10-decanediol.[206] Sc_2O_3 showed a special property: the first step dehydration mainly proceeded to produce 3B2OL at low temperatures while the complete dehydration to produce BD was catalyzed at temperatures higher than 400°C. The catalytic property of Sc_2O_3 resembled that of ThO_2 as reported by Winfield.

The selectivity to 3B2OL increased with increasing their calcination temperature in both cases of ZrO_2 and Sc_2O_3, indicating that smooth surface with high crystallinity is favorable for the dehydration. Different from the acid-base bifunctional monoclinic ZrO_2 catalyst and the ZrO_2 catalysts modified with alkaline Ln metal oxides, no acid sites and only a few basic sites were detected from the surface of Ln_2O_3. However, over Ln_2O_3, an O^{2-} anion presents a site B, and Ln^{3+} cations and/or oxygen defect sites act acidic site, A_1 and A_2. The basic site B eliminated the proton at position 1, following by the elimination of the neighboring OH^- group coordinated to the site A_1, to produce 3B2OL, while the site A_2 has a significant function for anchoring the diol molecule. Among Ln_2O_3 catalysts with In_2O_3, Sc_2O_3 has the smallest ionic radii, which must have conformed the best distance of the tridentate coordination sites over the active center for the formations of 3B2OL and BD from 2,3-BDO.

I also conducted my work with the catalytic dehydration of 2,3-BDO into the corresponding unsaturated alcohol, 3B2OL firstly, and then further to BD. Although complete dehydration of these 2,3-BDO into BD is possible, this route only occurred over Sc_2O_3 catalysts, and always needs higher reaction temperatures and also resulted in more by-products. However, 3B2OL can be readily formed as the first-step dehydration product from 2,3-BDO over Sc_2O_3, In_2O_3, m-ZrO_2 and also m-ZrO_2

modified with alkaline-earth metal oxides at low temperatures. In addition, the obtained 3B2OL, can be converted into BD easily over solid acid catalysts such as Al_2O_3 even at much lower reaction temperatures. In order to synthesize BD with high yield under mild reaction conditions, the 2,3-BDO could be dehydrated into BD step by step or in a process with a two-layer catalyst bed.

Biomass alternative to petroleum would be the raw material of chemicals in future. Bio-ethanol would be a chemical resource of BD in U.S. and Brazil where ethanol can be obtained as a chemical feedstock. However, the selectivity to BD is necessary for the industrial usage. In EU and Japan, C_4 alcohols such as 1-/2-butanol, 1,2-BDO, 1,3-BDO, 1,4-BDO and 2,3-BDO could be considered as the most prospect alternatives for the on-purpose synthesis of BD. Since these alcohols are four-carbon skeleton and suitable as the raw materials for the syntheses of BD. Besides, they are also biomass-derived feedstock for BD since they are all microbial produced possible from biomass with high yields and high purity. In addition, compared with other processes, dehydration of these C_4 alcohols is environmental friendly. In preparation for future shortage of BD supply, it is important to secure other supply routes of BD. Thus, I conducted my study on the dehydration of 2,3-BDO into BD during my doctoral couse and I hope one day my processes will be industrialized to meet the shortage of BD supply.

References:

[1] Cited from the homepage of U.S. energy information administration, https://www.eia.gov/forecasts/aeo/data/browser/.

[2] Cited from the homepage of RIBARIES MUSUMS GALERIES COUNTRY OF LAMBTON http://www.lclmg.org/lclmg/Museums/OilMuseumofCanada/BlackGold2/OilHeritage/OilSprings/tabid/208/Default.

[3] Cited from the homepage of oil150, http://www.oil150.com/about-oil/timeline/

[4] Cited from the homepage of U.S. energy information administration, https://www.eia.gov/beta/international/

[5] Cited from the homepage of oilfield businessnet work, https://oilfieldbusinessnetwork.com/petroleum/.

[6] J. E. Kostka1, O. Prakash, W. A. Overholt, S. J. Green, G. Freyer, A. Canion, J. Delgardio, N. Norton, T. C. Hazen, M. Huettel, *Appl. Environ. Microbiol.,* **2011**, *77*, 7962.

[7] J. G. Speight, M. R. Islam, *Technol. Eng.,* **2016**, *3*, 23.

[8] Cited from the homepage of genugreen. files. wordpress, https://genugreen.files.wordpress.com/2012/07/flow-chart-for-products-from-petroleum-based-feedstocks.

[9] B. Dimitriades, *Environ. Sci. Technol.***, 1972**, *6*, 253.

[10] J. Hansen, M. Sato, R. Ruedy, K. Lo, D. W. Lea, M. Medina-Elizade, *Proc. Natl. Acad. Sci. U. S. A.* **2006**, *103*, 14288.

[11] Cited from the homepage of U.S. energy information administration, https://www.eia.gov/dnav/pet/hist/LeafHandler.

[12] Cited from the homepage of U.S. energy information administration, https://www.eia.gov/todayinenergy/detail.

[13] Cited from the homepage of U.S. energy information administration, https://www.eia.gov/todayinenergy/detail.

[14] Cited from the homepage of FOOD AND AGRICULTURAL ORGANIZATION (FAO). Energy supply and demand: trends and prospects, ftp://ftp.fao.org/docrep/fao/010/i0139e/i0139e03.pdf.

[15] C. B. Field; M. J. Behrenfeld; J. T. Randerson; P. Falkowski, *Science,* **1998**, *281* (5374) 237.

[16] J. G. Canadell, E. D. Schulze, *Nature Commun.*, **2014**, *5* (5282) 1.

[17] L. A. Lucia, *BioResources,* **2008**, *3*, 981

[18] K. G. Satyanarayana, G. G. C. Arizaga, F. Wypych, *Prog. Polym. Sci.,* **2009**, *34*, 982.

[19] Y. Ahn, S. H. Lee, H. J. Kim, Y.-H. Yang, J. H. Hong, Y.-H. Kim, H. Kim, *Carbohydr. Polym.,* **2012**, *88*, 395.

[20] Cited from the homepage of climatetechvwiki,

http://www.climatetechwiki.org/technology/biomass.
[21] Cited from the homepage of GLOBAL ENERGY ENTERPRISE, https://www.e-education.psu.edu/.
[22] F. H. Isikgor, C. R. Becer, *Polym. Chem.,* **2015**, *6*, 4497.
[23] A. Barakat, H. de Vries, X. Rouau, *Bioresour. Technol.,* **2013**, *134*, 362.
[24] D. M. Alonso, S. G. Wettstein, J. A. Dumesic, *Green Chem.,* **2013**, *15*, 584.
[25] M. J. Taherzadeh, K. Karimi, *Int. J. Mol. Sci.,* **2008**, *9*, 1621.
[26] F. Cherubini, A. H. Strømman, Biofuels, *Bioprod. Biorefin.*, **2011**, *5*, 548.
[27] M. Altaf, M. Venkateshwar, M. Srijana, G. Reddy, *J. Appl. Microbiol.,* **2007**, *103*, 372.
[28] Z. Fang, *Pretreatment Techniques for Biofuels and Biorefineries, Berlin, Springer*, **2013**, *7*, 133.
[29] T. Ezeji, N. Qureshi, H. P. Blaschek, *Process Biochem.,* **2007**, *42*, 34.
[30] J. C. Serrano-Ruiz, R. M. West, J. A. Dumesic, *Annu. Rev. Chem. Biomol. Eng.,* **2010**, *1*, 79.
[31] Q. Wang, T. Chen, X. Zhao, J. Chamu, *Biotech. Bioeng.,* **2012**, *109*, 1610.
[32] J. B. Melpolder, R. F. Heck, *J. Org. Chem.,* **1976**, *41*, 265.
[33] J. W. Bode, E. M. Carreira, *J. Org. Chem.,* **2001**, *66*, 6410.
[34] C. Y. Ng, M. Y. Jung, J. Lee, M.-K. Oh, *Microb. Cell Fact.,* **2012**, *11*, 68.
[35] L. Zhang, Z. Guo, J. Chen, Q. Xu, H. Lin, K. Hu, X. Guan, Y. Shen, *Sci Rep.,* **2016**, *6*, 19257.
[36] M. Ehsani, M. R. Ferna´ndez, J. A. Biosca, A. Julien, S. Dequin, *Appl. Environ. Microbiol.,* **2009**, *75*, 3196.
[37] K. Weissermel, H.-J. Arpe, Industrial Organic Chemistry, 4th Ed., **2003**, 115.
[38] E. V. Makshina, M. Dusselier, W. Janssens, J. Degre've, P. A. Jacobs, B. F. Sels, *Chem. Soc. Rev.,* **2014**, *43*, 7917.
[39] S. C. Pandey, D. K. Ralli, A. K. Saxena and W. K. Alamkhan, *J. Sci. Ind. Res.,* **2004**, *63*, 276.
[40] R. A. M. Alselaa, F. M. Elfghi, *Chem. Pro. Eng. Res.,* **2015**, *34*, 10.
[41] Z. Belohlav, P. Zamostny, T. Herink, *Chem. Eng. Process.* **2003**, *42*, 461.
[42] Cited from the homepage of chemical industry cyclicality, https://musingsonfinance.com/2016/01/.
[43] P. C. A. Bruijnincx, B. M. Weckhuysen, Angew. Chem. Int. Ed., **2013**, *52*, 11980.
[44] M. P. Bailey, *Chem. Eng.,* **2014**, *121*, 19.
[45] M. D. Jones, *Chem. Cent. J.,* **2014**, *8*, 53.
[46] J. Sun, Y. Wang, *ACS Catal.,* **2014**, *4*, 1078.
[47] P. Lanzafame, G. Centi, S. Perathoner, *Chem. Soc. Rev.,* **2014**, *43*, 7561.
[48] J. M. R. Gallo, J. Buenob, U. Schuchardt, *J. Braz. Chem. Soc.,* **2014**, *25*, 2229.
[49] S.V. Lebedev, Z. Obshch. Khim., **1933**, *3*, 698.
[50] Y.A. Gorin, Z. Obshch. Khim., **1946**, *16*, 283.
[51] B. B. Corson, H. E. Jones, C. E. Welling, J. A. Hinckley, E. E. Stahly, *Ind. Eng. Chem.,* **1950**, *42*,

359.
[52] I. I. Ostromyslensky, *J. Russ. Phys.-Chem. Soc.,* **1915**, *47*, 1472.
[53] S. K. Bhattacharyya, B. N. Avasthi, *Ind. Eng. Chem. Process Des.,* **1963**, *2*, 45.
[54] S. K. Bhattacharyya, B. N. Avasthi, *J. Appl. Chem.,* **1966**, *16*, 239.
[55] H. Niiyama, S. Morii, E. Echigoya, *Bull. Chem. Soc. Jpn.,* **1972**, *45*, 655.
[56] R. Ohnishi, T. Akimoto, K. Tanabe, *J. Chem. Soc., Chem. Commun.,* **1985,** *22*, 1613.
[57] S. Kvisle, A. Aguero, R. P. A. Sneeden, *Appl. Catal.*, **1988**, *43*, 117.
[58] Y. Kitayama, A. Abe, *J. Chem. Soc. Jpn.*, **1989**, *11*, 1824.
[59] V. Gruver, A. Sun. J. J. Fripiat, *Catal. Lett.,* **1995**, *34*, 359.
[60] J. B. d'Espinose de la Caillerie, V. Gruver, J. J. Fripiat, *J. Catal.,* **1995**, *151*, 420.
[61] Y. Kitayama, M. Satoh, T. Kodama, *Catal. Lett.,* **1996**, *36*, 95.
[62] J. I. Di Cosimo, V. K. Diez, M. Xu, E. Iglesia, R. Apesteguıa, *J. Catal.,* **1998**, *178*, 499.
[63] T. Tsuchida, J. Kubo, T. Yoshioka, S. Sakuma, T. Takeguchi, W. Ueda, *J. Catal.,* **2008**, *259*, 183.
[64] M. Leon, E. Diaz, S. Ordonez, *Catal. Today,* **2011**, *16*4, 436.
[65] M. D. Jones, C. G. Keir, C. Di Iulio, R. A. M. Robertson, C. V. Williams, D. C. Apperley, *Catal. Sci. Technol.,* **2011**, *1*, 267.
[66] E.V. Makshina, W. Janssens, B.F. Sels, P.A. Jacobs, *Catal. Today,* **2012**, *198*, 338.
[67] H. Chae, T. Kim, Y. Moon, H. Kim, K. Jeong, C. Kim, S. Jeong, *Appl. Catal. B: Envir.*, **2014**, *150-151*, 596.
[68] G. O. Ezinkwo, V. F. Tretjakov, R. M. Talyshinky, A. M. Ilolov, T. A. Mutombo, *Catal. Commun*, **2014**, *43*, 207.
[69] M. Lewandowski, G. S. Babu, M. Vezzoli, M. D. Jones, R. E. Owen, D. Mattia, P. Plucinski, E. Mikolajska, A. Ochenduszko, D. C. Apperley, *Catal. Commun.,* **2014**, *49*, 25.
[70] V. L. Sushkevich, I. I. Ivanova, S. Tolborg, E. Taarning, *J. Catal.,* **2014**, *316*, 121.
[71] M. Gao, Z. Liu, M. Zhang, L.Tong, *Catal. Lett.,* **2014**, *144*, 2071.
[72] V. F. Tret'yakov, R. M. Talyshinskii, A. M. Ilolov, A. L. Maksimov, S. N. Khadzhiev, *Petro. Chem.,* **2014**, *54*, 195.
[73] C. Angelici, M. E. Z. Velthoen, B. M. Weckhuysen, P. C. A. Bruijnincx, *ChemSusChem,* **2014**, *7*, 2505.
[74] V. L. Sushkevich, I. I. Ivanova, V. V. Ordomsky, E. Taarning, *ChemSusChem,* **2014**, *7*. 2527.
[75] O. V. Larina, P. I. Kyriienko, S. O. Soloviev, *Catal. Lett.,* **2015**, *145*, 1162.
[76] O. V. Larina, P. I. Kyriienko, S. O. Soloviev, *Theor. Exp. Chem.,* **2015**, *51*, 252.
[77] Y. Sekiguchi, S. Akiyama, W. Urakawa, T. Koyama, A. Miyaji, K. Motokura, T. Baba, *Catal. Commun.,* **2015**, *68*, 20.
[78] V. L. Sushkevich, I. I. Ivanova, E. Taarning, *Green Chem.*, **2015**, *17*, 2552.
[79] N. La-Salvia, J. J. Lovón-Quintana,G. P. Valença, *J. Braz. Chem. Eng.,* **2015**, *32*, 489.

[80] S. Hanspal, Z. D. Young, H. Shou, R. J. Davis, *ACS Catal.,* **2015**, *5*, 1737.

[81] V. L. Sushkevich, D. Palagin, I. I. Ivanova, *ACS Catal.,* **2015**, *5*, 4833.

[82] C. Angelici, F. Meirer, A. M. J. Van der Eerden, H. L. Schaink, A. Goryachev, J. P. Hofmann, E. J. M. Hensen, B. M. Weckhuysen, P. C. A. Bruijnincx, *ACS Catal.,***2015**, *5*, 6005.

[83] T. W. Kim, J. W. Kim, S. Y. Kim, H. J. Chae, J. R. Kim, S. Y. Jeong, C. U. Kim, *Chem. Eng. J.,* **2015**, *278*, 217.

[84] T. De Baerdemaeker, M. Feyen, U. Mu¨ller, B. Yilmaz, F. Xiao, W. Zhang, T. Yokoi, X. Bao, H. Gies, D. De Vos, *ACS Catal.,* **2015**, *5*, 3393.

[85] A. Chieregato, O. J. Velasquez, C. Bandinelli, G. Fornasari, F. Cavani, M. Mella, *ChemSusChem,* **2015**, *8*, 377.

[86] W. Janssens, E. V. Makshina, P. Vanelderen, F. DeClippel, K. Houthoofd, S. Kerkhofs, J. A. Martens, P. A. Jacobs, B. F. Sel, *ChemSusChem,* **2015**, *8*, 994.

[87] M. Zhang, M. Gao, J. Chen, Y. Yu, *RSC Adv.,* **2015**, *5*, 25959.

[88] Z. Han, X. Li, M. Zhang, Z. Liu, M. Gao, *RSC Adv*., **2015**, *5*, 103982.

[89] R. A. L. Baylon, J. Sun, Y. Wang, *Catal. Today,* **2016**, *259*, 446.

[90] J. V. Ochoa, C. Bandinelli, O. Vozniuk, A. Chieregato, A. Malmusi, C. Recchi, F. Cavani, *Green Chem.,* **2016**, *18*, 1653.

[91] A. Klein, K. Keisers, R. Palkovits, *Appl. Catal. A: Gen.,* **2016**, *514*, 192.

[92] P. I. Kyriienko, O. V. Larina, S. O. Soloviev, S. M. Orlyk, S. Dzwigaj, *Catal. Commun.,* **2016**, *77*, 123.

[93] D. Cespi, F. Passarini, I. Vassura, F. Cavani, *Green Chem.,* **2016**, *18*, 1625.

[94] T. C. Ezeji, N. Qureshi, H. P. Blaschek, *Appl. Microbiol. Biotechnol.,* **2004**, *63*, 653.

[95] T. C. Ezeji, N. Qureshi, H. P. Blaschek, *J. Ind. Microbiol. Biotechnol.,* **2007**, *34*, 771.

[96] K. A. Taconi, K. P.Venkataramanan, D. T. Johnson, *Environ. Prog. Sust. Energy*, **2009**, *28*, 100.

[97] P. Ghiaci, J. Norbeck, C. Larsson, *PLoS One,* **2014**, *9*, 1.

[98] A. Matsuyama, H. Yamamoto, N. Kawada, Y. Kobayashi, J. Mol. Catal. B: Enzym., **2001**, *11*, 513.

[99] N. Itoh, M. Nakamura, K. Inoue, Y. Makino, *Appl. Microbiol. Biotechnol.,* **2007**, *75*, 1249.

[100] C. Q. Ma, A. L. Wang, J. Y. Qin, L. X. Li, X. L. Ai, T. Y. Jiang, *Appl. Microbiol. Biotechnol.,* **2009**, *82*, 49.

[101] K. K. Cheng, Q. Liu, J. A. Zhang, J. P. Li, J. M. Xu, G. H. Wang, *Process Biochem.,* **2010**, *45*, 613.

[102] N. Qureshi, M. Cheryan, *Appl. Microbiol. Biotechnol.,* **1989** b, *30*, 440.

[103] L. Y. Zhang, Y. L. Yang, J. A. Sun, Y. L. Shen, D. Z. Wei, J. W. Zhu, *Bioresour Technol.,* **2010**, *101*, 1961.

[104] J. Gao, H. Xu, Q. J. Li, X. H. Feng, S. Li, *Bioresour. Technol.,* **2010**, *101*, 7076.

[105] Z. Xiao, X. Wang, Y. Huang, F. Huo, X. Zhu, L. Xi, J. R Lu, *Biotechnol. Biofuels,* **2012**, *5*, 88.

[106] L. G. Lee, G. M. Whitesides, *J. Org. Chem.,* **1986**, *51*, 25.

[107] J. Hasegawa, M. Ogura, S. Tsuda, S. Maemoto, H. Kutsuki, T. Ohashi, *Agric. Bioil. Chem.,* **1990**, *54*, 1819.

[108] H. Yim, R. Haselbeck, W. Niu, C. Pujoi-Baxley, A. Burgard, J. Boldt, J. Khandurina, J. D. Trawick, R. E. Oterhout, R. Stephen, J. Estadilla, S. Tteisan, H. B. Schreyer, S. Andrae, T. H. Yang, S. Y. Lee, M. J. Burk, S. V. Dien, *Nat. Chem. Biol.,* **2011**, *7*, 445.

[109] M. Burk, A. Burgard, R. E. Oterhout, J. Sun Pat. WO 030,711, **2010**.

[110] G. R. M. Dowson, M. F. Haddow, J. Lee, R. L. Wingad, D. F. Wass, *Angew. Chem. Int. Ed.,* **2013**, *52*, 9005.

[111] D. L. Carvalho, R. R. de Avillez, M. T. Rodrigues, L. E. P. Borges, L. G. Appel, *Appl. Catal. A: Gen.,* **2012**, *415*, 96.

[112] A. S. Ndou, N. Plint, N. J. Coville, *Appl. Catal. A: Gen.,* **2003**, *251*, 337.

[113] S. Ogo, A. Onda, K. Yanagisawa, *Appl. Catal. A: Gen.,* **2011***, 402*, 188.

[114] C. R. Shen, J. C. Liao, *Metab. Eng.,* **2008**, *10*, 312.

[115] J. T. Hays, G. F. Hager, H. M. Engelman, H. M. Spurlin, *J. Am. Chem. Soc.,* **1951**, *73*, 5369.

[116] J. A. Dumesic, R. M. West, U.S. Pat. 685,887, **2010.**

[117] S. Murakami, T. Harada, A. Tai, *Bull. Chem. Soc. Jpn.,* **1980**, *53*, 1356.

[118] K. Hintzer, B. Koppenhoefer, V. Schurig, *J. Org. Chem.,* **1982**, *47*, 3850.

[119] W. E. Winfield, *J.Council Sci. Ind. Res.,* **1945**, *18*, 412.

[120] V. E. Wellman, U.S. Pat. 217,428,0 A, **1938**

[121] N. Ichikawa, S. Sato, R. Takahashi, T. Sodesawa, *J. Mol. Catal. A: Chem.,* **2006**, *256*, 106.

[122] L. Ott, S. Kohl, M. Bicker, H. Vogel, *Chem. Eng. Technol.,* **2005**, *28*, 1562.

[123] H. Duan, Y. Yamada, S. Sato, Unpublished data.

[124] U. Limbeck, C. Altwicker, U. Kunz, U. Hoffmann, *Chem. Eng. Sci.,* **2001**, *56*, 2171.

[125] M. Aghaziarati, M. Kazemeini, M. Soltanieh, S. Sahebdelfar, *Ind. Eng. Chem. Res.,* **2007**, *46*, 726.

[126] S. E. Hunter, C. E. Ehrenberger, P. E. Savage, *J. Org. Chem.,* **2006**, *71*, 6229.

[127] S. H. Vaidya, V. M. Bhandari, R.V. Chaudhari, *Appl. Catal. A: Gen.,* **2003**, *242*, 321.

[128] T. Richter, H. Vogel, *Chem. Eng. Technol.,* **2001**, *24*, 4.

[129] W. Reppe, *Justus Liebigs Ann. Chem.,* **1955**, *596*, 80.

[130] S. Sato, R. Takahashi, T. Sodesawa, N. Yamamoto, *Catal. Commun.,* **2004**, *5*, 397.

[131] R. R. Emerson, M. C. Flickinger, G. T. Tsao, *Ind. Eng. Chem. Prod. Res. Dev.,* **1982**, *21*, 473.

[132] A. N. Bourns, R. V. V. Nicholls, *Can. J. Res.,* **1947**, *25b*, 80.

[133] W. G. Zhang, D. H. Yu, X. J Jia, H. Huang, *Green Chem.,* **2012**, *14*, 3441.

[134] A. Multer, N. McGraw, K. Hohn, P. Vadlani, *Ind. Eng. Chem. Res.,* **2013**, *52*, 56.

[135] Q. Zheng, M. D. Wales, M. G. Heidlage, M. Rezac, H. Wang , S. H. Bossmann, K. L. Hohn, *J.*

Catal., **2015**, *330*, 222.

[136] T. Y. Kim, J. Baek, C. K. Song, Y. S. Yun, D. S. Park , W. Kim, J. W. Han, J. Yi, *J. Catal.,* **2015**, *323*, 85.

[137] M. A. Nikitina, I. I. Ivanova, *ChemCatChem,* **2016**, *8*, 1346.

[138] W. Kim, W. Shin, K. J. Lee, H. Song, H. S. Kim, D. Seung, I. N. Filimonov, *Appl. Catal. A: Gen.,* **2016**, *511*, 156.

[139] J. W. Bode, E. M. Carreira, *J. Am. Chem. Soc.* **2001**, *123*, 3611-3612.

[140] N. Shlechter, D. F. Othmer , R. Brand, *Ind. Eng. Chem.,* **1945**, *37*, 905.

[141] L. E. Schniepp , J. W. Dunning , H. H. Geller , S. A. Morell , E. C. Lathrop, *Ind. Eng. Chem.,* **1945**, *37*, 884.

[142] S. A. Morell , H. H. Geller , E. C. Lathrop, *Ind. Eng. Chem.,* **1945**, *37*, 877.

[143] J. Baek, T. Y. Kim, W. Kim, H. J. Lee, J. Yi, *Green Chem.,* **2014**, *16*, 3501.

[144] E. Arundale, M. Louis A, U.S. Pat. 244,9001 A, **1948**.

[145] C. A. McCombs, U.S. Pat. 610,3943 A, **2000**.

[146] S. N. Falling, U.S. Pat. 540,6007, **1995**.

[147] M. Kobune, S. Sato, R. Takahashi, *J. Mol. Catal. A: Chem.,* **2008**, *279*, 10.

[148] A. Igarashi, N. Ichikawa, S. Sato, R. Takahashi, T. Sodesawa, *Appl. Catal. A: Gen.,* **2006**, *300*, 50.

[149] S. Sato, R. Takahashi, T. Sodesawa, N. Honda, H. Shimizu, *Catal. Commun.,* **2003**, *4*, 77.

[150] S. Sato, R. Takahashi, T. Sodesawa, A. Igarashi, H. Inoue, *Appl. Catal. A: Gen.,* **2007**, *328*,109.

[151] T. Nozawa, S. Sato, R. Takahashi, *Top Catal.,* **2009**, *52*, 609.

[152] H. Gotoh, Y. Yamada, S. Sato, *Appl. Catal. A: Gen.,* **2010**, *377*, 92.

[153] S. Sato, F. Sato, H. Gotoh, Y. Yamada, *ACS Catal.,* **2013**, *3*, 721.

[154] S. Sato, R. Takahashi, T. Sodesawa, N. Honda, *J. Mol. Catal. A: Chem.,* **2004**, *221*, 177.

[155] N. Ichikawa, S. Sato, R. Takahashi, T. Sodesawa, H. Fujita, T. Atoguchi, A. Shiga, *J. Catal.,* **2006**, *239*, 13.

[156] M. Segawa, S. Sato, M. Kobune, T. Sodesawa, T. Kojima, S. Nishiyama, N. Ishizawa, *J. Mol. Catal. A: Chem.,* **2009**, *310*, 166.

[157] M. Magnin-Lachaux, Z. Tan, B. Liang, E. Negishi, *Org. Lett.,* **2004**, *6*, 1425.

[158] T. Min, B. Yi, P. Zhang, J. Liu, C. Zhang, H. Zhou, *Med. Chem. Res.,* **2009**, *18*, 495.

[159] R. Takahashi, I. Yamada, A. Iwata, N. Kurahashi, S. Yoshida, S. Sato, *Appl. Catal. A: Gen.,* **2010**, *383*, 134.

[160] A. Igarashi, S. Sato, R. Takahashi, T. Sodesawa, M. Kobune, *Catal.Commun.,* **2007**, *8*, 807.

[161] S. Sato, R. Takahashi, M. Kobune, H. Inoue, Y. Izawa, H. Ohno, K. Takahashi, *Appl. Catal. A: Gen.,* **2009**, *356*, 64.

[162] F. Sato, Y. Yamada, S. Sato, *Chem. Lett.,* **2012**, *41*, 593.

[163] N. Yamamoto, S. Sato, R. Takahashi, K. Inui, *Catal. Commun.,* **2005**, *6*, 480.

[164] H. Inoue, S. Sato, R. Takahashi, Y. Izawa, H. Ohno, K. Takahashi, *Appl. Catal. A: Gen.,* **2009**, *352*, 66.

[165] N. Yamamoto, S. Sato, R. Takahashi, K. Inui, *J. Mol. Catal. A: Chem.,* **2006**, *243*, 52.

[166] Q. Zhang, Y. Zhang, H. Li, C. Gao, Y. Zhao, *Appl. Catal. A: Gen.,* **2013**, *466*, 233.

[167] Q. Zhang, Y. Zhang, H. Li, C. Gao, Y. Zhao, M. Ma, Y. Yu, *Chin. J. Catal.,* **2013**, *34*, 1159.

[168] F. Sato, S. Sato, Y. Yamada, M. Nakamura, A. Shiga, *Catal. Today,* **2014**, *226*, 124.

[169] A. Auroux, A. Gervasini, *J. Phys. Chem.* **1990**, *94*, 6371.

[170] S. Lee, B. Kim, K. Park, Y. Um, J. Lee, Appl. *Biochem. Biotechnol.* **2012**, *166*, 1801.

[171] X. Ji, H. Huang, P. Ouyang, *Biotechnol. Adv.* **2011**, *29*, 351.

[172] A. Zeng, W.Sabra, *Curr. Opin. Biotechnol*. **2011**, *22*, 749.

[173] A. C. Neish, V. C. Haskell, F. J. MacDonald, *Can. J. Res.* **1945**, *23B*, 281.

[174] X. Liu, V. Fabos, S. Taylor, D. Knight, K. Whiston; G. J. Hutchings, *Chem. Eur. J.* **2016**, *22*, 12290.

[175] A. V. Tran, R. P. Chambers, *Biotechnol. Bioeng*. **1987**, *29*, 343.

[176] B. Török, I. Pálinkó, Á. Molnár, M. Rózsa-Tarjáni, *J. Mol. Struct.* **1999**, *482-483*, 329.

[177] M. A. Nikitina, V. L. Sushkevich, I. I. Ivanova, *Petrol. Chem.* **2016**, *56*, 230.

[178] C.P. Bezouhanova, F.A. Jabur, *J. Mol. Catal.* **1994**, *87*, 39.

[179] W. Zhang, D. Yu, X. Jia, H. Huang, *Green Chem.* **2012**, *14*, 3441.

[180] J. Zhao, D. Yu, W. Zhang, Y. Hu, T. Jiang, J. Fu, H. Huang, *RSC Adv*. **2016**, *6*, 16988.

[181] W. Kim, W. Shin, K. Lee, H. Song, H. Kim, D. Seung, I. Filimonov, *Appl. Catal. A* **2016**, *511*, 156.

[182] D. Tsukamoto, S. Sakami, M. Ito, K. Yamada, T. Yonehara, *Chem. Lett.* **2016**, *45*, 831.

[183] T. Kim, J. Baek, C. Song, Y. Yun, D. Park, W. Kim, J. Han, J. Yi, *J. Catal.* **2015**, *323*, 85.

[184] N. Ichikawa, S. Sato, R. Takahashi, T. Sodesawa, *J. Mol. Catal. A: Chem.* **2006**, *256*, 106.

[185] W. Zhang, D. H. Yu, X. J. Ji, H. Huang, *Green Chem.* **2012**, *14*, 3441.

[186] Q. Zhang, Y. Zhang, H. Li, C. Gao, Y. Zhao, *Appl. Catal. A: Gen.* **2013**, *466*, 233.

[187] N. Yamamoto, S. Sato, R. Takahashi, K. Inui, *Catal. Commun.* **2005**, *6*, 480.

[188] S. Sato, R. Takahashi, M. Kobune, H. Inoue, Y. Izawa, H. Ohno, K. Takahashi, *Appl. Catal. A: Gen.* **2009**, *356*, 64.

[189] R. Koirala, K. R. Gunugunuri, S. E. Pratsinis, P. G. Smirniotis, *J. Phys. Chem. C* **2011**, *115* 24804.

[190] H. Guo, S. Wang, C. Li, Y. Zhao, Q. Sun, X. Ma, *Ind. Eng. Chem. Res.* **2016**, *55*, 7873.

[191] G. Cabello, L. Lillo, C. Caro, G. E. Buono-Core, B. Chornik, M. Flores, C. Carrasco, C. A. Rodriguezd, *Ceram.Int.* **2014**, *40*, 7761.

[192] X. Y. Qiu, H. W. Liu, F. Fang, M. J. Ha, X. H. Zhou, J. M. Liu, *Appl. Phys. A* **2005**, *81*,

1431.
[193] H. Wang, S. Liu, W. Zhang, N. Zhao, W. Wei, Y. Sun, *Acta. Chim. Sinica,* **2006**, *64*, 2409.
[194] A. Y. Teterin, K. I. Maslakov, Y. A. Teterin, K. E. Ivanov, S. V. Yudintsev, S. V. Stefanovsky,T. S. Livshits, M. I. Lapina, *Nucl. Technol. Radiat.* **2010**, *25*, 157.
[195] J. Chen, S. Wu, F. Zhang, S. Lü, Y. Mao, *Mater. Chem. Phys.* **2016**, *172*, 87.
[196] S. Yan, M. Kim, S. Mohan, S. O. Salley, K. Y. Simon Ng, *Appl. Catal. A* **2010**, *373*, 104.
[197] Y. Yanagisawa, K. Takaoka, S. Yamabe, T. Ito, *J. Phys. Chem.* **1995**, *99*, 3704.
[198] J. I. Di Cosimo, V. K. Díez, C. Ferretti, C. R. Apesteguía, *Catalysis*, **2014**, *26*, 1.
[199] S. Liu, X. Zhang, J. Li, N. Zhao, W. Wei, Y. Sun, *Catal. Commun.* **2008**, *9*, 1527.
[200] F. Sato, S. Sato, Y. Yamada, M. Nakamura, A. Shiga, *Catal. Today*, **2014**, *226*, 124.
[201] S. Sato, R. Takahashi, T. Sodesawa, N. Honda, *J. Mol. Catal. A* **2004**, *221*, 177.
[202] M. Aslam, K. G. Davenport, *CA Pat.,* 2004042C, **1999**.
[203] S. Sato, R. Takahashi, M. Kobune, H. Gotoh, *Appl. Catal. A: Gen.* **2009**, *356*, 57.
[204] F. Sato, S. Sato, *Catal. Commun.* **2012**, *27*, 129.
[205] F. Sato, H. Okazaki, S. Sato, *Appl. Catal. A: Gen.* **2012**, *419*, 41.
[206] K. Abe, Y. Ohishi, T. Okada, Y. Yamada, S. Sato, *Catal. Today,* **2011**, *164*, 419.
[207] R. Takahashi, I. Yamada, A. Iwata, N. Kurahashi, S. Yoshida, S. Sato, *Appl. Catal. A*. **2010**, *383*, 134.
[208] R.D. Shanon, *Acta Cryst. A*, **1976**, *32*, 751.
[209] D. Sun, S. Arai, H. Duan, Y. Yamada, S. Sato, *Appl. Catal. A: Gen.* **2017**, 531, 21.

List of publications

		Location in the present thesis
1.	**Hailing Duan**, Daolai Sun, Yasuhiro Yamada, Satoshi Sato, Dehydration of 2,3-butanediol into 3-buten-2-ol catalyzed by ZrO_2, *Catal. Commun.* **48,** 2014, 1-4.	Chapter II Section 2.1-2.4; Chapter III Section 3.1-3.2
2.	**Hailing Duan**, Yasuhiro Yamada, Satoshi Sato, Selective dehydration of 2,3-butanediol to 3-buten-2-ol over ZrO_2 modified with CaO, *Appl. Catal. A: General* **487,** 2014, 226-233.	Chapter II Section 2.1-2.4; Chapter III Section 3.3
3.	**Hailing Duan**, Yasuhiro Yamada, Satoshi Sato, Vapor-phase Catalytic Dehydration of 2,3-butanediol into 3-buten-2-ol over Sc_2O_3, *Chem. Lett.* **43,** 2014, 1773-1775.	Chapter II Section 2.1-2.4; Chapter III Section 3.5
4.	**Hailing Duan**, Yasuhiro Yamada, Satoshi Sato, Efficient production of 1,3-butadiene in the catalytic dehydration of 2,3-butanediol, *Appl. Catal. A: General* **491,** 2015, 163-169.	Chapter IV Section 4.1-4.5; Chapter V Section 5.1-5.2; Chapter VI
5.	**Hailing Duan**, Yasuhiro Yamada, Satoshi Sato, Future prospect of the production of 1,3-butadiene from butanediols, *Chem. Lett.* **45,** 2016, 1036-1047.	Chapter I Section 1.8
6.	**Hailing Duan**, Yasuhiro Yamada, Shingo Kubo, Satoshi Sato, Vapor-phase Catalytic Dehydration of 2, 3-Butanediol to 3-Buten-2-ol over alkaline earth metal oxide modified ZrO_2 Catalysts, *Appl. Catal. A: General* **530**, 2017, 66-74.	Chapter II Section 2.1-2.4; Chapter III Section 3.4